Tree-stem methane emissions in the Amazon: the role of below-ground drivers and stem methane cycling

Holly Rebecca Blincow

Thesis submitted for the degree of Doctor of Philosophy

October 2025

Lancaster Environment Centre, Lancaster University, UK

Dedicated to

Mario, Jailson, Joney, Adrinaldo, Erivam & Elso.

Abstract

Tropical wetlands are the largest natural source of atmospheric methane (CH_4), with Amazonian floodplain trees alone contributing approximately 15% of global wetland CH_4 emissions. Although stem CH_4 emissions in the Amazon floodplain exceed those in other tropical regions, they are highly variable across landscapes and individual trees. The mechanisms driving this variability remain poorly understood.

To investigate CH_4 flux variability at both ecosystem and species levels, fieldwork was conducted across three floodplain systems in the Brazilian Amazon during wet and dry seasons, spanning multiple field campaigns. Stem CH_4 fluxes were measured from two tree species with contrasting wood densities (*Eschweilera coriacea* and *Hevea spruceana*) and compared with below-ground porewater chemistry and root biomass. Results revealed substantial spatial and seasonal variation in stem CH_4 emissions, with fluxes differing across floodplain types but not consistently by species, suggesting that site-level biogeochemistry plays a stronger role than species identity in regulating emissions.

Vertical declines in stem CH_4 flux were examined alongside dual isotope enrichment ($\delta^{13}C$-CH_4 and $\delta^{2}H$-CH_4), indicating internal CH_4 oxidation occurring within stems at rates comparable to those in subtropical forests, despite differences in overall emission magnitudes. While oxidation did not vary substantially across species or ecosystems, species-specific patterns highlighted variability in oxidation which requires further investigation.

Stable isotopes ($\delta^{13}C$), wood decay and radiocarbon (^{14}C) analysis of porewater, wood cores and tree chambers revealed species-level differences that may help explain why some trees emit more CH_4 than others. Wood decay was identified as a potential alternative pathway for CH_4 production, and sonic tomography is proposed as a promising tool for scaling decay-related emissions across forest systems. However, distinguishing soil-derived from tree-derived CH_4 using ^{14}C and $\delta^{13}C$ remains challenging due to complex interactions among microbial oxidation, internal transport, and tree-specific traits.

By studying two tree species with contrasting wood densities across multiple Amazonian floodplain ecosystems and seasons, this research confirms the significant role

of CH_4 cycling within trees. CH_4 production inside tree stems contributes to emissions year-round and appears to dominate during the dry season, calling for a reassessment of how emissions are measured in tropical floodplain trees and how ecosystem and regional CH_4 budgets are estimated. Furthermore, internal oxidation was confirmed in both species and shown to influence net CH_4 fluxes by reducing emissions. However, oxidation rates varied across species and sites, suggesting that the underlying controls of this process warrant further investigation due to their implications for ecosystem-level and regional CH_4 budgets. These findings have important consequences for process-based modelling and the refinement of regional CH_4 budget, emphasizing the need to integrate tree-level dynamics into broader assessments of tropical wetland CH_4 fluxes.

Contents

List of Figures and Tables

List of Figures

List of Tables

Table 2.2 | Below-ground parameters measured at three soil depths (0-50 cm, 50-100 cm, and 100-150 cm) during the wet seasons of 2019 and 2021. Samples are presented separately by site (igapó and várzea) and by the tree species associated with the piezometer locations. Results are expressed as mean ± standard deviation (SD).

Table S2.1 | Pearson correlation coefficients (r) and corresponding p-values (p) between stem methane (CH_4) flux measured at two heights (30 cm and 70 cm) and below-ground variables measured at 0-50 cm soil depth across igapó and várzea floodplain forests. Statistically significant correlations are in bold ($p < 0.05$).

Table S2.2 | Pearson correlation coefficients (r) and associated p-values (p) between stem CH_4 flux measured at two heights (30 cm and 70 cm) and below-ground variables measured at 0-50 cm soil depth. Data are presented separately for two Amazonian floodplain forest types (igapó and várzea) and for two tree species, *H. spruceana* and *E. coriacea*. Statistically significant correlations ($p < 0.05$) are shown in bold.

Table S3.3 | Tree-level stem CH_4 fluxes (wet season, lower stem: 30-60 cm above the water surface), wood density, and diameter at breast height (DBH) by plot. Species codes: B = *Hevea spruceana*, M = *Eschweilera coriacea*; the numeric suffix is the tree tag. Wood density (g cm^{-3}) and DBH (cm) were measured 1 m above the flood line. Stem CH_4 fluxes are expressed per unit emitting surface area (mg CH_4 m^{-2} hr^{-1}). "–" denotes data not available.

Table 3.1 | Summary of field measurements conducted across forest plots. The table lists the type of analysis performed (flux measurements, stable isotope analysis), the corresponding flood height at the time of sampling (in meters), and the sampling year and month for each plot. Data were collected during both wet and dry seasons across igapó, high várzea, and low várzea forest types to capture seasonal and hydrological variability.

Table 3.2 | Mean (± SD) percentage decrease in CH_4 flux between two stem heights (H1 = 30-60 cm; H2 = 70-100 cm) and mean (± SD) isotopic shifts ($\delta^{13}C$-CH_4 and $\delta^{2}H$-CH_4) from H1 to H2 across two tree species and three floodplain types. Sample sizes (n) indicate the number of trees measured for each parameter.

Table S4.1 | Sample sizes for wood decay, $\delta^{13}C$-CH_4 and Stem CH_4 flux

Table 5.1 | Summary of published estimates of tree-mediated CH_4 fluxes across a range of wetland forest types. Fluxes are reported as daily emissions per hectare (nmol CH_4 ha^{-1} d^{-1}), alongside the proportion of total wetland CH_4 emissions attributed to trees in each study. The table also includes the percentage of tree coverage within the surveyed area, where available, to provide context for the relative contribution of stem emissions.

List of Abbreviations and Acronyms

AIC	Akaike's Information Criterion
AMS	Accelerator mass Spectrometry
ASDR	Amanã Sustainable Development Reserve
CH_4	Methane
CO_2	Carbon dioxide
DBH	Diameter at breast height
DO	Dissolved oxygen
DOC	Dissolved organic carbon
EC	Electric conductivity
F_{ox}	Fraction oxidised
GC	Gas Chromatography
GHG	Greenhouse gases
MOB	Methane oxidising bacteria
MSDR	Mamirauá Sustainable Development Reserve
N_2	Nitrogen
NEIF	National Environmental Isotope Facility
NPP	Net primary production
PTFE	Polytetrafluoroethylene
PVC	Polyvinyl chloride
SE	Standard Error
SUREC	Scottish Universities Environmental Research Centre
Tg	Terra grams
Tukey HSD	Tukey's Honest Significant Difference (HSD)

ZTL	Zero Tension Lysimeters

Acknowledgements

Firstly, I am profoundly grateful to my supervisory team. Sunitha Pangala, I especially thank you for your efforts in securing the funding that made this project possible, and for your unwavering guidance throughout. Over these four years, you have been not only a dedicated mentor but also a friend; conducting fieldwork with you was a particular highlight of my PhD. To Niall McNamara, thank you for the tough love over the years. I have been grateful for your guidance and appreciated you being a sounding board for all my thoughts and ideas. Alison Hoyt, thank you for your support and encouragement. You always made me feel so welcome on my visits to Stanford.

Beyond my supervisors, I am profoundly grateful to the many people who have helped make this project possible. To the Mamirauá Institute for Sustainable Development, thank you for your assistance and hospitality during my many visits to Brazil. The Plant-Soil Interactions team at UKCEH and the Terrestrial Carbon Cycle group at Stanford, thank you for your guidance and valuable input in this project. To Carla, you have been a constant on nearly every field campaign. This work would not be what it is without all the hours of work in the field, and I am incredibly grateful to you. Clarice, the weekly phone calls have been a wonderful source of support and grounding, and I have appreciated your constant guidance. Sue, muito obrigada por tudo! Your Portuguese lessons were instrumental in helping me immerse myself in life in Brazil, and I greatly value the friendship we have built along the way.

I owe a special thanks to my parents, you have always supported me and believed in my ability to achieve anything, and for that I am deeply grateful. Dad, I know this faith was truly tested when I asked you to accompany me to the Amazon with only three days' notice. Not only were you an excellent research assistant, but the memories from that trip are among my favourites together. I hope the experience, even with the stomach bug, was worth it.

To Mario, Jailson, Joney, Eviram, Adrinaldo, Elso and Marcela: your tireless work through weeks in the field made all of this possible. Your knowledge of these incredible ecosystems is unmatched, and I loved learning from you all. In return, I hope to have left you with a love of Uno, Dobble and a friendship that spans the globe.

Para Mário, Jailson, Joney, Eviram, Adrinaldo, Elso e Marcela: o trabalho incansável de vocês ao longo de semanas no campo tornou tudo isso possível. O conhecimento de vocês sobre esses ecossistemas incríveis é incomparável, e eu adorei aprender com cada um. Em troca, espero ter deixado com vocês o carinho pelo Uno, pelo Dobble e uma amizade que atravessa o mundo.

To the girls – Cat, Imogen, and Hannah. It has been a privilege to go on this journey with you. Weekly dips in Windermere, Christmas's and New Years spent together and countless espresso martinis later. You have kept me sane when sanity was in short supply these past 4 years. Thank you for being the greatest of friends.

Lastly, to my partner Graham: no challenge is too big, no dream goes unsupported. Thank you for the endless cups of coffee, for walking the dog while I was immersed in work, for listening patiently to my constant chatter about methane, and for joining me during weeks of fieldwork in Brazil. This work would not have been possible without your unwavering support - both financial and emotional.

Authors Declaration

This thesis has not been submitted in support of an application for another degree at this or any other university. It is the result of my own work and includes nothing that is the outcome of work done in collaboration except where specifically indicated. Many of the ideas in this thesis were the product of discussion with my supervisors: Dr Sunitha Pangala (Lancaster University, UK), Prof. Niall McNamara (UK Centre for Ecology & Hydrology, Lancaster, UK) and Dr Alison Hoyt (Stanford University, USA).

This thesis word length is 32,956 (excluding reference lists) and therefore does not exceed the permitted maximum.

Statement of Authorship

This thesis has been prepared in the alternative format, as a set of three papers presented in Chapters 2-4. These chapters have co-authors in addition to my supervisory team. Please find below details of these publications. Chapters 1 and 5 are introductory and discussion chapters and are not intended for submission.

Chapter 2 -

Blincow, H, McNamara, N, Hoyt, A, Elias, D, Gomez, C, Lamb, J, Nunes de Sousa, Rodrigo, Gris, D, Pequeno Reis, L, Pangala, S. *Site-level biogeochemistry dominates over species identity in regulating stem methane emissions in Amazon floodplain forests*. In preparation

Chapter 3 -

Blincow H, McNamara N, Hoyt A, Perryman C, Elias D, Gomez C, Lamb J, Gris D, Ariza Carricondo C, Pequeno Reis L, Pangala SR. *Stem methane oxidation as a driver of tree stem methane variability*. In preparation.

Chapter 4 -

Blincow, H, McNamara N, Hoyt A, Perryman C, Garnett M, Elias D, Gomez C, Lamb J, Gris D, Pequeno Reis L, Pangala SR. *Wood rot as an alternative source of methane production in flooded Amazonian trees*.

Chapter 1 - General Introduction

Atmospheric methane (CH_4) has increased in the environment and is now 2.6 times greater than estimated pre-industrial times (Figure 1.1) (Lan et al., 2025). In comparison to carbon dioxide (CO_2), the global warming potential of CH_4 is 27 times higher over a 100 year period (Forster et al., 2023) and due to its relatively short lifespan in the environment compared to CO_2, CH_4 is seen to be a stronger option for mitigating climate change in the short term (UNEP, 2021).

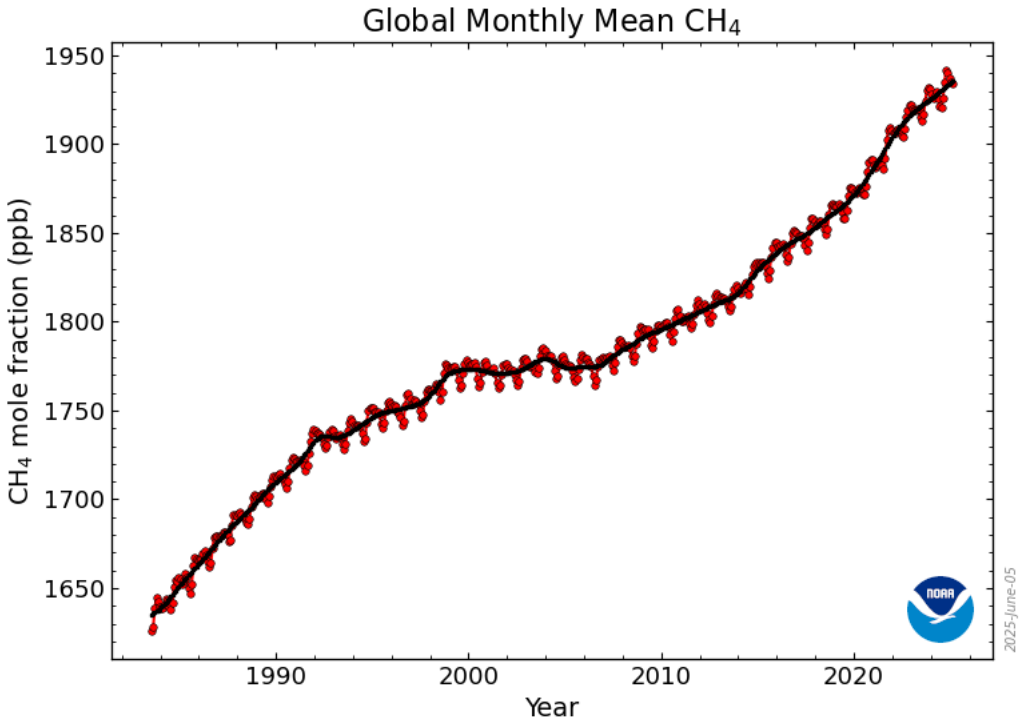

Figure 1.1 | Globally-averaged, monthly mean atmospheric CH_4 abundance determined from marine surface sites by NOAA Global Monitoring Laboratory (Lan et al., 2025).

To devise effective strategies for mitigating CH_4 emissions, it is essential to improve our understanding of its sources and sinks (Saunois et al., 2025), and to reduce the uncertainty between top-down atmospheric measurements and bottom-up inventory estimates. CH_4 is released through a range of pathways, encompassing both direct anthropogenic and natural sources. Among anthropogenic biogenic sources, agriculture and waste management are the largest, emitting an estimated 211 to 228 Tg CH_4 per year,

whilst in natural systems, wetlands represent the most significant source, releasing between 165 and 248 Tg CH_4 annually (Saunois et al., 2025).

1.1 The role of wetlands in the global CH_4 budget

Wetlands rank among the largest natural sources of atmospheric CH_4, and their emissions are expected to increase significantly, reaching 338 ± 28 Tg CH_4 yr^{-1} by 2100 (Zhang et al., 2017). They also represent the greatest source of uncertainty in the global CH_4 budget (Saunois et al., 2025) driving increased interest in understanding wetland fluxes. Tropical wetlands, in particular, account for the largest share of wetland CH_4 emissions (Bloom et al., 2017) but remain comparatively under-studied (Delwiche et al., 2021). This imbalance contributes to substantial uncertainty in global CH_4 estimates. As wetland emissions have the potential to surpass anthropogenic sources, reducing this uncertainty requires robust, localised measurements of CH_4 production, transport, emission, and consumption processes (Saunois et al., 2025).

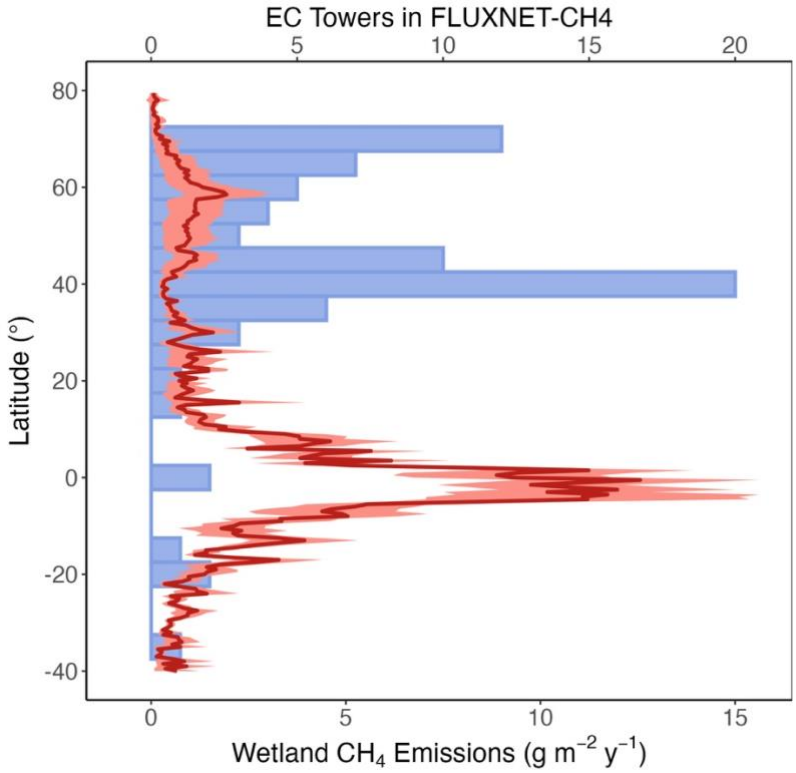

Figure 1. 2| Latitudinal distribution of eddy covariance (EC) towers in the FLUXNET-CH_4 network and corresponding wetland CH_4 emissions derived from the global wetland CH_4 emission model (WetCHARTs version 1.0) (Bloom et al., 2017). The red line indicates mean annual CH_4 emissions (g m^{-2}

y^{-1}) across latitudes, with shaded areas representing variability. Blue bars denote the number of EC towers per latitude band, highlighting observational coverage relative to emission hotspots (Perryman, unpublished based on FLUXNET data)

1.2 Wetland CH_4 production and emissions

CH_4 emissions from wetlands result from a balance between microbial production and oxidation processes that occur simultaneously within the system (Figure 1.3). CH_4 production (methanogenesis) is carried out by anaerobic archaea known as methanogens, which thrive in the anoxic conditions typical of saturated soils. This process primarily occurs via two main pathways: acetoclastic fermentation, where acetate is converted into CH_4 and CO_2, and hydrogenotrophic methanogenesis, which reduces CO_2 with hydrogen (Conrad, 1989; Whalen, 2005). These pathways are fuelled by the microbial decomposition of organic matter, often derived from plant litter and root exudates.

Conversely, CH_4 oxidation is facilitated by methanotrophic bacteria, which consume CH_4 as an energy source in the presence of oxygen. This oxidation typically occurs in oxic microzones, such as the soil-water interface and the rhizosphere (Le Mer & Roger, 2001). Methanotrophs are classified into low-affinity and high-affinity types, with the latter capable of oxidizing CH_4 even at atmospheric concentrations, whereas low-affinity methanotrophs dominate under high CH_4 concentrations typically found in wetland soils (Knief, 2015).

The net CH_4 flux from wetlands is thus controlled by the interactions between production and oxidation, as well as by various environmental factors including temperature, water table depth, vegetation type, and substrate availability (Bloom et al., 2021; Inubushi et al., 2005; Murguia-Flores et al., 2023; Sjögersten et al., 2020). CH_4 can be emitted to the atmosphere through three main pathways: ebullition (bubbling), diffusion through porewater, and plant-mediated vascular transport. Among these, vascular transport has often been considered the dominant pathway in vegetated wetlands, as plants can directly channel CH_4 from the anoxic soil layers to the atmosphere via aerenchyma tissue, bypassing oxidation zones (J. P. Chanton & Whiting, 1995; Limpert et al., 2020). In addition to herbaceous plants, trees in forested wetland systems are now

well established as conduits for CH_4 release, with multiple studies confirming their role in mediating significant stem emissions (Gauci et al., 2010; Terazawa et al., 2007).

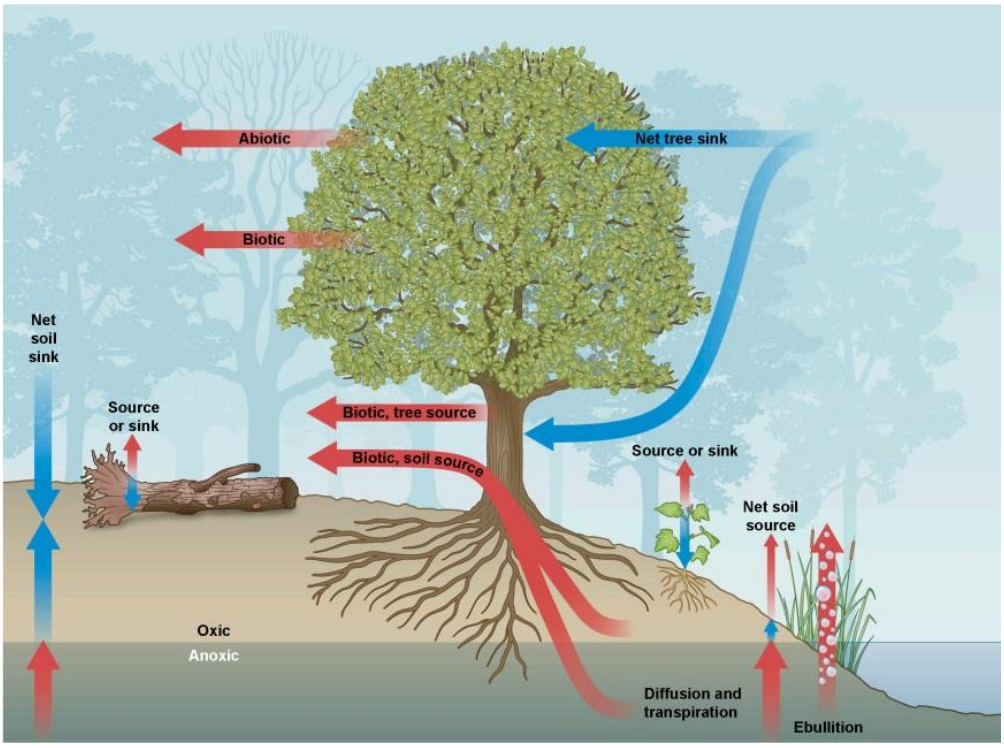

Figure 1.3 | The Variety of CH_4 sources and sinks in upland and wetland forests. Red arrows are CH_4 sources and blue arrows are sinks. Taken from Covey & Megonigal (2019).

1.3 Tree CH_4 in wetlands

Forested wetlands represent a significant component of the global wetland area, covering an estimated 880,000 to 2,562,000 km^2 of Earth's land surface (Lehner et al., 2025), and therefore have significant potential to influence the global CH_4 budget. Early studies highlighted the importance of wetland trees in CH_4 cycling (Gauci et al., 2010; Terazawa et al., 2007), suggesting they may help reconcile discrepancies between top-down and bottom-up CH_4 flux estimates in flooded ecosystems. Initial investigations suggested that trees could emit CH_4 at concentrations 10,000 times higher than atmospheric levels (Terazawa et al., 2007). Since these early studies, tree stem CH_4 emissions have been measured across temperate wetland regions and have been extended to tropical floodplains. There is large uncertainty in these measurements, with fluxes [ranging from 0.0032 to 3.76 mg m^{-2} hr^{-1} in temperate systems (Gauci et al., 2010; Pitz et

al., 2018) whilst tropical wetland tree flux ranges from 0.00 to 380 mg m^{-2} hr^{-1} (Pangala et al., 2014, 2017). Tropical wetland trees currently host the largest uncertainty and understanding more about these systems could help close the gap in bottom-up estimates in the global CH_4 budget.

1.4 Tropical Tree CH_4 emissions

Stem CH_4 emissions display significant spatial variability, strongly influenced by regional ecosystem type. Compared to boreal and temperate systems, tropical stem CH_4 emissions are up to 200 times larger (Pangala et al., 2015, 2017), accounting for 62-87% of total ecosystem CH_4 flux in tropical Indonesian forests (Pangala et al., 2013) and contributing up to half of all emitted CH_4 in the Amazon floodplain (Pangala et al., 2017). Reasons for increased stem emissions in the tropics compared to temperate and boreal regions is likely due to increased temperature and CH_4 availability in soils (Turetsky et al., 2014), known to influence stem emissions (Sjögersten et al., 2020).

1.5 Trees as a conduit of soil-derived CH_4

Previous studies have shown that trees are capable of transporting gases through their stems (Bloemen et al., 2013), a pathway that has also been proposed for the movement of soil-derived CH_4 from roots to the atmosphere (Anttila et al., 2024; Takahashi et al., 2022). The majority of stem-emitted CH_4 has been attributed to microbial production in anoxic soils, with emissions often correlating strongly with water table depth (Machacova et al., 2016; Sjögersten et al., 2020; Terazawa et al., 2015), soil temperature (Jeffrey et al., 2023; Vainio et al., 2022) and soil CH_4 flux (Jeffrey et al., 2023). Once produced in the soil, CH_4 can move into tree root systems and are transported up the stem either by passive diffusion or through convective flow driven by pressure gradients, creating diel variability (Takahashi et al., 2022) and gas exchange processes (Maier et al., 2018; Pitz & Megonigal, 2017; Plain & Epron, 2021; Sakabe et al., 2021). CH_4 is then emitted via the stem surface, controlled by lenticel density, wood density (Pangala et al., 2013) and stem diameter (Covey & Megonigal, 2019). Fluxes subsequently decline with stem height (Pangala et al., 2013; Sjögersten et al., 2020), which further supports soil as the dominant source of CH_4. However, emerging research now indicates that trees themselves may also act as sources of CH_4.

1.6 Tree stems as a Source of CH_4

Beyond serving as conduits for soil-derived CH_4, trees are increasingly recognised as sites of in-stem CH_4 production, occurring within the heartwood and sapwood of living trees (Feng et al., 2022; Mochidome et al., 2025; Smits et al., 2022; Wang et al., 2016; Yip et al., 2019). The mechanisms behind this production are diverse and not yet fully understood. Evidence from wetwood indicates that microbial processes associated with decay and rot can release CH_4 (Schink et al., 1981; Zeikus & Ward, 1974), and decay-causing saprotrophic fungi have been shown to generate CH_4 under certain conditions (Lenhart et al., 2012). At the same time, endophytic and epiphytic microbial communities within stem tissues are suggested as additional contributors (Epron et al., 2023; Jeffrey, Maher, Tait, et al., 2021). Together, these findings point to a combination of processes driving in-stem CH_4 production.

Despite these insights, the contribution of internal microbial activity to whole-stem CH_4 fluxes remains unclear, particularly across different species and climatic zones. In Japanese upland forests, up to 89% of emissions were measured above 3 m, suggesting that internal production can dominate stem flux in some systems (Mochidome et al., 2025), whereas tropical trees appear to have limited internal CH_4 production potential (Pangala et al., 2017). However, the scarcity of measurements, the temporal and spatial variability of emissions, and the difficulty in separating soil-derived from stem-derived CH_4 limit our understanding at broader scales, particularly in the tropics where in-stem CH_4 production has not been widely studied.

1.7 Trees stems as a CH_4 sink

Trees are increasingly recognized not just as passive conduits transporting soil-derived CH_4 to the atmosphere, but as active sites of methane cycling, capable of both producing and oxidising CH_4 within their tissues. This dual role means that trees can shape net CH_4 fluxes through internal processes that vary across species, stem height, and environmental conditions. Microbial oxidation by methane-oxidising bacteria (MOB) inhabiting stem and bark tissues can consume CH_4 before it reaches the atmosphere, with uptake influenced by factors such as oxygen availability, substrate concentration, stem height, and tissue (Covey & Megonigal, 2019; Jeffrey, Maher, Chiri, et al., 2021).

Vertical gradients along the stem also play a role: CH_4 emissions often decrease with height, suggesting that upper stem sections may function as net CH_4 sinks (Gauci et al., 2024). Despite this, the drivers of MOB activity and their variability across tree species, tissue types, and environmental conditions remain poorly understood.

At the regional scale, CH_4 uptake by trees varies with hydrology and soil CH_4 availability. In upland, free-draining forests, decreased soil CH_4 sources allow stems to act as net sinks, particularly in upper sections (Gauci et al., 2024). By contrast, flooded or wetland trees may simultaneously emit and oxidise CH_4 (Jeffrey et al., 2019), meaning that even trees contributing net emissions can still take up CH_4, albeit to a lesser degree. The potential for wetland trees to function as sinks, for example during dry periods when soil CH_4 production is reduced, is largely unexplored. Limited measurements, especially at height, make it difficult to determine whether these trees behave like upland trees under certain conditions (Saunois et al., 2025). Similarly, subtropical trees may host bark-dwelling MOB, but the environmental and physiological drivers of microbial CH_4 consumption in these systems remain largely unstudied (Jeffrey, Maher, Chiri, et al., 2021).

At the global scale, trees could represent a substantial terrestrial CH_4 sink, although estimates are uncertain due to limited data. In upland, non-flooded systems, trees are estimated to take up 24.6 - 49.9 Tg CH_4 per year, potentially rivalling soils as a major sink (Gauci et al., 2024). However, global upscaling is constrained by limited measurements above 2 m, the ability for stems to emit CH_4 at height (Mochidome et al., 2025) and an incomplete understanding of microbial oxidation processes across ecosystems (Jeffrey, Maher, Tait, et al., 2021). Furthermore, studies have demonstrated that removing bark layers reduced CH_4 oxidation (Jeffrey, Maher, Chiri, et al., 2021), confirming that bark-associated MOB play a critical role in regulating emissions. Improving knowledge of small-scale mechanisms is therefore critical for accurately predicting regional and global CH_4 uptake by trees.

1.8 Controls and variability of stem emissions

Stem CH_4 emissions in forested wetlands are shaped by seasonal, environmental, and biological controls that interact across scales, with seasonality playing a particularly prominent role. In temperate and tropical forest systems alike, seasonal rainfall,

temperature, and water table depth changes are key controls (Pangala et al., 2015; Sjögersten et al., 2020; Welch et al., 2019). However, in flooded forest ecosystems, seasonal controls remain understudied, with most research focused on the flooded period rather than the dry season. Studies have shown that CH_4 fluxes increase with rising water tables (Gauci et al., 2022; Jeffrey et al., 2023), but once inundation occurs, emissions plateau, suggesting that flooding acts as an on/off switch for CH_4 release. This response is particularly pronounced in tropical forests, where seasonal flooding can trigger some of the highest stem CH_4 fluxes recorded globally (Pangala et al., 2017).

While seasonal dynamics set the broader framework, ecosystem-scale factors further shape CH_4 fluxes. Environmental conditions such as oxygen availability and substrate supply regulate CH_4 production and its movement in stems (Feng et al., 2022; Gauci et al., 2022; Girkin et al., 2020; Jeffrey et al., 2023; Pangala et al., 2015). Flood longevity is a particularly important driver: as soils become anoxic, microbial methanogenesis intensifies, increasing CH_4 concentrations available for stem uptake (Gauci et al., 2022; Pitz et al., 2018; Terazawa et al., 2015). Comparisons with upland systems, where CH_4 availability is lower, show significantly reduced stem emissions (Bubier et al., 2005; Pitz et al., 2018). However, even when soils act as net CH_4 sinks, trees can continue to emit CH_4, likely due to internal production or localized emission hotspots within the stem (Mochidome & Epron, 2024; Warner et al., 2017).

Temporal dynamics add further variability. Diurnal patterns have been observed in several systems, with some trees emitting more CH_4 during the day due to increased sap flow (Takahashi et al., 2022), while others show a negative correlation between flux and sap flow (Bréchet et al., 2025). These contrasting trends suggest that CH_4 transport mechanisms may differ across climates and forest types, warranting further investigation.

At the tree scale, a wide range of physiological and anatomical traits influence the capacity of stems to produce, transport, and emit CH_4. These include lenticel density, wood density, aerenchyma development, sap flow rates, and stem pH, all of which can modulate gas exchange and microbial activity within the stem (Gauci et al., 2010; Moisan et al., 2024; Pangala et al., 2014; Takahashi et al., 2022). However, the influence of these traits is not consistent across systems. For example, wood density has been shown to both moderate CH_4 fluxes (Pangala et al., 2013) and have inconsistent effects (Sjögersten et

al., 2020) suggesting that CH_4 controls are dynamic and shaped by multiple interacting factors.

Species-level differences also contribute to variability in stem CH_4 emissions. Studies have documented significant flux variation across species, often linked to differences in wood anatomy, heartwood volume, and physiological traits (Covey et al., 2012; Epron et al., 2023; Sjögersten et al., 2020). Both heartwood and sapwood have been identified as potential sources of CH_4 (Covey et al., 2012; Wang et al., 2016), and interspecific variation in their relative proportions may help explain species-specific emission patterns.

Beyond production, CH_4 consumption within stems adds another layer of complexity. Bark-dwelling methanotrophs can oxidize CH_4 before it escapes to the atmosphere, thereby reducing net emissions (Jeffrey, Maher, Tait, et al., 2021). However, the abundance and activity of methane-oxidizing bacteria vary across individuals and species, further contributing to flux heterogeneity.

1.9 The Amazon forest and its role in tree CH_4 emissions

The Amazon is the largest tropical forest in the world and home to over 10,000 recorded tree species (Ter Steege et al., 2019) with a wetland extent of over 834,300 km^2 (Lehner et al., 2025), due to seasonal rainfall linked to the yearly shift of the Intertropical Convergence Zone, turning riparian forests into forested wetland systems.

Amazonian floodplains are the most species-rich floodplains on earth (F. Wittmann, Schöngart, Montero, et al., 2006) and as well as being a huge carbon store (Malhi et al., 2006), they are estimated among the highest for net primary production (NPP) known for tropical forests (Schöngart & Wittmann, 2010). These floodplains are not one large ecosystem, but are an accumulation of different ecosystems, characterised by different flood waters with contrasting fertility and alluvium (F. Wittmann et al., 2022).

The two dominant floodplain systems are igapó and várzea forest floodplains. Várzea is a white-water system and covers an area approximately 456,000km^2 wide (Melack & Hess, 2010). These rivers and their floodplains are light in colour but appear browner due to suspension of alluvium (Prance, 1979) (Figure 1.4). Várzea forests can be further split

into high and low várzea; high várzea is classed as forests with annual inundation <3m in height, corresponding to a mean flooded period of <50 days a year and has elevated nutrient content from alluvial soils. In contrast, low várzea have annual inundation of >3 m and >50 day's a year of flooding (F. Wittmann et al., 2002). Because of the differences in flood duration, trees within high várzea are not as adapted to flooding compared with low várzea (da Silva Marinho et al., 2010; Junk & Piedade, 1997).

Figure 1.4 | Contrasting flood water colours of the forest plots. An igapó forest on the left and várzea forest on the right.

Contrastingly, igapó floodplains are fed by blackwater river systems and appear dark in colour (Figure 1.4) but contain clear water which is darkened by suspended plant matter (Prance, 1979). They have higher oxygen concentrations in the water near the bottom of black-water lakes in comparison to white-water lakes (Junk & Piedade, 1997). Igapó's forests are less species rich and overall, have more sandy soils (Worbes, 1997), covering 302,000 km^2 (Melack & Hess, 2010). Due to this, they are often nutrient poor compared to várzea forests. They also have a lower pH of 4.6-5.2 compared to várzea's 6.5-7.5 (Schmidt, 1972).

White-water and black-water systems differ in their nutrient content, driven by the source of the water. Blackwaters originate from the Guiana and central Brazilian shields whereas white-waters originate from Andes and sub-Andean regions (Furch & Junk, 1997). These Andean regions have a larger sediment input and are nutrient-rich in comparison to black-water systems.

CH_4 emissions across these floodplains are some of the highest ever reported from tree stems (Pangala et al., 2017) and even in riparian systems are shown to contribute to global CH_4 estimates (Gauci et al., 2022). Pangala et al. (2017) highlights how fluxes across the different Amazonian floodplains can vary but very little is known as to what causes these fluxes to differentiate. Possible causes could be due to different river systems, species differences, flood level or variations in adaptations of trees across the floodplain. There are over 5,000 flood tolerant species found across these wetlands (Ter Steege et al., 2019), with some developing aerenchyma which provides enlarged gas spaces to increase oxygenation of the tree roots (Evans, 2004). Not only does this enlarged tissue facilitate oxygen exchange, but it can also increase CH_4 exchange (Pangala et al., 2013). This is suggested to be one reason why tree CH_4 emissions are greatest in wetland systems . However, emissions remain highly variable across the floodplain. Floating chamber measurements in igapó forests along the Jaú River recorded mean annual CH_4 emissions of 30 mg CH_4 m^{-2} d^{-1} (Rosenqvist et al., 2002), while várzea systems showed much higher rates, averaging 110 mg CH_4 m^{-2} d^{-1} (Barbosa et al., 2021). Stem fluxes also differ markedly: mature trees in igapó forests (black-water) emit 472 ± 206 mg CH_4 m^{-2} d^{-1}, whereas those along the Solimões River (white-water) emit 1,330 ± 518 mg CH_4 m^{-2} d^{-1} (Pangala et al., 2017). These differences may reflect underlying variation in physicochemical conditions between black-water and white-water systems, including sediment load, pH, and nutrient availability (Ji et al., 2016), which can influence microbial CH_4 production. Carbon inputs such as litterfall, macrophyte biomass, and root productivity also vary across floodplain types (Melack & Forsberg, 2001), potentially affecting substrate availability for methanogenesis. Nutrient richness and species composition further differ between river systems (Junk et al., 2015); igapó soils are nutrient-poor, with up to 10- or more-fold lower content of elements such as P, K, Ca, and Mg when compared to várzea soils (Furch, 1997), adding complexity to the spatial patterns of CH_4 emissions. Despite these known ecological gradients, current studies have

largely focused on upscaling stem fluxes to regional budgets, without resolving the site-specific or species-level factors that may drive variability (Gauci et al., 2022; Pangala et al., 2017).

2.0 Knowledge gap

Although tree-mediated CH_4 emissions in tropical wetlands are increasingly recognized, there remains limited understanding of what drives the large variability in stem fluxes across Amazonian floodplain forests. Most existing studies have prioritized regional-scale estimates and broad emission patterns (Gauci et al., 2022; Pangala et al., 2017) without accounting for biogeochemical context, species-level traits, or site-specific conditions. As a result, the observed spatial heterogeneity in stem CH_4 fluxes remains poorly constrained, and the mechanisms behind this variability are largely unknown. In addition, the internal dynamics of CH_4 within tree stems are not well characterized. While emission hotspots have been observed (Epron et al., 2023), and fungal decay has been shown to produce CH_4 in temperate systems (Hietala et al., 2015; Lenhart et al., 2012), no direct link between wood decay and stem CH_4 fluxes has been demonstrated in tropical forests. Similarly, stem-mediated CH_4 oxidation is an emerging area of study (Jeffrey, Maher, Tait, et al., 2021), and whilst the process is known to exist, its role in Amazonian floodplain trees remains unknown.

Another limitation is the seasonal bias in measurements. Most studies focus on the wet season, when trees are inundated and belowground CH_4 transport is likely enhanced. Far less is known about stem fluxes during the dry season, when trees are no longer submerged. While riparian trees outside the floodplain have been studied (Gauci et al., 2022), the behaviour of floodplain trees during the dry season remains poorly understood. It is plausible that emissions resemble those of upland species, where stem CH_4 hotspots have also been observed (Bréchet et al., 2025; Epron et al., 2023), but this has not been tested in the Amazon context.

Together, these gaps highlight the need to move beyond broad emission estimates and toward identifying the specific causes of stem CH_4 variability. This thesis addresses that need by investigating how species-level traits, wood decay, oxidation potential, and belowground CH_4 availability and production potential influence stem emissions across

contrasting floodplain systems. By doing so, we aim to highlight potential causes of uncertainty in regional CH_4 budgets.

2.1 Research objectives

The specific objectives of this study are:

Obj. 1. To assess how soil biogeochemical properties influence stem CH_4 emissions across contrasting Amazonian floodplain ecosystems.

Obj.2. To investigate the potential for CH_4 oxidation within Amazonian floodplain tree stems.

Obj.3. To determine the relative contribution of soil-derived CH_4 versus in-stem CH_4 production to overall stem emissions.

Obj.4. To evaluate whether wood decay contributes to CH_4 production and influences stem CH_4 flux variability.

2.2 Structure of the thesis

This thesis is organised into five chapters. Chapter **one** provides the background to key topics covered in this thesis and highlights the knowledge gaps and objectives for this research. Chapter **two**, **three** and **four** are written in paper format and include an introduction, methods section, results and discussion.

Chapter **two** studies the ecosystem variability and below-ground controls that influence tree stem CH_4 emissions in the amazon. Chapter **three** explores the role oxidation plays in limiting tree stem CH_4 emissions and its variability across species and floodplain ecosystems. Chapter **four** examines wood decay as an alternative sources of CH_4 in trees and how tree-derived sources can be teased apart from soil-dominating sources. Finally, chapter **five** revisits the objectives raised in chapter one, providing a synthesis of the key findings and a general discussion with future recommendations for scientific research to refine the global CH_4 budget. References are included at the end of the thesis, with supplementary information at the end of each chapter.

Chapter 2 - Tree stem methane emissions are regulated by site-level biogeochemistry over species identity in Amazon floodplain forests

In prep for New Phytologist

Holly R Blincow[1*], Niall P McNamara[2], Alison M. Hoyt[3], Dafydd Elias[2], Carla Gomez[1,4], Jack Lamb[3], Rodrigo Nunes de Sousa[1], Darlene Gris[5], Leonardo Pequeno Reis[6], Sunitha Rao Pangala[1,4*]

[1]Lancaster Environment Centre, Lancaster University, Bailrigg, Lancaster, UK

[2]UK Centre for Ecology & Hydrology, Lancaster, UK

[3]Department of Earth System Science, Stanford University, Stanford, CA, USA

[4]Department of Life Sciences, Imperial College London, Silwood Park Campus, Ascot, Berkshire, UK

[5]Mamirauá Institute for Sustainable Development, Amazonia, Brazil

[6]Universidade Federal Rural da Amazônia, Belém, Para, Brazil

*Corresponding authors: h.r.blincow@bham.ac.uk; s.pangala@imperial.ac.uk

Orchid ID: HRB:0009-0009-1866-1089; SRP:0000-0002-0650-7721

2.1 Abstract

- Tree stems in Amazonian floodplains are major methane (CH_4) emission pathways, yet controls on their variability remain unclear. Emissions vary by orders of magnitude between várzea (nutrient-rich white-water) and igapó (nutrient-poor black-water) forests, and among trees, suggesting controls beyond flooding. We tested whether site-level biogeochemistry better explains stem CH_4 variability than species identity.
- Stem CH_4 emissions from two species - *Eschweilera coriacea* and *Hevea spruceana* - were measured in várzea and igapó forests during the flooded

season and paired with porewater chemistry (pH, electrical conductivity, dissolved oxygen, dissolved CH_4, dissolved organic carbon), methane-production potential (MPP), and root biomass.

- Stem CH_4 emissions were significantly higher in várzea than igapó, independent of species or stem height. Várzea porewaters displayed higher conductivity, dissolved CH_4 and MPP, near-neutral pH, and lower oxygen, with fine roots concentrated in the 0-50 cm soil layer. Basal stem emissions in várzea correlated with shallow biogeochemical variables and fine-root biomass, whereas relationships in igapó were weak.
- Together, these results suggest that tree-stem CH_4 emissions can be linked to site-level below-ground biogeochemistry, while species traits modulate fluxes secondarily. Amazon-wide CH_4 budgets and models should integrate ecosystem geochemistry and root-soil interactions alongside tree traits to capture spatial variability in stem emissions.

Keywords: Tree stem methane, CH_4, Amazon, Tropical Floodplain forests, várzea, igapó, wetland

2.2 Introduction

Tropical wetlands are the largest natural source of atmospheric methane (CH_4), with the Amazon basin contributing a substantial proportion due to widespread annual flooding, which transforms over 900,000 km^2 into forested wetlands (Hess et al., 2015; Saunois et al., 2020). While CH_4 emissions have previously been attributed to emissions from anoxic soils and waterbodies, recent studies have identified tree stems as major emission pathways, with fluxes in Amazonian floodplain forests exceeding those of tropical peatlands and temperate wetlands by up to two orders of magnitude (Pangala et al., 2013, 2017). Despite their global significance, the controls on CH_4 emissions from Amazonian tree stems remain poorly understood.

Two basin-scale studies show strong hydrological control on seasonal patterns (Gauci et al., 2022; Pangala et al., 2017), yet stem fluxes vary by orders of magnitude among ecosystems and among trees within sites at single time points, implying additional controls beyond flood stage patterns (Gauci et al., 2022; Pangala et al., 2017). Proposed

explanations point to interactions between tree functional traits (e.g. wood density, porosity, lenticel abundance) and below-ground biogeochemistry that sets methanogenic potential and CH_4 availability (Epron et al., 2023; Moisan et al., 2024; Pangala et al., 2015; Soosaar et al., 2022; van Haren et al., 2021). In the Amazonian floodplains, where within-season temperature is relatively stable, hydrology typically dominates seasonality (Gauci et al., 2022; Pitz et al., 2018); however, once flooded, increasing water depth does not necessarily increase emissions (Gauci et al., 2022; Jeffrey et al., 2023), suggesting that flooding serves as an "on/off" switch for soil-driven methanogenesis, with finer-scale variability controlled by other variables.

Woody traits such as wood density, porosity, and anatomical adaptations have previously been linked to variability in stem CH_4 fluxes. Lower-density wood is often associated with higher fluxes due to reduced diffusion resistance (Pangala et al., 2014; Soosaar et al., 2022; van Haren et al., 2021), while porosity, parenchyma, lenticel density, and moisture content also influence emissions (Epron et al., 2023; Pangala et al., 2015). Tree functional traits shaped by flood adaptation may also interact with internal CH_4 production or oxidation processes within woody tissues (Moisan et al., 2024; Parolin et al., 2004), making stem emissions potentially sensitive to species-specific anatomical characteristics. Because many of these traits co-vary among species (Chave et al., 2009; Poorter et al., 2010; Yang et al., 2024), comparing species with contrasting wood density provides a practical way to test whether species identity helps explain variation in stem CH_4 emissions when the full suite of woody traits is not measured directly. However, in Amazonian floodplain forests it remains unclear whether variation in stem CH_4 emissions is better explained by species identity, as a proxy for differences in wood structure and transport potential, or by site-level below-ground biogeochemistry that governs CH_4 production and availability.

Amazonian flooded forests, with their unique water chemistry, present a particularly complex setting. White-water várzea floodplains receive Andean-derived, sediment-rich waters (EC 50-140 $\mu S\ cm^{-1}$, near-neutral pH) while black-water igapó forests receive acidic (pH 4-5), low-EC ($<40\ \mu S\ cm^{-1}$), nutrient-poor waters from weathered Guiana and Brazilian shields (Furch & Wolfgang, 1997; Junk et al., 2011) - contrasts that shape microbial communities and methanogenic activity. These hydrochemical differences likely modulate soil CH_4 production and dissolved CH_4 availability for stem transport, driving spatial variability across the basin. Furthermore,

porewater properties such as pH, dissolved oxygen (DO), electrical conductivity (EC), DOC and dissolved CH_4 are also known to play significant roles in regulating soil methanogenesis and CH_4 availability (Liu et al., 2012; Teh et al., 2005; Wang et al., 1996), while fine-root biomass density regulates local CH_4 production and availability through substrate supply and access to soil CH_4 pool (Liu et al., 2012; Baird et al., 2024; Pumpanen et al., 2024).

Although flooding is a prerequisite for anaerobic processes, the rate and magnitude of CH_4 production and emissions including stem emissions, are expected to be shaped by these finer-scale below-ground conditions. Yet, stem CH_4 measurements have not been systematically paired with tree-specific porewater chemistry, MPP, and root biomass across this hydro-chemical gradient. Here we address this gap by quantifying stem CH_4 emissions from two co-occurring species with contrasting wood density - *Eschweilera coriacea* and *Hevea spruceana* - in nutrient-rich várzea and nutrient-poor igapó during the flooded season. Using species identity as a proxy for contrasting wood density, we paired stem flux measurements with tree-specific porewater chemistry (pH, EC, DO, DOC, dissolved CH_4), MPP, and fine-root biomass to 150 cm depth. We tested whether below-ground biogeochemistry better explains variability in stem CH_4 emissions than species identity across contrasting black- and white-water systems.

2.2.1 Aims

This study examines whether below-ground biogeochemical differences (porewater chemistry, MPP and root biomass), may account for observed variability in tree stem CH_4 emissions both within flooded forest plots and between black- and white-water river systems.

We hypothesise that:

1) For a given tree species, stem CH_4 fluxes will differ significantly between várzea and igapó forests, reflecting site-level differences,

2) Site-level variation in CH_4 emissions is explained by differences in belowground biogeochemistry

3) Among the below-ground variables, dissolved CH_4 and DOC concentrations in porewater are the strongest predictors of stem CH_4 emission variability, reflecting their role in fuelling methanogenesis.

2.3 Materials and Methods

2.3.1 Study site

Figure 2.1 | Location of the igapó field site, located within the Amanã Sustainable Development Reserve (in blue) and the várzea field site, situated within the Mamirauá Sustainable Development Reserve (in red). Both sites are located within the Brazilian Amazon.

The study was conducted in the central Amazonian floodplain of Brazil (~500 km west of Manaus) within two sustainable development reserves (Figure 2.1): a blackwater igapó forest plot in Amanã Sustainable Development Reserve (ASDR; S2° 38.598' W64° 39.980'south of Amanã lake) and ii) a white-water várzea forest plot in Mamirauá Sustainable Development Reserve (MSDR; S2° 48.916' W65° 05.192'; near Japurá river). The igapó plot is influenced by two hydrologically distinct river systems: the white-water Solimões-Japurá confluence and the black-water Negro River. During the dry season, the Solimões-Japurá dominates, while the Rio Negro prevails during the flooded season. At

the time of sampling, the site was inundated with ~1.5 m of water. The igapó forest plot contains approximately 500 trees within the 1hectare plot from 80 species (data provided by the Mamirauá Institute). The várzea forest plot was bounded by the Solimões, Japurá, and Auati Paraná Rivers and located close to the Japurá river along a smaller river channel. The várzea forest plot contains approximately 400 trees within the 1 hectare plot from 100 species (data provided by the Mamirauá Institute), with an inundation of 2-3 meters of floodwater at the time of sampling. The understory vegetation is characteristically greater in igapo forests than várzea. Previous leaf litter measurements in these forest systems are also greater in igapó compared to várzea(Camargo et al., 2015; Schöngart & Wittmann, 2010), as is nitrogen (Furch, 1997). However, biomass production has been measured to be over double in várzea (17.4 t ha^{-1}) compared to igapó forests (8.7 t ha^{-1})(Furch, 1997).

The two sites were chosen based on their contrasting hydrology: a nutrient-rich, sediment-laden white-water várzea with 2-3 m inundation for up to three months (várzea plot), versus a nutrient-poor, low-pH, relatively high-DO black-water igapó with 1-2 m inundation for up to 45 days (igapó plot). The mean annual temperatures at both plots were 27°C.

Within our 1 ha plots, two tree species: *Hevea spruceana* (commonly known as Seringa Barriguda) and *Eschweilera coriacea* (commonly known as Matamata) were selected for this study. Five mature individuals of each species were sampled per plot. These species were chosen because they were among the few species occurring in both plots and represented contrasting wood densities, making them ideal for testing species identity as proxy for woody traits. Across the two plots, only ten species were shared, and *H. spruceana* and *E. coriacea* were the only pair with markedly different wood density (0.5 ± 0.2 g cm^{-3} for H. spruceana and 0.8 ± 0.08 g cm^{-3} for *E. coriacea*). Both species were sufficiently abundant (≥10 mature individuals per plot) and spatially distributed across each plot (trees ≥3-6 m apart), ensuring representative sampling without clustering bias. Both species are large canopy trees that occur in Amazonian forests but differ in habitat specialization and wood structure. *Hevea spruceana* (Euphorbiaceae), a relative of the rubber tree *Hevea brasiliensis*, is primarily associated with seasonally flooded riverine environments and is characteristic of várzea and igapó forests, where it is adapted to periodic inundation (F. Wittmann, Schöngart, Montero, et al., 2006; F. Wittmann et al., 2010). In contrast, *E. coriacea* (Lecythidaceae) is one of the most widespread and

abundant canopy tree species in Amazonia and occurs across a broader range of habitats, including both terra firme and seasonally flooded forests (Heuertz et al., 2020; Steege et al., 2013; F. Wittmann, Schöngart, Montero, et al., 2006). The two species therefore represent contrasting ecological strategies and wood densities, with *E. coriacea* typically forming dense hardwood characteristic of Lecythidaceae taxa, whereas *H. spruceana* exhibits lower wood density typical of many Euphorbiaceae species (Wycherley, 1992). Tree diameter at breast height ranged from 18-52 cm for *H. spruceana* and 19-50 cm for *E. coriacea.* All ten trees samples from were mature trees.

2.3.2 Tree stem CH_4 measurements

Tree stem CH_4 fluxes were measured during daylight hours over three weeks in May 2022 in the flooded season at both plots (Table 2.1). Fluxes were measured at two heights: 30-60 cm and 70-100 cm above the floodwater line (~1.5 m in igapó and ~3 m in várzea), using chambers as described in . The chambers were strapped to the tree using ratchet straps and visible gaps around the edges were plugged using a modelling clay (Play-Doh). Once attached to the tree stems, the chambers were connected via tubing to the microportable GHG analyser (ABB LGR GLA131-GGA) and CH_4 fluxes were calculated based on the linear change in methane concentration over time within the chamber headspace. A linear regression was applied to each 5-minute chamber closure time series, and only flux estimates with a correlation coefficient (R^2) greater than 0.97 were retained for analysis (all fluxes met this threshold). Final flux values are reported as mg CH_4 m^{-2} hr^{-1}, normalized to the surface area enclosed by the chamber.

2.3.3 Below-ground measurements

Porewater chemistry

Subsurface porewater samples were collected within a two-week period from standpipe piezometers constructed from PVC pipes, installed at depths of 0-50 cm, 50-100 cm and 100-150 cm with end caps installed to exclude rainwater. For each piezometer, 3 mm holes were drilled approximately 2 cm apart within its designated 50 cm segment (e.g., 0-50 cm, 50-100 cm, or 100-150 cm) to allow for water sampling at the corresponding depth using tubing attached to a peristaltic pump. Piezometers were installed 50 cm from each tree where tree flux samples were to be taken (20 trees in total) during the dry season (Nov-Dec 2019) and allowed to stabilise before sampling began in May 2021 (Table 2.1). Each tree under investigation had its own set of piezometers (at

all three depths), allowing for assessment of the role of that specific tree vs. belowground parameters. No samples were collected during the 2022 campaign as piezometers were submerged under water.

Water samples extracted from piezometers were analysed for dissolved CH_4, DOC, pH, EC, and DO. Dissolved CH_4 concentrations were measured from the equilibrated headspace of porewater samples. 60 ml of porewater and 40 ml of atmospheric air were shaken vigorously for five minutes inside a 100 ml syringe, after which a 10 ml aliquot was added to an Exetainer 3 ml vial (Labco, UK) for analysis of CH_4 concentrations using gas chromatography (GC) analysis (Clarus 480 Perkin Elmer). Samples were corrected for atmospheric contamination, and dissolved CH_4 concentrations were calculated from the headspace CH_4 mixing ratio using Henry's law, accounting for partitioning between water and gas phases and corrected for temperature at the time of equilibration using the neoDissGas package (Cawley et al., 2020).

Samples for DOC concentration were collected from piezometers at all depths and filtered through a Whatman 40-micron filter. Due to the remote location of sampling, all samples were placed on ice to keep them < 4 °C whilst in the field. Samples were frozen within 14 days of collection for preservation (Cook et al., 2016) and analysed using a Shimadzu TOC-L CPH analyser.

EC and pH were sampled using a multi-parameter pocket tester (Apera Instruments PC60 Premium). The handheld device was calibrated against a Hanna Instruments HI 2003 Edge® EC Meter and Hanna Instruments HI5221 pH Meter. Dissolved oxygen was analysed in porewater using Hanna Dissolved Oxygen Meter (Model HI9143). Below-ground samples were collected in the wet seasons of May 2019 and 2021. In May 2019, only DO, EC and pH were measured, with analysis expanded in 2021 to include DOC and dissolved CH_4.

Below-ground and above-ground parameters were not all measured in the same year (Table 2.1). EC, pH, and DO were measured in both 2019 and 2021. No significant interannual differences were found in these parameters after accounting for soil depth ($p > 0.05$; see Statistical analysis, Table S2.1 and Table S2.2). Based on the absence of detectable year effects, we assumed that below-ground parameters measured in 2021 were representative of below-ground conditions during the 2022 stem CH_4 flux

measurements. Accordingly, tree stem CH_4 fluxes were modelled against below-ground parameters measured in 2021.

CH_4 production potential (MPP)

Intact soil cores were extracted to 150 cm during the wet season in 2021 using a Russian type peat auger (Eijkelkamp, Netherlands) and sectioned into depth intervals of 0-5, 5-30, 30-50, 50-100 and 100-150 cm. Each section was placed into a gas-tight incubation container, consisting of a PVC pipe cut to fit the intact core and sealed with two PVC end caps. One end cap was used to seal the bottom of the core, and the other was attached at the top and fitted with a three-way valve for gas sampling.It was flushed with N_2 to establish anoxia, and incubated in the dark at field temperature (average of 26 °C) for 14 days. Headspace gas (2 ml) was withdrawn at 0, 6, 12, 24, 48 and 72 h, then every 24 h to day 7 and every 48 h until day 14, analysed for CH_4 on a Shimadzu GC-FID, and replaced with equal volumes of N_2 to maintain pressure. MPP was calculated from the cumulative increase in CH_4 concentration, corrected for dilution from N_2 backfilling and dissolved fractions using Henry's law, and expressed as mmol CH_4 m^{-2} d^{-1} based on the core cross-sectional area.

Root biomass

Three soil cores were extracted per tree, totalling 20 samples using a soil auger (5 cm diameter, 150 cm long) in Nov andDec 2019. The soil cores were extracted within a 75 cm radius around the tree, with samples taken at three soil depths, with three replicates at each depth: 0-50 cm, 50-100 cm, and 100-150 cm. The cores from each depth were combined to create a homogeneous sample, which was then used to analyse root biomass.

Root biomass was measured by separating roots from the soil by wet sieving and manual sorting, and separating roots > 2 mm (coarse roots) and < 2 mm (fine roots) in diameter. Roots were then oven-dried at 60 °C for 72 hours and weighed to determine root biomass per volume of soil.

Although roots from neighbouring trees may also have been present within the sampled volume, focal trees were generally well spaced (most separated from their nearest neighbour by c. 3 m in igapó and 5 m in várzea), so sampling within a 75 cm radius of each stem likely captured a substantial proportion of roots from the focal tree and its immediate neighbourhood, while not guaranteeing exclusive attribution.

Table 2.1 | Analysis conducted at each individual field campaign.

Year	*Site*	*Analysis*
2019	igapó (blackwater) & high várzea (whitewater)	EC, pH, DO, fine root biomass and coarse root biomass from 3 soil depths (0-50 cm, 50-100 cm and 100-150 cm)
2021	igapó (blackwater) & high várzea (whitewater)	EC, pH, Dissolved CH_4, DO, DOC, MPP from 3 soil depths (0-50 cm, 50-100 cm and 100-150 cm)
2022	igapó (blackwater) & high várzea (whitewater)	Stem fluxes, at two heights (30-60 cm and 70-100 cm) from 5 of each species (*E. coriacea* and *H. spruceana*) per plot

2.3.4 Statistical analysis

All statistical analyses were conducted in R v12.0. Normality was visually assessed and data were transformed where necessary. Stem CH_4 fluxes were analyzed with linear models (log-transformed), including site, species, height, and two-way interactions. Model simplification was guided by Akaike's Information Criterion (AIC), with residuals inspected for assumption violations.

The effect of below-ground parameters (EC, DO, pH, MPP) on dissolved CH4 were analyzed with linear mixed effect models including tree species, site, soil depth, with tree identity as a random effect. We also tested for species-dependent effects by including an interaction between tree species and site. Model selection was based on AIC values, and the final model retained only significant predictors.

Fine and coarse root biomass were analysed using linear mixed-effects models. For each root type, a global model included soil depth, tree species, site, and the

interaction between species and site as fixed effects, with tree identity included as a random effect to account for repeated sampling.

To examine the relationship between stem CH_4 fluxes and below-ground variables we used Pearson's correlation coefficients. Correlations were performed separately for várzea and igapó forests, and then further stratified by species and stem height. Fine and coarse root biomass were analysed at depths of 50, 100, and 150 cm. A significance threshold of $p < 0.05$ was used throughout, with p-values between 0.05 and 0.1 interpreted as indicative of trends. All reported correlations include Pearson's r and associated p-values.

2.4 Results

2.4.1 Stem CH_4 emission magnitude and variability across sites and species

Across both forest types and species there was a pronounced vertical decline in emissions: stem CH_4 fluxes were consistently higher at 30 cm than at 70 cm ($p < 0.001$; Figure 2.2). At a given height, fluxes were also higher in várzea than in igapó forests ($p = 0.041$; Figure 2.2). Although mean fluxes differed between tree species within sites, species identity did not explain significant variation in stem CH_4 emissions once site and height were accounted for - the final model for CH_4 emissions only retained site and height as fixed effects. Stem CH_4 fluxes exhibited substantial variability among individual trees, particularly at 30 cm height, with the greatest variability observed in the várzea forest.

In the igapó forest, mean stem CH_4 fluxes at 30 cm were lower overall, averaging 3.14 ± 3.86 mg CH_4 m^{-2} h^{-1} for *E. coriacea* and 0.92 ± 0.53 mg CH_4 m^{-2} h^{-1} for H. spruceana. At 70 cm, fluxes further declined to 0.75 ± 0.79 mg CH_4 m^{-2} h^{-1} for *E. coriacea* and 0.24 ± 0.14 mg CH_4 m^{-2} h^{-1} for *H. spruceana*. At 30 cm stem height in the várzea forest, mean stem CH_4 fluxes were 13.3 ± 15.0 mg CH_4 m-² h-1 for *E. coriacea* and 4.71 ± 2.77 mg CH_4 m^{-2} h^{-1} for *H. spruceana*. At 70 cm, fluxes declined substantially in both species, averaging 2.12 ± 2.91 mg CH_4 m^{-2} h^{-1} for *E. coriacea* and 1.77 ± 1.55 mg CH_4 m^{-2} h^{-1} for *H. spruceana*.

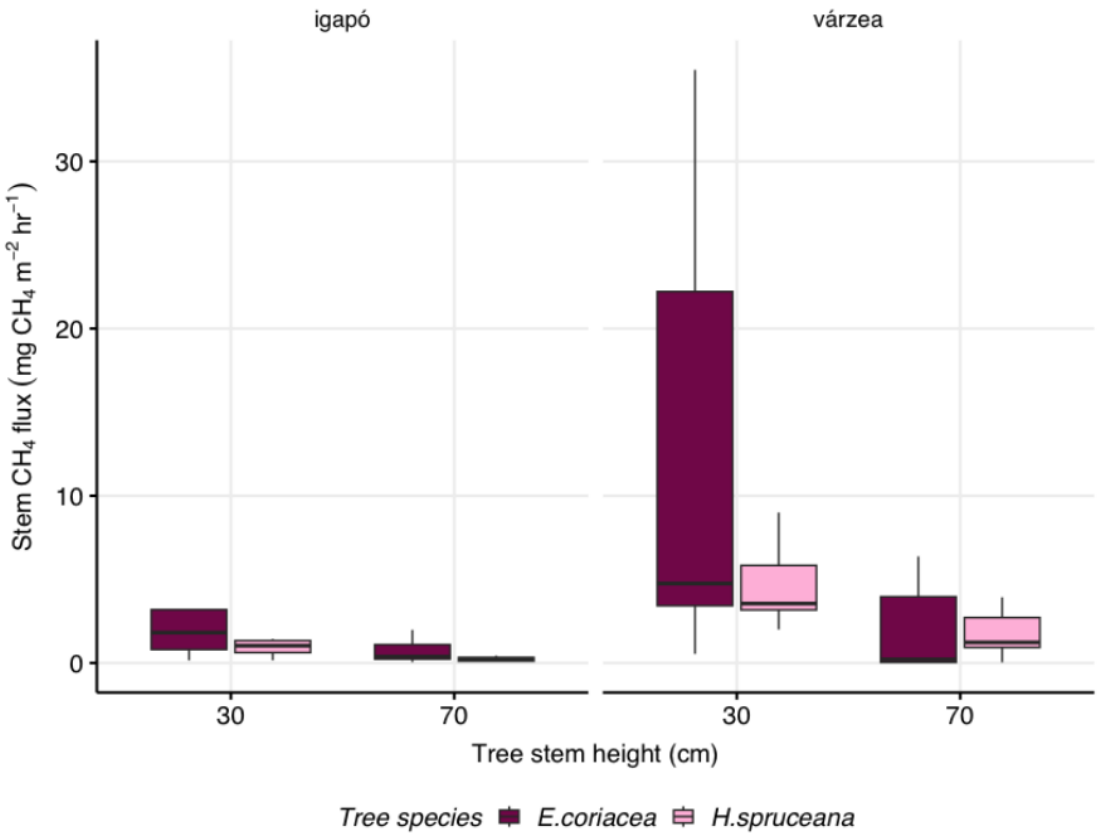

Figure 2.2 | Stem CH_4 fluxes for two species (*E. coriacea*, n = 10; *H. spruceana*, n = 10) in two floodplain forest types (várzea, igapó), measured at two heights (30-60 cm and 70-100 cm relative to the water surface). Fluxes (mg CH_4 m^{-2} hr^{-1}) are reported per unit area of the stem surface enclosed by the chamber.

2.4.2 Variability in Porewater Chemistry and CH_4 Production Potential Across Sites

Dissolved CH_4 concentrations exhibited strong vertical patterns across soil profiles, with concentrations highest in shallow soils and declining with depth (Table 2.2, Figure 2.3). In the mixed-effects model, dissolved CH_4 decreased significantly with increasing soil depth, was higher beneath *H. spruceana* than *E. coriacea*, and increased with increasing MPP. Dissolved CH_4 concentrations were highest in the 0-50 cm layer, intermediate at 50-100 cm, and lowest at 100-150 cm. All relationships were identified on square-root-transformed dissolved CH_4 concentrations.

Across both sites, porewater chemistry and MPP displayed pronounced depth-related gradients. In igapó soils, dissolved CH_4 concentrations were lower overall but followed similar depth-related declines, peaking at 50 cm and averaging 64.6 µmol L^{-1}. MPP was lower than in várzea, averaging 1.14 mg CH_4 m-2 hr^{-1} at 30 cm and declining to 0.29 mg CH_4 m-2 hr^{-1} at 150 cm. Igapó soils remained more acidic and less conductive than várzea soils, with pH ranging from 3.82 to 6.7 and EC averaging 38.8 µS cm^{-1} at 50 cm, declining further with depth. DO concentrations decreased from 4.56 mg L^{-1} at 50 cm to 1.11 mg L^{-1} at 150 cm, while DOC declined from 19.7 to 3.9 mg L^{-1} across the profile.

In várzea soils, dissolved CH_4 averaged 129 µmol L^{-1} at 50 cm and declined to 23.2 µmol L^{-1} at 150 cm, while MPP was greatest in shallow soils (mean 9.27 mg CH_4 m-2 hr^{-1} at 30 cm) and decreased sharply with depth. DO concentrations declined from 3.0 mg L^{-1} at 50 cm to 0.25 mg L^{-1} at 150 cm, and DOC concentrations decreased from 8.32 to 2.9 mg L^{-1} across the same depth interval. Soil pH ranged from near-neutral values in surface soils to slightly lower values at depth, while EC remained comparatively high throughout the profile.

Dissolved CH_4 differed significantly across tree species, with greater quantities found in depths associated with *H. spruceana*, compared to *E. coriacea* ($p < 0.01$) - a pattern repeated in both igapó and várzea. Despite clear site-level differences in porewater chemistry and MPP, site, pH, DO, EC, DOC, and the site × species interaction did not explain additional variation in dissolved CH4 once soil depth, tree species, and MPP were included in the model ($p > 0.05$).

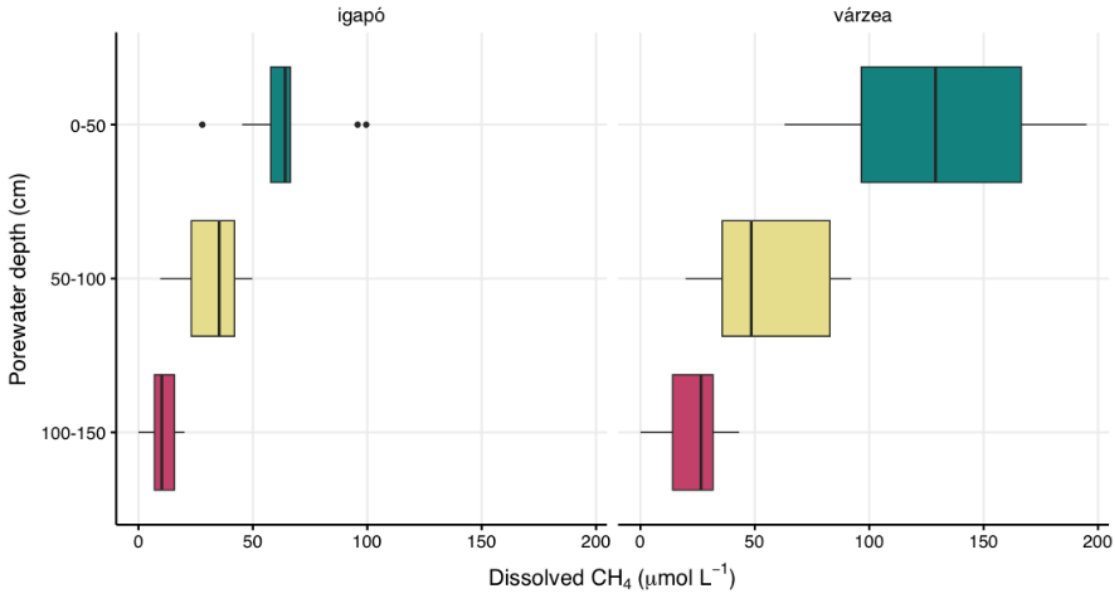

Figure 2.3 | Dissolved CH_4 concentrations (µmol L^{-1}) at three soil depths (0–50, 50–100, 100–150 cm) around each sampled tree across igapó and várzea forest plots.

2.4.3 Root biomass Distribution Across Depth and Sites

Root biomass was strongly structured by soil depth, with both fine and coarse roots concentrated in the upper 0-50 cm soil layer (Table 2.2). Root biomass declined sharply with increasing depth and was negligible below 50 cm. No significant differences were found between the two tree species for either fine or coarse root biomass at any depth.

In the igapó forest, fine root biomass at 0-50 cm averaged 945 ± 486 g m^{-3}, while coarse root biomass was 949 ± 606 g m^{-3}. Root biomass at greater depths was negligible: fine roots averaged 23.9 ± 31 g m^{-3} at 50-100 cm and 0.113 ± 0.621 g m^{-3} at 100-150 cm. Coarse root biomass at these depths was 4.38 ± 14.7 g m^{-3}; and 1.93 ± 7.56 g m^{-3}, respectively (Table 2.2). The várzea forest exhibited a similar depth-related pattern, but with higher biomass values than igapó (Table 2.2). Fine root biomass at 0-50 cm averaged 1257 ± 700 g m^{-3}, while coarse root biomass averaged 978 ± 540 g m^{-3}. At 50-100 cm, fine and coarse root biomass declined to 5.07 ± 13.6 g m^{-3} and 1.99 ± 5.29 g m^{-3}, respectively, and decreased further at 100-150 cm to 2.61 ± 14.3 g m^{-3} for fine roots, with coarse roots at 7 ± 20.3 g m^{-3} (Table 2.2).

2.4.4 Relationships Between Below Ground Variables and Stem CH_4 Emissions

With lower overall stem CH_4 fluxes in igapó, the relationship between below-ground variables and emissions was weaker and not statistically significant (Table S2.1). Across all trees, moderate positive trends were observed for MPP ($r = 0.52$, $p = 0.067$) and EC ($r = 0.49$, $p = 0.081$), but these relationships were not significant. Fine root biomass at 0-50 cm depth was weakly correlated with 30 cm stem flux ($r = 0.26$, $p = 0.36$), and no relationship was detected with coarse root biomass. Species-level analyses revealed no meaningful correlations for E. coriacea and for H. spruceana. At 70 cm stem height, emissions were lower, and all correlations with below-ground variables diminished and were statistically non-significant (Table S2.2).

In várzea, stem CH_4 emissions at 30 cm height showed moderate to strong correlations with several below-ground variables. Across all trees, pH ($r = 0.60$, $p = 0.026$) and EC ($r = 0.57$, $p = 0.034$) were the best predictors of stem emissions at 30 cm (Table S2.1). MPP in topsoil (0-50 cm) was also correlated positively with 30 cm fluxes ($r = 0.62$, $p = 0.021$). Root biomass further explained variation in stem fluxes. Fine root biomass at 0-50 cm depth showed a positive correlation with stem flux at 30 cm ($r = 0.49$, $p = 0.048$). Coarse root biomass was not significantly associated with stem emissions. Species-specific patterns revealed stronger below-ground coupling in E. coriacea. For this species, 30 cm stem flux was significantly correlated with EC ($r = 0.70$, $p = 0.043$) and MPP ($r = 0.68$, $p = 0.048$), with a borderline association with fine root biomass ($r = 0.56$, $p = 0.061$). For H. spruceana, correlations were weaker and non-significant (e.g., MPP: $r = 0.41$, $p = 0.18$). As in igapó, correlations weakened at 70 cm stem height (Table S2.2).

.

Table 2.2 | Below-ground parameters measured at three soil depths (0-50 cm, 50-100 cm, and 100-150 cm) during the wet season. Samples are presented separately by site (igapó and várzea) and by the tree species associated with the piezometer locations. All parameters collected in 2021 except for fine and coarse root biomass which were collected in 2019. Results are expressed as mean ± standard deviation (SD).

Plot type	Tree species	Soil depth (cm)	EC ± SD ($\mu S\ cm^{-1}$)	pH ± SD	Dissolved CH_4 ± SD (μmol^{-1})	DO ± SD ($mg\ l^{-1}$)	DOC ± SD ($mg\ l^{-1}$)	MPP ± SD ($mmol\ CH_4\ m^{-2}\ d^{-1}$)	Fine root biomass ($g\ m^{-3}$)	Course root biomass ($g\ m^{-3}$)
Igapó	*H. spruceana*	0-50	39.5 ± 7.4	4.7 ± 0.7	69.6 ± 15.1	4.3 ± 1	19.8 ± 7.1	1.28 ± 0.16	629 ± 275	289 ± 140
		50-100	26.7 ± 7.5	4.5 ± 0.7	42.7 ± 5.4	2.9 ± 0.6	10.9 ± 3.6	0.66 ± 0.11	6.5 ± 9.2	2.8 ± 4.0
		100-150	16.3 ± 3.6	4.4 ± 0.8	12.8 ± 5.6	1.3 ± 0.6	4.0 ± 2.3	0.44 ± 0.07	1.4 ± 3.1	1.2 ± 2.5
	E. coriacea	0-50	38.3 ± 5.5	5.0 ± 1.1	59.6 ± 26.7	4.8 ± 0.9	19.6 ± 7.8	1.23 ± 0.18	743 ± 303	348 ± 132
		50-100	23.6 ± 4.2	4.8 ± 1.1	20.9 ± 10.4	2.7 ± 0.8	8.1 ± 1.0	0.7 ± 0.13	5.8 ± 9.6	2.5 ± 4.3
		100-150	11.9 ± 1.4	4.7 ± 1.3	7.9 ± 7.8	0.9 ± 0.3	3.8 ± 2.2	0.44 ± 0.03	1.5 ± 3.6	1.3 ± 2.9
Várzea	*H. spruceana*	0-50	111 ± 19.7	6.5 ± 0.3	153 ± 37.3	2.7 ± 1.3	9.5 ± 1.3	7.58 ± 1.46	1134 ± 379	930 ± 412
		50-100	75.4 ± 11.1	6.2 ± 0.7	76.0 ± 22.1	1.3 ± 0.5	4.7 ± 2.6	4.8 ± 0.98	18.6 ± 20.1	18.2 ± 25.0

	100-150	50.8 ± 9.4	5.7 ± 1.4	34.2 ± 8.3	0.2 ± 0.2	2.6 ± 0.6	2.15 ± 0.36	6.5 ± 11.8	3.6 ± 6.1
E. coriacea	0-50	117 ± 31.7	6.83 ± 0.3	104.1 ± 41	3.3 ± 0.8	7.1 ± 2.1	8.13 ± 0.96	1287 ± 461	967 ± 424
	50-100	76.6 ± 18.8	6.76 ± 0.3	35.8 ± 13.7	1.6 ± 0.5	5.7 ± 2.2	4.13 ± 0.56	20.4 ± 20.6	17.7 ± 24.6
	100-150	52.9 ± 14.3	6.6 ± 0.4	12.1 ± 12.6	0.3 ± 0.1	3.2 ± 1.3	1.79 ± 0.54	7.2 ± 12.0	3.7 ± 6.2

2.5 Discussion

Our study demonstrates that stem CH_4 emissions in Amazonian floodplain forests are more strongly regulated by site characteristics (white-water vs black-water), than species identity (*E. coriacea vs. H. spruceana*). In the high-emitting white-water site, we found that shallow soil biogeochemical properties were the best predictor of stem flux magnitude at 30 cm height.

2.5.1 Site-level biogeochemistry as the dominant control

As hypothesised, stem CH_4 fluxes were substantially higher in our várzea site than our igapó site, irrespective of species or stem height (Figure 2.2), consistent with basin-scale assessments that white-water floodplains emit more CH_4 than black-water systems (Gauci et al., 2022; Pangala et al., 2017). Várzea porewaters had higher EC, near-neutral pH, lower DO, and higher dissolved CH_4, conditions favourable for methanogenesis (Bridgham et al., 2013; Conrad, 2007; Segers, 1998). By contrast, igapó porewaters were acidic, less conductive, and more oxygenated, conditions that constrain methanogenesis and favour CH_4 oxidation (Laanbroek, 2010; Teh et al., 2005; Table 2.2). Independent observations from Amazon floodplain lakes likewise report higher CH_4 production and greater diffusive and ebullitive fluxes in chemically reduced, higher-conductivity white-water settings than in acidic, more oxygenated black-water environments (Barbosa et al., 2016, 2021; Engle & Melack, 2000), reinforcing our inference that site-level geochemistry governs emission strength. While hydrology governs seasonality (Gauci et al., 2022; Jeffrey et al., 2023), our single-season comparison indicates that, within a stable flood phase, spatial heterogeneity in soil chemistry exerts significant control on stem-flux variability.

Across both forests, the co-occurrence of high MPP, dissolved CH_4 and fine-root biomass in the shallow 0-50 cm layer (Table 2.2) is consistent with an active near-surface zone where root activity, oxygen drawdown, and fresh carbon inputs promote methanogenesis, creating a shallow CH_4 pool - patterns widely observed in rice paddies and wetlands (Aulakh et al., 2001; Le Mer & Roger, 2001; Liu et al., 2012; Määttä & Malhotra, 2024; Segers, 1998).

In várzea, basal stem emission was strongly related to near-surface porewater chemistry and MPP, rather than to bulk carbon supply: pH, EC, and MPP at 0-50 cm were significant predictors, whereas DOC was not (Table S2.2). Fine roots at 0-50 cm were positively associated with basal emission, and coarse roots were not. By contrast, in igapó, relationships between basal emission and below-ground variables were weak or absent, and species-level associations were similarly non-significant (Table S2.2). Despite relatively high DOC, acidic and more oxygenated conditions likely constrained methanogenesis and muted any root-linked enhancement of supply, echoing findings from Amazon black-water systems and Southeast Asian peat swamps, where DOC-rich conditions nonetheless exhibit low CH_4 production (Gauci et al., 2022; Pangala et al., 2013, 2017).

Our measurements of MPP and dissolved CH_4 integrate the net outcome of several below-ground processes that we did not quantify but are known to regulate methanogenesis and CH_4 availability in wetlands. Variation in litter inputs and quality, carbon-to-nitrogen (C/N) ratios, and nutrient status (e.g., availability of alternative electron acceptors such as nitrate, ferric iron, and sulfate) can stimulate or suppress methanogenesis by altering substrate supply and redox constraints, as well as by shifting competition among microbial communities (Bridgham et al., 2013; Conrad, 2007; Le Mer & Roger, 2001). The strong correlation we found between basal stem emission (30-60 cm) and MPP and dissolved CH_4 in the 0-50 cm layer in várzea indicates that these unmeasured processes likely acted through their effects on shallow methanogenesis, but explicitly quantifying litter inputs/quality, C/N, and nutrient/redox chemistry may help explain residual within-site variability.

2.5.2 Species identity as a secondary driver

Tree species identity exerted only a secondary influence on stem CH_4 fluxes relative to site-level biogeochemistry. Contrary to expectations based on wood density, *E. coriacea* (high density, 0.6-0.9 g cm^{-3}; Table S2.3) consistently emitted more CH_4 than *H. spruceana* (low density, 0.23-0.7 g cm^{-3}; Table S2.3), especially in várzea. Fluxes ranged from 0.007-35.5 mg CH_4 m^{-2} hr^{-1} in *E. coriacea*, nearly fourfold higher at maximum than *H. spruceana* (0.04-9.15 mg CH_4 m^{-2} hr^{-1}). Yet across both species, site-level differences overshadowed species identity, with emissions consistently higher in várzea than igapó. Our results showed strong effects of site and height, but not species;

after accounting for site and height, species explained little additional variance, consistent with earlier work indicating that traits modulate rather than control stem CH_4 emissions (Barba, Bradford, et al., 2019; Covey & Megonigal, 2019; Pitz et al., 2018; Warner et al., 2017). Other stem and /bark traits, including porosity and permeability, sapwood moisture, parenchyma fraction, lenticel abundance, and bark and /stem methanotrophy, likely govern gas conductance and in-stem transformations and may interact with site biogeochemistry to shape emissions (Covey & Megonigal, 2019; Epron et al., 2023; Jeffrey, Maher, Chiri, et al., 2021; Moisan et al., 2024; Pangala et al., 2015; Soosaar et al., 2022).

2.5.3 Vertical flux gradients and transport mechanisms

Stem CH_4 fluxes declined significantly with stem height (30 cm > 70 cm; Figure 2.2). Similar decreases with height are widely reported across tropical, temperate and boreal forests and are consistent with predominantly diffusive transport from a soil source, with strongest gradients at the stem base (Gauci et al., 2022; Jeffrey, Maher, Tait, et al., 2021; Machacova et al., 2023; Pangala et al., 2017; Pitz & Megonigal, 2017; Rusch & Rennenberg, 1998; Sjögersten et al., 2020). The magnitude of this gradient is scaled with subsurface CH_4 supply: in the várzea, dissolved CH_4 at 0-50 cm and MPP at 30 cm were higher than in the igapó and within the várzea *E. coriacea* tended to have higher dissolved CH_4 and MPP than *H. spruceana* (Table S2.3), mirroring its higher basal flux and steeper attenuation. Although these species differences in pools were not statistically significant, they are directionally consistent with diffusion from a larger near-surface reservoir. Fine roots were concentrated in the upper 0-50 cm and were more abundant in the várzea (with *E. coriacea* slightly higher), providing a plausible pathway for enhanced shallow methanogenesis and delivery. Superimposed on these supply-side effects, interspecific contrasts in attenuation likely reflect anatomical and internal cycling differences – permeability, vessel connectivity and moisture that govern axial conductance and basal degassing (Covey & Megonigal, 2019; Mochidome & Epron, 2024) and potential in-stem CH_4 production/oxidation (H. L. Li et al., 2020; Mochidome & Epron, 2024; Yip et al., 2019; Zhou et al., 2021). Our observations of wet, degraded heartwood in *E. coriacea* are consistent with (but do not prove) in-stem methanogenesis. Taken together, the conserved vertical declines indicate diffusion dominates transport, absolute magnitudes scale with below-ground CH_4 supply (higher in the várzea), and

profile shape is modulated by species-specific anatomy with possible in-stem cycling (Li et al., 2020; Mochidome & Epron, 2024; Yip et al., 2019; Zhou et al., 2021).

2.5.4 Root-Soil Interactions and CH_4 Supply

Across both forest types, the upper 0-50 cm soil layer showed consistently elevated MPP, dissolved CH_4 and fine root biomass relative to deeper soils (50-100 cm and 100-150 cm; Table 2.2). This pattern indicates a shallow active zone for potential CH_4 supply (increased CH_4 production and availability), consistent with previous wetland studies showing that fresh carbon inputs, strong redox gradients and root activity concentrate methanogenesis in near-surface soils (Conrad, 2007; Segers, 1998; Silver et al., 1999).

Root biomass measurements preceded stem CH_4 flux measurements by approximately two years (2019 vs. 2022). Although absolute root biomass may vary between years due to turnover, the vertical distribution of roots in mature Amazon floodplain forests is largely structured by the annual flood pulse, which regulates oxygen availability and root development (Parolin et al., 2004; F. Wittmann et al., 2010). Root dynamics typically vary more across hydrological phases within a year than between years within the same season. As both root sampling and flux measurements were conducted during the flooded season, they represent comparable stages of the flood cycle. We therefore interpret the observed root distribution as representative of the relative rooting environment influencing methane supply, recognising that interannual turnover may affect absolute biomass but is unlikely to change the vertical pattern or its relationship with stem CH_4 emissions.

Within várzea, basal stem CH_4 flux was positively associated with fine-root biomass at 50 cm, whereas coarse roots showed no relationship - consistent with higher metabolic activity and surface area of fine roots and their control over rhizosphere processes including the role of fine roots in water uptake, CH_4 then being dissolved in that water that moves into the stem (Aulakh et al., 2001; Bridgham et al., 2013). These patterns support a shaollow, root-influenced source zone that supplies CH_4 for stem transport.

In várzea, the two species exhibited distinct associations with below-ground variables measured (Table S2.2): for E. coriacea, basal emissions were strongly correlated with EC and MPP, and showed a near-significant correlation with fine root biomass; for

H. spruceana, pH and EC were the dominant controls. In igapó, correlations between stem emissions and below-ground variables were weak or absent, consistent with acidic, more oxygenated porewaters limiting methanogenesis and reducing variation in CH_4 supply.

Our data collectively suggest a supply-then-transport hypothesis: where shallow porewater chemistry favours methanogenesis (várzea), dense fine roots likely enhance CH_4 supply to stems, increasing mean emissions and tree-to-tree variance; where chemistry constrains methanogenesis (igapó), this root-stem coupling weakens, and emissions remain low. In this framework, species and wood traits act downstream of supply, modulating transport and in-stem processing once CH_4 is available, rather than determining supply itself (Covey & Megonigal, 2019; Moisan et al., 2024; Pangala et al., 2015; Soosaar et al., 2022; van Haren et al., 2021) For upscaling, shallow (0-50 cm) pH, EC, MPP and fine-root density are the most informative predictors; DOC or species identity alone will mischaracterise spatial patterns.

2.5.5 Intra- and Interspecific Variability

Pairing each tree's stem flux with its own below-ground profile allowed us to test variability both within sites and between co-occurring species. Despite the dominant role of site-level biogeochemistry, stem CH_4 fluxes varied by nearly two orders of magnitude among co-located trees in várzea (e.g. *E. coriacea* at 30 cm: 0.54-35.5 mg CH_4 m^{-2} hr^{-1}), whereas ranges in igapó were much narrower (e.g. *H. spruceana* at 30 cm: 0.16-1.43 mg CH_4 m^{-2} hr^{-1}) (Figure 2.2). This within site variability has been reported in other wetland forests (Cugler et al., 2024; Pangala et al., 2013) and in global syntheses (Barba, Bradford, et al., 2019), but our results show it is site-contingent: variance is amplified in nutrient-rich, near-neutral várzea and dampened in acidic, more oxygenated igapó, consistent with geochemical constraints on methanogenesis and oxidation (Li et al., 2020; Wang et al., 2021; Yip et al., 2019). For example, *H. spruceana* in várzea emitted 2.0–9.0 mg CH_4 m^{-2} hr^{-1} versus 0.16-1.43 mg CH_4 m^{-2} hr^{-1} in igapó (Figure 2.2). Thus, when porewater chemistry is conducive to CH_4 production, there is an increase in stem flux variability, but the cause of increased variability is unknown.

Stem CH_4 emissions declined significantly with stem height (30-60 cm > 70-100 cm; Figure 2.2). Similar decreases with height are widely reported across tropical, temperate and boreal forests and are consistent with predominantly diffusive transport from a soil source, with strongest gradients at the stem base (Gauci et al., 2022; Jeffrey,

Maher, Chiri, et al., 2021; Machacova et al., 2023; Pangala et al., 2017; Sjögersten et al., 2020). Vertical stem CH_4 emission patterns differed between species: emissions declined ~6-fold with height in *E. coriacea* but ~2-3-fold in *H. spruceana* across sites, suggesting species differences attributed to species traits that regulate gas conductance or /transport and degassing (Covey & Megonigal, 2019; Mochidome & Epron, 2024). Potential in-stem cycling (production and/or oxidation) may further reshape these vertical emissions (Epron et al., 2023; H. L. Li et al., 2020; Yip et al., 2019; Zhou et al., 2021). Our observations of wet, degraded heartwood in *E. coriacea* are consistent with this possibility, though confirmation would require further investigation.

Species also differed in their coupling to below-ground variables, consistent with stronger chemical constraints on methanogenesis. The below-ground variables explain only part of the observed variation, with interspecific and root-associated controls likely being context-dependent. It appears that once CH_4 is available in the near-surface, additional species-linked processes likely shape emissions (e.g., bark and /lenticel traits, wood permeability, bark methanotrophy, CH_4 production within tree stems; (Epron et al., 2023; Jeffrey, Maher, Chiri, et al., 2021; H. L. Li et al., 2020; Mochidome & Epron, 2024; Yip et al., 2019; Zhou et al., 2021).

2.6 Conclusions

Our findings demonstrate that stem CH_4 emissions from Amazonian floodplain forests are shaped primarily by site-level below-ground biogeochemistry rather than by tree species identity alone. In the várzea plot we studied, nutrient-rich, near-neutral soils with higher conductivity and dense shallow roots were associated with greater methanogenesis and stem fluxes, whereas the igapó plot, characterized by nutrient-poor, acidic, and more oxygenated soils, showed lower emissions. These differences suggest contrasting biogeochemical controls on CH_4 production between the two study sites. Tree traits such as wood density exerted secondary influences, modulating but not overriding the dominant role of soil chemistry.

These results suggest that Amazon-wide budgets and process models should incorporate geochemical context and root-soil interactions, alongside tree traits, to capture spatial variability in stem emissions. Scaling based solely on species composition or wood properties could misrepresent flux patterns. More broadly, the distinct behaviours of these two contrasting sites can be viewed as natural analogues of potential

future change. Shifts in flood regimes, soil chemistry, or hydrological balance, such as those projected under climate change, could alter these emission patterns, potentially transforming currently strong sources into weaker ones or vice versa (Flores et al., 2024; Gedney et al., 2024). Understanding such ecosystem-specific sensitivities will be critical for reducing uncertainty in Amazon climate feedbacks and for refining the representation of tropical wetlands in global CH_4 budgets.

2.7 Acknowledgements

This research was funded by a Royal Society Research Grant (RGF\R1\180042) awarded to SRP. HB was supported by a studentship associated with this grant. SRP acknowledges support from the Royal Society Dorothy Hodgkin research fellowship (DH160111) and Royal Society enhancement award (RGF\EA\180042). The authors would like to thank the Mamirauá Institute for Sustainable Development for support throughout the study. We thank M. Castro, J. Castro, A. Silva, J. Carvalho and E. Martins for all their fieldwork support and guidance.

2.8 Authorship contributions

SRP and HRB conceived the study. HRB was supervised by SRP, NPM and AMH. HRB coordinated logistics and led fieldwork with support from CG, JL, and RNS. RNS and SRP collected the 2019 and 2021 below-ground datasets; SRP and RNS also established plots and installed instrumentation. DE supervised and trained HRB in laboratory analyses of below-ground properties and supported subsequent data interpretation. DG and LPR facilitated site access and permissions. HRB, SRP, and NPM analysed data and wrote the manuscript; all authors contributed to revisions and approved the final version.

2.9 Supplementary Information

Table S3.1 | Below-ground parameters measured at three soil depths (0-50 cm, 50-100 cm, and 100-150 cm) during the wet season of 2019. The data is presented to document interannual variability relative to measurements reported for 2021 in the main text. Samples are presented separately by site (igapó and várzea) and by the tree species associated with the piezometer locations. Results are expressed as mean ± standard deviation (SD).

Plot type	Tree species	Soil depth (cm)	EC ± SD ($\mu S\ cm^{-1}$)	pH ± SD	DO ± SD ($mg\ l^{-1}$)
Igapó	*H. spruceana*	0-50	40.2 ± 6.4	4.9 ± 0.6	4.5 ± 1.1
		50-100	26.7 ± 6.6	4.4 ± 0.8	3.1 ± 0.3
		100-150	17 ± 4.6	4.2 ± 0.7	1.3 ± 0.6
	E. coriacea	0-50	38.4 ± 3.97	5.29 ± 1.01	4.93 ± 1.08
		50-100	24.9 ± 5.14	5.29 ± 1.07	2.78 ± 0.51
		100-150	12.6 ± 2.39	4.67 ± 1.42	1.08 ± 0.46
Várzea	*H. spruceana*	0-50	128 ± 33.1	7.04 ± 0.44	3.17 ± 1.43
		50-100	72.7 ± 11.5	6.61 ± 0.98	1.47 ± 0.38
		100-150	54.5 ± 9.26	5.78 ± 1.34	0.37 ± 0.21
	E. coriacea	0-50	114 ± 26.6	6.55 ± 0.49	3.5 ± 0.77
		50-100	77.5 ± 15.4	6.75 ± 0.44	1.6 ± 0.27
		100-150	57.2 ± 11.2	6.41 ± 0.22	0.39 ± 0.16

Table S2.2 | Results of linear models testing for interannual differences in below-ground physicochemical parameters. EC, DO, and pH were modelled as a function of sampling year, soil depth, and their interaction (Year × soil depth). F-statistics and associated p-values are shown for each fixed effect. EC was log-transformed prior to analysis to meet model assumptions. No significant effects of year or Year × soil depth interactions were detected for any parameter ($p > 0.05$).

RESPONSE VARIABLE	***EFFECT***	***DF***	***F VALUE***	***P VALUE***
EC (LOG)	Year	1	0.08	0.77
	Soil depth	2	19.90	<0.001
	Year × soil depth	2	0.01	0.99

DO	Year	1	0.78	0.38
	Soil depth	2	113.37	<0.01
	Year × soil depth	2	0.07	0.93
PH	Year	1	0.08	0.78
	Soil depth	2	1.92	0.15
	Year × soil depth	2	0.11	0.89

Table S2.1 | Pearson correlation coefficients (r) and corresponding p-values (p) between stem methane (CH_4) flux measured at two heights (30 cm and 70 cm) and below-ground variables measured at 0–50 cm soil depth across igapó and várzea floodplain forests. Statistically significant correlations are in bold ($p < 0.05$).

Site	*Variables measured at 0-50 cm soil depth*	*Correlation between 30 cm stem flux and below ground variables measured at 0-50 cm (r, p)*	*Correlation between 70 cm stem flux and below ground variables measured at 0-50 cm (r, p)*
Igapó	DOC (mg l^{-1})	-0.29, 0.416	0.08, 0.822
	Dissolved CH_4 (µmol l^{-1})	0.13, 0.729	-0.25, 0.485
	DO (mg l^{-1})	0.14, 0.693	-0.05, 0.888
	pH	0.38, 0.277	0.22, 0.539
	EC (µS cm^{-1})	0.49, 0.081	0.16, 0.666
	MPP (mmol CH_4 m^{-2} d^{-1})	0.52, 0.067	-0.13, 0.725
	course root (g m^{-3})	0.07, 0.857	-0.09, 0.804
	Fine root (g m^{-3})	0.26, 0.360	0.53, 0.118
Várzea	DOC (mg l^{-1})	0.07, 0.769	0.14, 0.557
	Dissolved CH_4 (µmol l^{-1})	0.44, 0.050	0.42, 0.062
	DO (mg l^{-1})	0.22, 0.347	0.35, 0.125
	pH	**0.60, 0.026**	0.42, 0.064
	EC (µS cm^{-1})	**0.57, 0.034**	0.39, 0.077

MPP (mmol CH_4 m^{-2} d^{-1})	**0.62, 0.021**	0.37, 0.070
course root (g m^{-3})	0.40, 0.081	0.32, 0.089
Fine root (g m^{-3})	**0.49, 0.048**	0.35, 0.082

Table S2.2 | Pearson correlation coefficients (r) and associated p-values (p) between stem CH_4 flux measured at two heights (30 cm and 70 cm) and below-ground variables measured at 0–50 cm soil depth. Data are presented separately for two Amazonian floodplain forest types (igapó and várzea) and for two tree species, *H. spruceana* and *E. coriacea*. Statistically significant correlations ($p < 0.05$) are shown in bold.

Tree species	*Site*	*Measurement height for stem CH_4 flux*	*Below-Ground Variable (0–50 cm soil depth)*	*Correlation coefficient (r)*	*p value*
E. coriacea	Igapó	30 cm	DOC (mg l^{-1})	-0.28	0.603
			Dissolved CH_4 (µmol l^{-1})	0.05	0.901
			DO (mg l^{-1})	0.21	0.702
			pH	0.47	0.27
			EC (µS cm^{-1})	0.43	0.31
			MPP (mmol CH_4 m^{-2} d^{-1})	0.37	0.384
			Coarse root (g m^{-3})	0.33	0.442
			Fine root (g m^{-3})	0.17	0.756
		70 cm	DOC (mg l^{-1})	-0.08	0.865
			Dissolved CH_4 (µmol l^{-1})	-0.14	0.763
			DO (mg l^{-1})	-0.26	0.634
			pH	0.25	0.654
			EC (µS cm^{-1})	0.17	0.758
			MPP (mmol CH_4 m^{-2} d^{-1})	-0.02	0.969
			Coarse root (g m^{-3})	0.19	0.726
			Fine root (g m^{-3})	0.37	0.386
	Várzea	30 cm	DOC (mg l^{-1})	0.26	0.586

			Dissolved CH_4 (µmol l^{-1})	0.39	0.406
			DO (mg l^{-1})	0.38	0.408
			pH	0.42	0.352
			EC (µS cm^{-1})	**0.7**	**0.043**
			MPP (mmol CH_4 m^{-2} d^{-1})	**0.68**	**0.048**
			Coarse root (g m^{-3})	0.45	0.317
			Fine root (g m^{-3})	0.56	0.061
		70 cm	DOC (mg l^{-1})	0.33	0.489
			Dissolved CH_4 (µmol l^{-1})	0.42	0.354
			DO (mg l^{-1})	0.41	0.364
			pH	0.5	0.253
			EC (µS cm^{-1})	0.51	0.242
			MPP (mmol CH_4 m^{-2} d^{-1})	0.47	0.296
			Coarse root (g m^{-3})	0.48	0.28
			Fine root (g m^{-3})	0.51	0.246
H. spruceana	Igapó	30 cm	DOC (mg l^{-1})	-0.12	0.739
			Dissolved CH_4 (µmol l^{-1})	0.1	0.798
			DO (mg l^{-1})	0.05	0.9
			pH	0.15	0.672
			EC (µS cm^{-1})	0.13	0.71
			MPP (mmol CH_4 m^{-2} d^{-1})	0.07	0.849
			Coarse root (g m^{-3})	0.03	0.934
			Fine root (g m^{-3})	0.33	0.413
		70 cm	DOC (mg l^{-1})	-0.21	0.552
			Dissolved CH_4 (µmol l^{-1})	-0.31	0.397
			DO (mg l^{-1})	-0.42	0.223
			pH	-0.01	0.983
			EC (µS cm^{-1})	0.08	0.849

Várzea	30 cm	MPP (mmol CH_4 m^{-2} d^{-1})	-0.27	0.469
		Coarse root (g m^{-3})	-0.02	0.95
		Fine root (g m^{-3})	0.17	0.658
		DOC (mg l^{-1})	0.09	0.814
		Dissolved CH_4 (µmol l^{-1})	0.49	0.178
		DO (mg l^{-1})	0.03	0.926
		pH	**0.72**	**0.011**
		EC (µS cm^{-1})	**0.62**	**0.031**
	70 cm	MPP (mmol CH_4 m^{-2} d^{-1})	0.41	0.18
		Coarse root (g m^{-3})	0.33	0.241
		Fine root (g m^{-3})	0.12	0.714
		DOC (mg l^{-1})	0.34	0.318
		Dissolved CH_4 (µmol l^{-1})	0.38	0.257
		DO (mg l^{-1})	0.07	0.856
		pH	0.43	0.194
		EC (µS cm^{-1})	0.32	0.347
		MPP (mmol CH_4 m^{-2} d^{-1})	0.36	0.286
		Coarse root (g m^{-3})	0.36	0.278
		Fine root (g m^{-3})	0.13	0.698

Table S2.4 | Tree-level stem CH_4 fluxes (wet season, lower stem: 30–60 cm above the water surface), wood density, and diameter at breast height (DBH) by plot. Species codes: B = *Hevea spruceana*, M = *Eschweilera coriacea*; the numeric suffix is the tree tag. Wood density (g cm^{-3}) and DBH (cm) were measured 1 m above the flood line. Stem CH_4 fluxes are expressed per unit emitting surface area (mg CH_4 m^{-2} h^{-1}). "–" denotes data not available.

Plot type	*Tree ID*	*Wet season flux (mg CH_4 m^{-2} hr^{-1})*	*Wood density (g cm^{-3})*	*DBH (cm)*
Várzea	B1	9	0.23	39.1

	B2	5.83	0.31	38.1
	B3	3.17	0.48	24.2
	B4	3.55	0.35	47.2
	B5	2	0.36	43.0
	M6	3.42	0.7	20.1
	M7	0.54	0.72	21.9
	M8	4.75	-	22.9
	M9	22.2	0.64	33.8
	M17	35.5	-	-
Igapó	B10	0.62	0.7	20.2
	B11	1.34	0.63	22.0
	B12	1.03	0.61	31.4
	B13	1.43	0.47	25.9
	B18	0.16	-	52.6
	M15	0.81	0.78	50
	M16	1.81	0.82	28.3
	M19	9.74	-	42.2
	M20	3.19	-	-
	M14	0.15	0.87	31.9

Chapter 3 - Variable Stem Methane Oxidation Shapes Tree Emissions Across Amazonian Ecosystems

In prep for New Phytologist

Holly Blincow[1*], Niall McNamara[2], Alison Hoyt[3], Clarice Perryman[3], Carla Gomez[1], Dafydd Elias[2], Jack Lamb[3], Darlene Gris [5], Cristina Ariza Carricondo[6], Leonardo Pequeno Reis[5,7], Sunitha Rao Pangala[1,4*]

[1]Lancaster Environment Centre, Lancaster University, Bailrigg, Lancaster, UK

[2]UK Centre for Ecology & Hydrology, Lancaster Environment Centre, Lancaster, UK

[3]Department of Earth System Science, Stanford University, Stanford, CA, USA

[4]Department of Life Sciences, Imperial College London, Silwood Park Campus, Ascot, Berkshire, UK

[5]Mamirauá Institute for Sustainable Development, Amazonas, Brazil

[6]University of Antwerp, Antwerp, Belgium

[7] Universidade Federal Rural da Amazônia, Belém, Para, Brazil

*Corresponding authors: h.r.blincow@bham.ac.uk; s.pangala@imperial.ac.uk

Orchid ID: HRB:0009-0009-1866-1089; SRP:0000-0002-0650-7721

3.1 Abstract

- Methane (CH_4) is the second most important greenhouse gas (GHG), with natural wetlands representing the largest biogenic source. In Amazonian floodplain forests, trees act as significant conduits for CH_4 emissions.
- Stem CH_4 emissions typically decline with increasing stem height in wetland systems, a trend often attributed to diffusion. However, emerging evidence suggests oxidation plays a role in reducing stem emissions in subtropical forests. The extent to which oxidation regulates stem-emitted CH_4 in Amazon floodplain forests is unknown.
- We combined stem CH_4 flux measurements with natural abundance dual isotope analysis ($\delta^{13}C$ and $\delta^{2}H$), across two tree species in three floodplain

ecosystems (high várzea, low várzea and igapó), during the wet season to investigate the role of CH_4 oxidation on vertical emission dynamics.

- We observed declining CH_4 fluxes accompanied by isotopic enrichment (heavier $\delta^{13}C$ and $\delta^{2}H$) at increasing stem heights, indicating 20 ± 25% of CH_4 is oxidised in tree stems. However, oxidation varied across all trees, with high variability observed in low wood density species across floodplain ecosystems.
- Fine-scale chamber flux and $\delta^{13}C$ measurements at 15 cm vertical intervals revealed departures from the general decline in stem CH_4 with height: in some segments, flux increased with stem height, while $\delta^{13}C$-CH_4 became more depleted, consistent with in-stem production rather than oxidation alone. These patterns were largely obscured in typical sampling intervals, likely due to oxidation co-occuring in stems.
- Together, these findings suggest that both oxidation and in-stem production of CH_4 co-occur in Amazonian floodplain trees, varying across species and ecosystems, underscoring the need for further research into CH_4 production and consumption processes in tropical wetlands.

3.2 Introduction

Methane (CH_4) is the second most important anthropogenic greenhouse gas after CO_2, accounting for ~26% of the total anthropogenic radiative forcing since 1750 (Etminan et al., 2016; Lan et al., 2025), with emissions projected to rise substantially by 2100 (Z. Zhang et al., 2017). Natural wetlands are the largest biogenic CH_4 source (~26% of global emissions; Saunois et al., 2025) and tropical floodplain trees alone contribute 5-10% of wetland fluxes via their stems (Pangala et al., 2013, 2017), making our understanding of them critical for future climate predictions. For flooded systems, tree stems are understood to act primarily as passive conduits for soil-derived CH_4, transported upwards through roots and stem tissues (Barba, Poyatos, et al., 2019; Covey & Megonigal, 2019; Pitz & Megonigal, 2017; Plain & Epron, 2021; Sjögersten et al., 2020; Terazawa et al., 2007). Under this model, the high wet-season CH_4 concentrations reported in Amazonian flooded forests (Gauci et al., 2022; Pangala et al., 2017; van Haren et al., 2021) would be

expected to reach the atmosphere largely unattenuated. However, recent evidence suggests that CH_4 oxidation in tree stems has a significant influence on stem CH_4 emissions. In subtropical forests ~30-35% of CH_4 transported from soils into tree stems is oxidised within stems (Jeffrey, Maher, Tait, et al., 2021). Furthermore, stem CH_4 fluxes consistently decline with height, a pattern that is too steep to be explained by passive venting alone (Covey & Megonigal, 2019; Gauci et al., 2024). Despite mounting evidence of methanotrophy in woody tissues (Gauci et al., 2024; Jeffrey, Maher, Chiri, et al., 2021) and in standing deadwood (Martinez et al., 2022), no study has yet quantified CH_4 oxidation in trees in the flooded forests of the Amazon – the ecosystems where stem emissions are largest.

Stable isotope analysis provides a powerful tool to understand patterns of CH_4 oxidation in the environment. The stable carbon isotope composition of CH_4 ($\delta^{13}C\text{-}CH_4$) is highly sensitive to CH_4 oxidation because methanotrophs preferentially consume $^{12}CH_4$, enriching the residual CH_4 in ^{13}C. As such, vertical $\delta^{13}C$ gradients in tree stems could be used to understand when and where oxidation occurs (Jeffrey, Maher, Tait, et al., 2021; Liptay et al., 1998). Although $\delta^{13}C\text{-}CH_4$ has been sampled in Amazonian trees (Gauci et al., 2024; Pangala et al., 2017), the lack of measurements taken at multiple stem heights limits the ability to quantify in-stem oxidation with confidence. However, the presence of in-stem CH_4 production (Epron et al., 2023; Wang et al., 2016) can complicate our ability to interpret $\delta^{13}C\text{-}CH_4$ as changes in the methanogenic pathway between the soil and stem/within stems also influence $\delta^{13}C\text{-}CH_4$ (Whiticar et al., 1986). Often, use of a second isotopic constrain can help distinguish between shifts in $\delta^{13}C\text{-}CH_4$ due to oxidation vs. those due to changes in methane production. For example, CH_4 oxidation also influences the stable hydrogen isotopic composition of CH_4 ($\delta^{2}H\text{-}CH_4$) as oxidation leaves residual CH_4 enriched in ^{2}H (Figure 3.1), where a shift to larger $\delta^{13}C\text{-}CH_4$ and $\delta^{2}H\text{-}CH_4$ values clearly indicates the influence of CH_4 oxidation instead of a shift in production pathways.

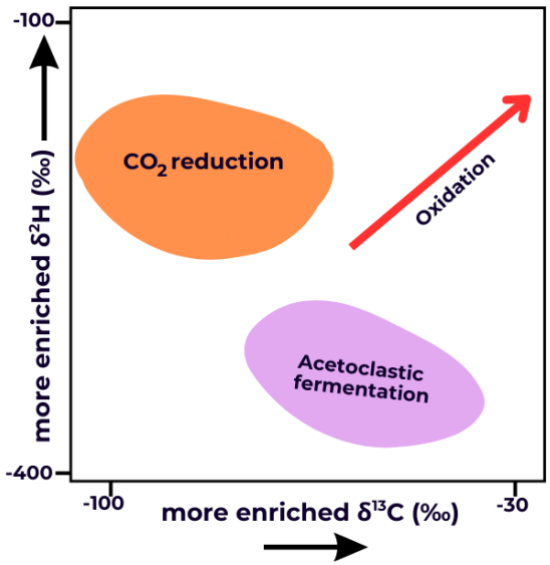

Figure 3.1 | Isotopic composition of $\delta^{13}C$ and $\delta^{2}H$ signalling CH_4 production and consumption pathways (adapted from Whiticar, 1999).

Dual-isotope analysis has already demonstrated in-stem oxidation in deadwood and snags (Martinez et al., 2022). This approach could be particularly powerful in flooded forests, where steep flux declines with height could reflect either microbial oxidation or cumulative diffusive loss. By measuring both isotopes across vertical gradients, we can partition these mechanisms more robustly and determine the extent to which oxidation mitigates Amazonian stem emissions. Together, analysis of $\delta^{13}C$ and $\delta^{2}H$ allow for characterization of the source of stem CH_4 emissions (soil vs in-stem production) and for assessment of CH_4 oxidation in tree stems.

Here, we apply a dual-isotope approach ($\delta^{13}C$-CH_4 and $\delta^{2}H$-CH_4) to tree stems and soils in Amazonian floodplain forests to: (i) test whether soil CH_4 is the dominant source of stem emissions; (ii) quantify the degree of in-stem CH_4 oxidation across species and floodplains and (iii) assess whether oxidation varies across floodplain types and seasons in proportion to CH_4 availability. By combining flux, isotopic, and vertical gradient analyses across várzea and igapó forests, this study will provide new insights into CH_4 cycling in tropical wetland forests and refine our understanding of the processes that regulate methane emissions at the ecosystem scale.

3.3 Methods

3.3.1 Study site

The study was conducted in the central Amazonian floodplain of Brazil, approximately 500 km west of Manaus, within two sustainable development reserves: Mamirauá Sustainable Development Reserve (MSDR) and Amanã Sustainable Development Reserve (ASDR) (Figure 3.2). The first plot, an igapó forest, was located in ASDR, at the South of Amanã lake (S2° 38.598', W 64° 39.980"). This catchment is influenced by three rivers: the Solimões, Japurá and Negro River, with the Japurá dominating the south of Amanã Lake in the dry season and the Negro River dominating in the flooded season. When samples were collected in flooded conditions, the flood level was ~1.5 m. The second and third plots were in the MSDR, a várzea forest bounded by the Solimões, Japurá, and Auati Paraná Rivers. A high várzea plot was located close to the Japurá river (S 2°48.916′, W 65°05.192′) along a smaller river channel, with an average flood level of 2-3 m, lasting approximately 3 months. The low várzea plot was located along the same section of the floodplain channel (S 2°49′56.20″, W 65°00′14.35″) approximately 10 km downstream of high várzea, and like the high várzea plot, receives floodwater from the whitewater rivers of the Solimões and Japurá. Unlike high várzea forests, these systems receive >50 days of flooding a year over 3 meters deep. This plot was established in the wake of the El Niño event of 2023 and 2024 which caused low flood levels throughout the Amazon floodplain. This meant the previously established plots of igapó and high várzea did not flood in 2024 and therefore sampling was moved to low várzea as its elevation to the riverbed meant this site still received flood water, even during a low flood season. The flood levels at each plot varied between sites and across sampling years (Table 3.1).

These plots were chosen to reflect the contrasting hydrology of the Amazon floodplain. At the time of sampling, the igapó forest was flooded by the Negro River, creating a blackwater site, meaning it is characterised by nutrient-poor water systems (Prance, 1979) with acidic waters ranging from 4.6-5.2 pH (Schmidt, 1972). In contrast, the high and low várzea plots were fed by whitewater rivers, known for their higher nutrient levels (Prance, 1979), lower oxygen concentrations (Junk & Piedade, 1997) and near neutral pH (F. Wittmann et al., 2022).

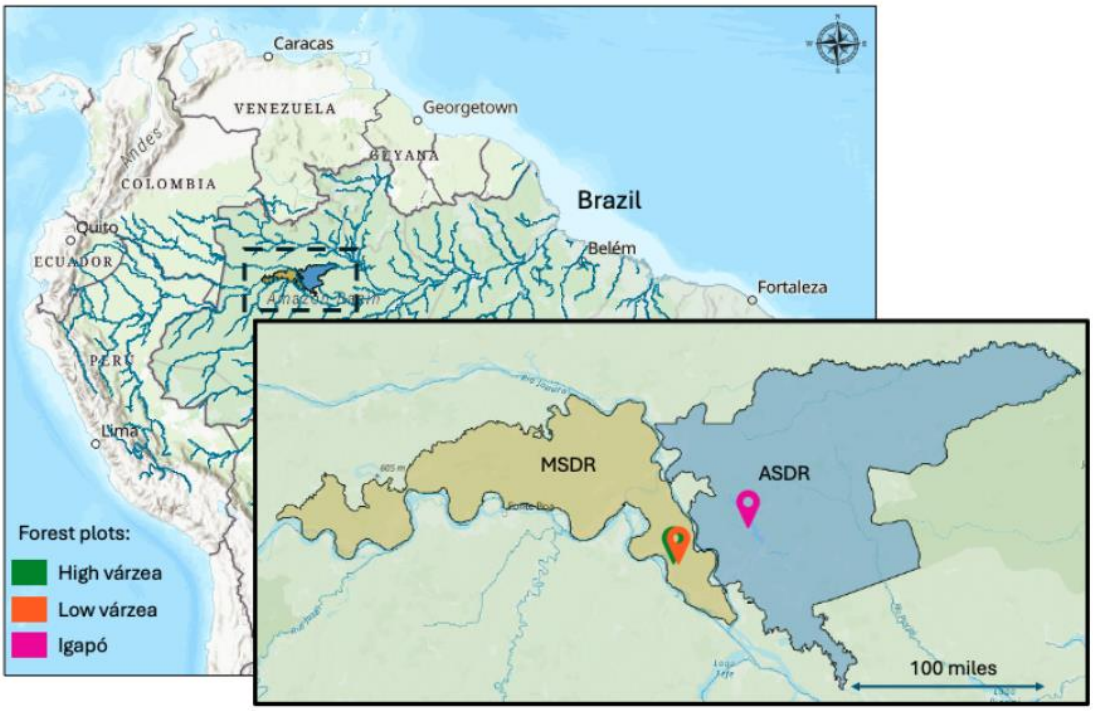

Figure 3.2 | Location of field sites across the Mamirauá Sustainable Development Reserve (MSDR) and Amaná Sustainable Development Reserve (ASDR). High várzea and low várzea plots are situated 5km apart.

3.3.2 Tree CH_4 Flux and Isotope Sampling

Tree stem CH_4 fluxes were measured during daylight hours in both the flooded (wet) and non-flooded (dry) seasons (Table 3.1). Two tree species were selected for this study based on their abundance across floodplain zones and contrasting wood densities: *Hevea spruceana* (Serengi Barriguda; 0.5 ± 0.2 g cm^{-3}) and *Eschweilera coriacea* (Matamata; 0.8 ± 0.08 g cm^{-3}). In igapó and high várzea plots, five trees per species were sampled during flooded and non-flooded conditions, and in the low várzea plot, 10 trees of each species were sampled during the flooded season. Diameter at breast height averaged 22.6 ± 3.8 cm, 35.2 ± 10.3 cm and 40 ± 11.7 cm in igapó, high and low várzea respectively for *H. spruceana* and 42 ± 7.9 cm, 26.3 ± 4.2 cm and 33.4 ± 11.7 cm in igapó, high and low várzea respectively for *E. coriacea*.

Stem CH_4 fluxes were measured at two stem heights (30-60 cm and 70-100 cm above the flood line in flooded season, or above the forest floor in the dry season) to assess how emissions vary with height. Measurements were conducted in both seasons at the igapó and high várzea plots. To capture finer-scale vertical variation, an additional series of stem CH_4 flux measurements was conducted at 15 cm intervals, five height

increments (starting 30 cm above the flood line) in the low várzea plot during the 2024 wet season, when El Niño-driven drought left the igapó and high várzea plots unflooded. This higher-resolution profile tested whether small chambers revealed sharper vertical gradients otherwise obscured when larger stem areas were enclosed.

Fluxes were measured using flexible static stem chambers following Pangala et al. (2017). Rectangular polycarbonate chambers of varying size to enclose 70% of the stem surface area with neoprene foams attached around the chamber edges were attached to the tree stems using ratchet straps. The chambers were connected to a microportable GHG analyser (ABB LGR GLA131-GGA) via PTFE tubing, and real-time CH_4 fluxes were derived from the linear change in chamber headspace concentration over time, converted to mass using the ideal gas law (accounting for temperature, pressure, and the molecular weight of CH_4), and normalised to chamber volume and the enclosed stem surface area, with CH_4 fluxes reported in mg CH_4 m^{-2} hr^{-1}.

For CH_4 isotope analysis ($\delta^{13}C$-CH_4 and $\delta^{2}H$-CH_4), gas samples were collected from the stem chambers just before the end of each 5-minute flux measurement, while the system remained as a closed-loop. A 30 ml gas sample was withdrawn into a syringe from the chamber outlet port and transferred into 12 ml double-wadded exetainer vials (Labco, UK). $\delta^{13}C$-CH_4 was analysed using a Picarro G2201-i cavity ring-down spectrometer with a custom-built autosampler, calibrated with isotopic reference gases (-23.9‰, -54.5‰, and -66.5‰; Isometric Instruments). $\delta^{2}H$-CH_4 was analysed at the UC Davis Stable Isotope Facility using a ThermoScientific Delta V Plus isotope ratio mass spectrometer (ThermoScientific, Bremen, Germany).

The fraction of CH_4 oxidised within the stem was calculated using the equation from Liptay et al. (1998):

$$F_{ox} = \frac{\left(\delta^{13}C_{70} - \delta^{13}C_{30}\right)}{((a_{ox} - 1) \times 100)}$$

where $\delta^{13}C_{70}$ and $\delta^{13}C_{30}$ represent isotope values at 70-100 cm and 30-60 cm heights respectively, and α_{ox} denotes the fractionation factor for CH_4 oxidation (1.028), calculated as the mean from 12 floodplain trees reported in (Jeffrey, Maher, Tait, et al., 2021).

Table 3.1 | Summary of field measurements conducted across forest plots. The table lists the type of analysis performed (flux measurements, stable isotope analysis), the corresponding flood height at the

time of sampling (in meters), and the sampling year and month for each plot. Data were collected during both wet and dry seasons across igapó, high várzea, and low várzea forest types to capture seasonal and hydrological variability.

Year	*Site*	*Flood water level*	*Analysis*
2022	igapó (blackwater)	150 cm	Stem fluxes, $\delta^{13}C\text{-}CH_4$ & $\delta^{2}H\text{-}CH_4$ isotopes at two heights (30-60 cm and 70-100 cm). Belowground CH_4 concentration and isotopes at depths of 5 cm and 30 cm
2023	high várzea (whitewater)	150 cm	Stem fluxes, $\delta^{13}C\text{-}CH_4$ & $\delta^{2}H\text{-}CH_4$ isotopes at two heights (30-60 cm and 70-100 cm). Belowground CH_4 concentration and isotopes at depths of 5 cm and 30 cm
2024	igapó (blackwater)	No flooding	Stem flux at two heights, $\delta^{13}C\text{-}CH_4$ & $\delta^{2}H\text{-}CH_4$ isotopes
2024	high várzea (whitewater)	No flooding	Stem flux at two heights, $\delta^{13}C\text{-}CH_4$ & $\delta^{2}H\text{-}CH_4$ isotopes
2024	low várzea (whitewater)	200 cm	Stem fluxes, $\delta^{13}C\text{-}CH_4$ & $\delta^{2}H\text{-}CH_4$ isotopes at two heights (30-60 cm and 70-100 cm). Fine scale CH_4 fluxes at 15 cm increments from 30 cm above floodline

3.3.3 Soil (Porewater) CH_4 and Isotope Sampling

Below-ground dissolved CH_4 concentrations and isotopic compositions ($\delta^{13}C\text{-}CH_4$ and $\delta^{2}H\text{-}CH_4$) were analysed from water samples extracted using cylindrical zero-

tension lysimeters (ZTLs) as described in Cristina et al. (2022). Each ZTL consisted of a rigid Nylon-12 cylinder (5 cm diameter, ~250 ml collection volume) capped with a fine mesh to allow gravitational drainage of soil water while excluding particulates and roots. Unlike piezometers, ZTLs do not apply suction but passively collect soil porewater under natural hydraulic gradients, making them particularly suitable for flooded forest soils. Flexible tubing connected to each lysimeter extended above the flood line, permitting long-term sample retrieval during high-water periods. ZTLs were installed in 2019 during the non-flooded season at 5, 30, 75, and 150 cm depths, with later sampling concentrated at 5 and 30 cm where root biomass was highest (see Chapter 1).

Water was extracted from the lysimeters using a peristaltic pump (0.06 L/min) into a 100 ml syringe. For equilibration, 60 ml of water sample was combined with 40 ml of atmospheric air to establish a defined headspace-to-water ratio. The syringe was shaken vigorously for 3 minutes, ensuring equilibration of dissolved gases between water and headspace, based on equilibration times reported in Garnett et al. (2016) and Chanton (2005). After settling, 30 ml of the gas phase was transferred to 12 ml exetainers (Labco, UK) for isotope analysis, and 10 ml to 3 ml vials for CH_4 concentration analysis via gas chromatography (GC; Clarus 480, Perkin Elmer).

Dissolved CH_4 concentrations were calculated from the headspace CH_4 mixing ratio using Henry's law, accounting for partitioning between water and gas phases and corrected for temperature at the time of equilibration using the neoDissGas package (Cawley et al., 2020). $\delta^{13}C$-CH_4 of the gas samples was analysed using a Picarro G2201-i cavity ring-down spectrometer, and $\delta^{2}H$-CH_4 was analysed at the UC Davis Stable Isotope Facility.

3.3.4 Statistical analysis

Linear models were used to investigate the influence of site, species and height (30-60 cm, 70-100 cm) on CH_4 flux and $\delta^{13}C$-CH_4. Separate models were used to test the relationships during the wet and dry season, as a smaller number of sites were sampled during the dry season. Site, species, $\delta^{13}C$-CH_4, height and an interaction between site and species were included in the global models for CH_4 flux. The global model for $\delta^{13}C$-CH_4 included site, species, CH_4 flux, height and an interaction between site and species.

To investigate the fine-scale influence of vertical height on CH_4 emissions and $\delta^{13}C\text{-}CH_4$, we constructed linear models testing the effects of height (15 cm intervals), tree species and an interaction between height and tree species on both CH_4 emissions and $\delta^{13}C\text{-}CH_4$. Additionally, CH_4 flux was included in the model for $\delta^{13}C\text{-}CH_4$ and $\delta^{13}C\text{-}CH_4$ was included in the model for CH_4 flux. Estimated marginal means were used for post-hoc comparisons, with Dunnett-adjusted contrasts applied to compare each stem height to the lowest chamber using the emmeans package (Lenth & Piaskowski, 2017).

To test the influence of porewater depth and site on dissolved CH_4, the global linear model included depth, site and the interaction between them. Dual-isotope patterns were explored descriptively by plotting $\delta^{13}C\text{-}CH_4$ against $\delta^{2}H\text{-}CH_4$ across stem heights to visualise coordinated isotopic shifts. Relationships between $\delta^{13}C\text{-}CH_4$ and $\delta^{2}H\text{-}CH_4$ were assessed using regression slopes, calculated using paired $\delta^{13}C\text{-}CH_4$ and $\delta^{2}H\text{-}CH_4$ measurements (*E. coriacea*, n = 10; *H. spruceana*, n = 15), grouped by species. Relationships between changes in CH_4 flux and corresponding shifts in $\delta^{13}C\text{-}CH_4$ across individual trees were assessed using Kendall's rank correlation coefficient (τ), selected due to non-normality and heteroscedasticity in change metrics.

All statistical analyses were performed in R Studio (Version 2024.09.0+375; R Core Team). Backwards step selection was used to identify the most parsimonious model in each instance. A significance level of $p < 0.05$ was applied throughout. Normality was assessed visually, and where sample sizes were <4, data were presented descriptively without formal statistical testing. Results are reported as means ± standard deviation unless otherwise stated.

3.4 Results

3.4.1 Flooded season

Stem CH_4 fluxes and $\delta^{13}C\text{-}CH_4$ at two heights

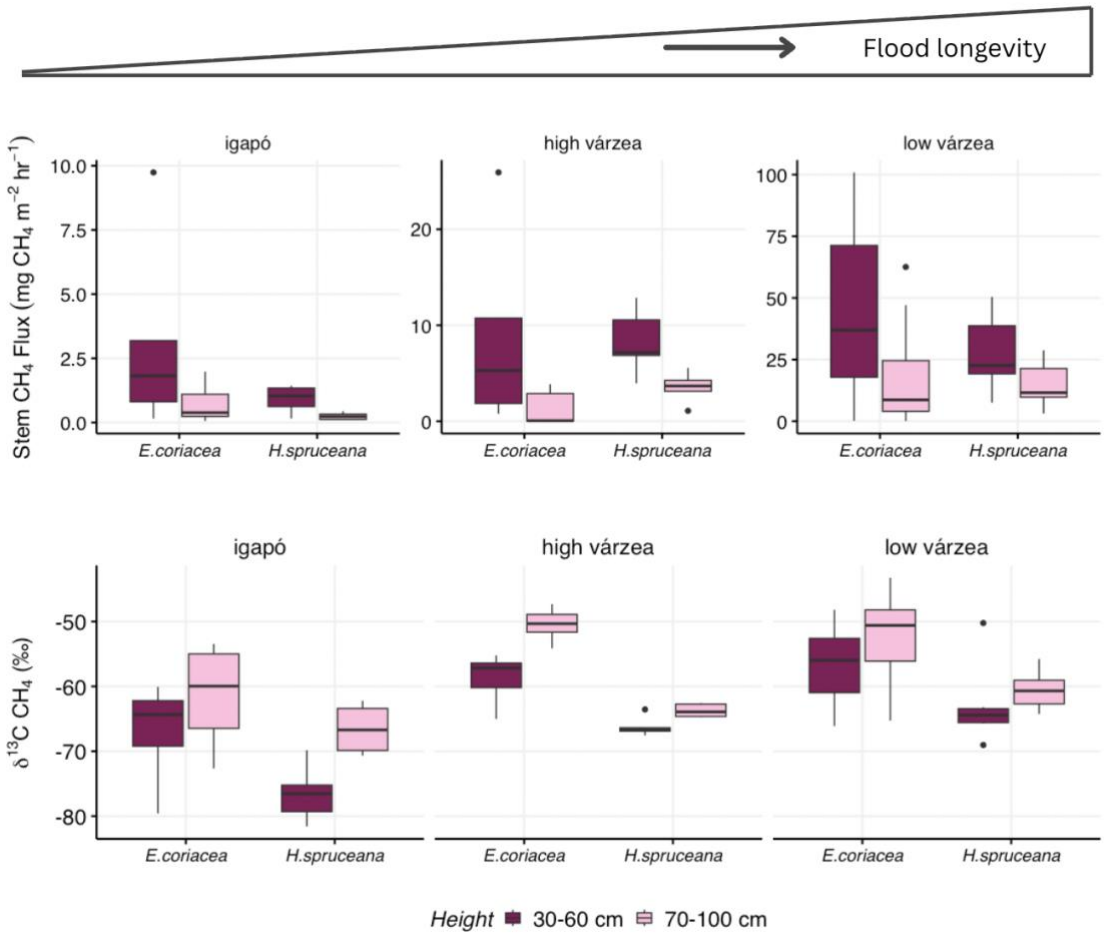

Figure 3.3 | Stem CH_4 fluxes (mg CH_4 m^{-2} hr^{-1}) and corresponding stem $\delta^{13}C$-CH_4 values measured during the flooded season at two stem heights (30-60 cm and 70-100 cm above the flood line) for two tree species (*E. coriacea* and *H. spruceana*) and across three plots. Sample sizes: high várzea (n = 5 trees per species), igapó (n = 5 trees per species), low várzea *(E. coriacea* n = 16; *H. spruceana* n = 9).

Stem CH_4 fluxes varied significantly between sites and declined with increasing stem height ($p < 0.001$ and $p < 0.01$, respectively). Across species, fluxes were highest in low várzea, intermediate in high várzea, and lowest in igapó (Figure 3.3). At the lower stem height (30 cm), mean fluxes ranged from 3.1-43.5 mg m^{-2} h^{-1} in *E. coriacea* and 0.9-28.1 mg m^{-2} h^{-1} in *H. spruceana*, with consistently higher emissions in low várzea for both species. Fluxes decreased between 30 and 70 cm across all sites, with the greatest proportional declines observed in igapó and high várzea.

$\delta^{13}C$-CH_4 values increased with stem height across forest types and species ($p < 0.05$), coinciding with declining CH_4 fluxes. Mean $\delta^{13}C$-CH_4 shifts between heights ranged from 5.6-8.3‰ in *E. coriacea* and 2.5-9.9‰ in *H. spruceana*, though the magnitude of isotopic enrichment did not differ significantly among sites. In a pooled linear model, stem CH_4

flux was significantly associated with site and height and showed a negative relationship with $\delta^{13}C\text{-}CH_4$ ($p < 0.05$), indicating lower fluxes at greater stem heights and more ^{13}C-enriched CH_4.

Comparisons between várzea forest types revealed that mean stem CH_4 fluxes were substantially higher in low várzea than high várzea, while $\delta^{13}C\text{-}CH_4$ values differed only modestly between the two plots. Species-level patterns were consistent across várzea types, with *E. coriacea* exhibiting higher fluxes and larger $\delta^{13}C\text{-}CH_4$ shifts than *H. spruceana*.

Across all individuals, the magnitude of CH_4 flux reduction between heights was positively correlated with the corresponding increase in $\delta^{13}C\text{-}CH_4$ (Kendall's $\tau = 0.31$, $p < 0.001$). Estimates of the fraction of CH_4 oxidised in tree stems varied widely among individuals and sites but showed no significant effects of species or forest type (all $p > 0.2$), reflecting high within-site variability (Table 3.2).

Table 3.2 | Mean (± SD) percentage decrease in CH_4 flux between two stem heights (H1 = 30-60 cm; H2 = 70-100 cm) and mean (± SD) isotopic shifts ($\delta^{13}C\text{-}CH_4$ and $\delta^{2}H\text{-}CH_4$) from H1 to H2 across two tree species and three floodplain types. Sample sizes (n) indicate the number of trees measured for each parameter.

		Mean ±SD decrease in flux between stem heights (%)	*Mean ± SD isotopic shift of $\delta^{13}C\text{-}CH_4$ from H1 to H2 (‰)*	*Mean ± SD isotopic shift of $\delta^{2}H\text{-}CH_4$ from H1 to H2 (‰)*	*F_{ox} (α)*
Igapó	*H.spruceana*	66.9 ± 19.8	9.9 ± 4.2 (n=5)	50.4 ± 33 (n = 2)	0.35 ± 0.15 (n = 5)
	E.coriacea	86.8 ± 4.85	5.6 ± 12.5 (n=4)	69.2 ± 53.1 (n = 3)	0.2 ± 0.45 (n = 4)
High várzea	*H.spruceana*	57.2± 14.5	2.5 ± 1.02 (n=5)	16 ± 11.2 (n = 3)	0.09 ± 0.04 (n=5)
	E.coriacea	90.5 ± 11.2	8.3 ± 5.4 (n=5)	65.4 ± 56 (n = 4)	0.3 ± 0.2 (n = 5)
Low várzea	*H.spruceana*	21.3 ± 13.1	2.7 ± 6.9	16.5 ± 21.7	0.1 ± 0.2

		(n=7)	(n = 6)	(n = 7)
E.coriacea	49.07 ± 11.3	6.5 ± 7.2 (n=10)	5.9 ± 28.8 (n=13)	0.17 ± 0.3 (n = 10)

Fine-scale stem fluxes and CH_4 isotope composition

Isotopic composition of stem-emitted CH_4 varied significantly with stem height and between species in low várzea ($p < 0.001$ for both effects; Figure 3.4). In *E. coriacea*, $\delta^{13}C$-CH_4 increased monotonically with height, from -61.35 ± 4.87 at 30-45 cm to progressively more enriched values of -50.68 ± 4.15 at 90–105 cm, with significant enrichment detected from 60-75 cm upwards relative to the basal chamber ($p \leq 0.01$). In contrast, $\delta^{13}C$-CH_4 in *H. spruceana* did not differ significantly among stem heights ($p > 0.05$) and showed no consistent directional trend along the stem. Vertical shifts in $\delta^{2}H$-CH_4 followed similar species-specific patterns, with enrichment with height in *E. coriacea* and greater variability but no systematic change in *H. spruceana* (Table S3.1).

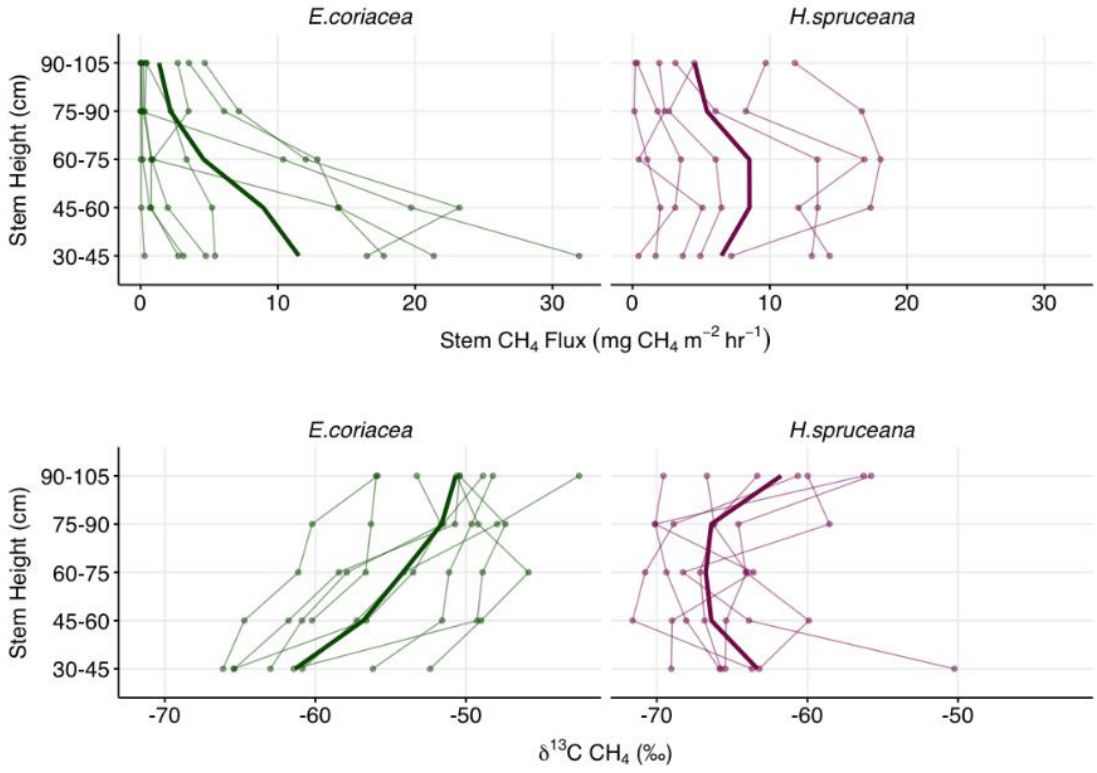

Figure 3.4 | CH_4 fluxes and corresponding stem $\delta^{13}C$-CH_4 values measured at fine-scale stem height increments (15 cm steps) beginning 30 cm above the flood line in the low várzea site. Individual trees (*H. spruceana*, n = 7; *E. coriacea*, n = 9) are shown as thin lines, with species means shown as bold lines.

Dual isotope patterns

Both δ^{13}C-CH_4 and δ^{2}H-CH_4 values increased between 30-70 cm and 70-100 cm, with more enriched values observed at 70-100 cm compared to 30-70 cm (Figure 3.5). Comparing δ^{13}C-CH_4 and δ^{2}H-CH_4 revealed a slope of 5.4 ± 12.4 (n = 10) for *E. coriacea* and 5.5 ± 8.3 (n = 15) for *H. spruceana*, indicating broadly similar isotope trajectories despite substantial variability.

Univariate models showed that δ^{13}C-CH_4 varied significantly among species and sites ($p < 0.05$). The magnitude of that δ^{13}C-CH_4 enrichment differed between sites and species: in várzea, *E. coriacea* exhibited a larger vertical shift in that δ^{13}C-CH_4 than *H. spruceana*, whereas in igapó, *H. spruceana* showed a greater mean change (Table 3.2). Overall, *E. coriacea* displayed greater variability in isotopic shifts between successive stem heights.

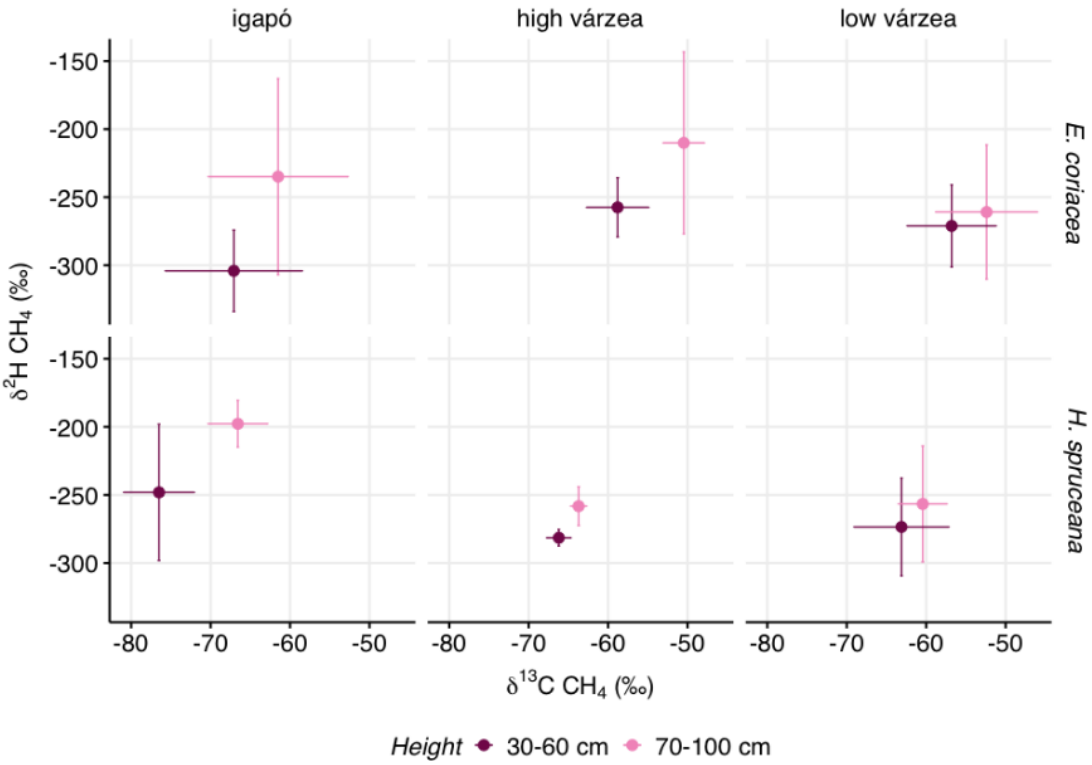

Figure 3.5 | Dual-isotope composition (δ^{13}C-CH_4 and δ^{2}H-CH_4) of CH_4 from tree stem chambers. Values represent mean ± SD for each species, grouped by site and stem height. Across all sites and species, isotopic enrichment increases with stem height. Sample sizes: *E. coriacea* and *H. spruceana* in

igapó and high várzea (n = 5 each), *E. coriacea* in low várzea (n = 16), and *H. spruceana* in low várzea (n = 9).

Below-ground CH_4 concentrations and isotope composition

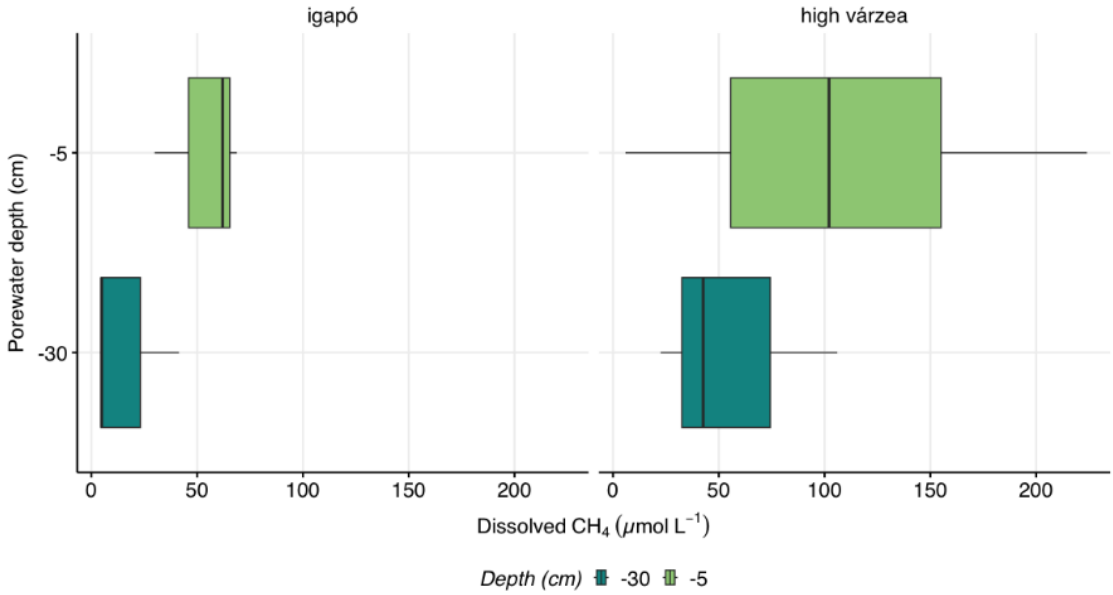

Figure 3.6 | Dissolved CH_4 concentrations (mean ± SD) from porewater sampled at depths of 5 cm (igapó n = 3, high várzea n = 4) and 30 cm (igapó n = 3, high várzea n = 3), determined by headspace equilibrium of porewater.

In the wet season, dissolved CH_4 concentrations were greater in high várzea compared to igapó at 5 cm depth (109 ± 92.6 µmol L^{-1} and 53.6 ± 20.8 µmol L^{-1} respectively), but these differences were not significant (Figure 3.6). At 30 cm, concentrations dropped to 16.9 ± 21.3 µmol L^{-1} in igapó and 57 ± 43.6 µmol L^{-1} in high várzea, but no significant effect of depth was observed. Dissolved CH_4 concentrations overall were more variable in high várzea than in igapó.

At 5 cm and 30 cm depths, belowground $\delta^{13}C$-CH_4 in igapó was lower (-66.3 ± 7.7‰ and -72.1 ± 8.4‰ respectively) than in high várzea (-54.0 ± 4.1‰ at 5 cm and -66.3 ± 7.7‰ at 30 cm). Mean $\delta^{2}H$-CH_4 was similar across sites at both depths: -293 ± 53.7‰ at 5cm and -332 ± 15.3‰ at 30 cm in igapó and -293 ± 52‰ and -318 ± 8.1‰ at 5 cm and 30 cm depths in high várzea (Figure 3.7).

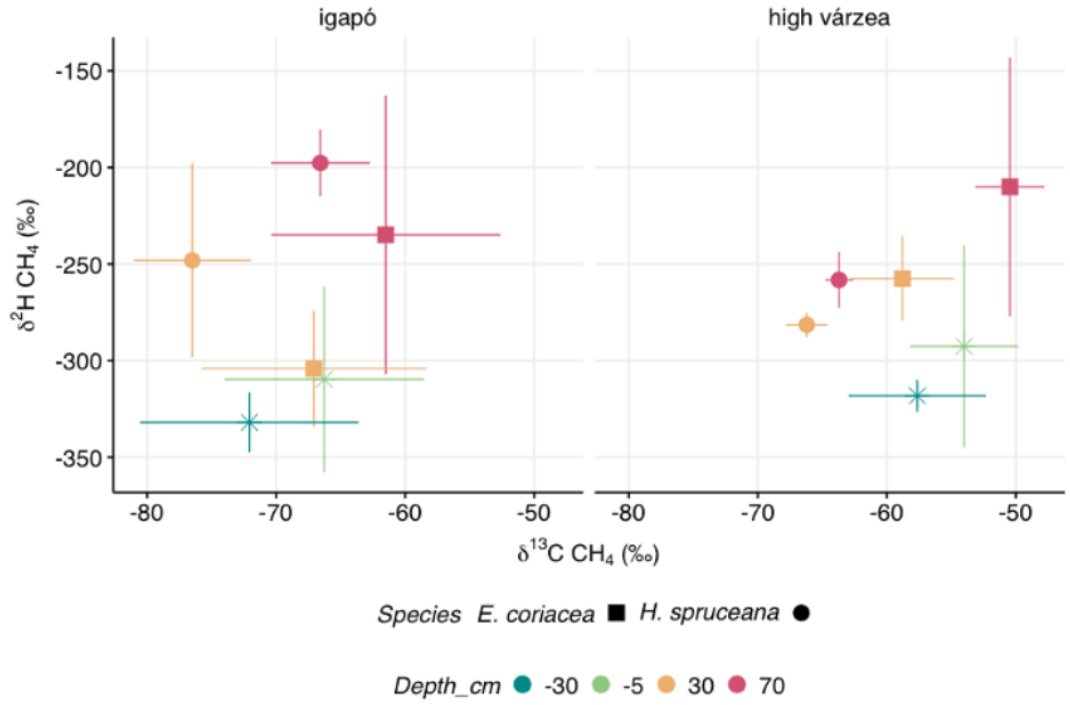

Figure 3.7 | Mean $\delta^{13}C$-CH_4 and $\delta^{2}H$-CH_4 values (± SD) of dissolved CH_4 from porewater (headspace equilibration at 5 cm and 30 cm depths) and CH_4 from stem chambers measured at 30-60 cm and 70-100 cm stem height. Sample were collected across both plots: 30 cm depth (igapó n = 3; high várzea n = 3) and 5 cm depth (igapó n = 2; high várzea n = 2). Samples were collected across the plots: 30 cm depth (igapó n = 3; high várzea n = 3) and 5 cm depth (igapó n = 2; high várzea n = 2).

3.4.2 Dry season

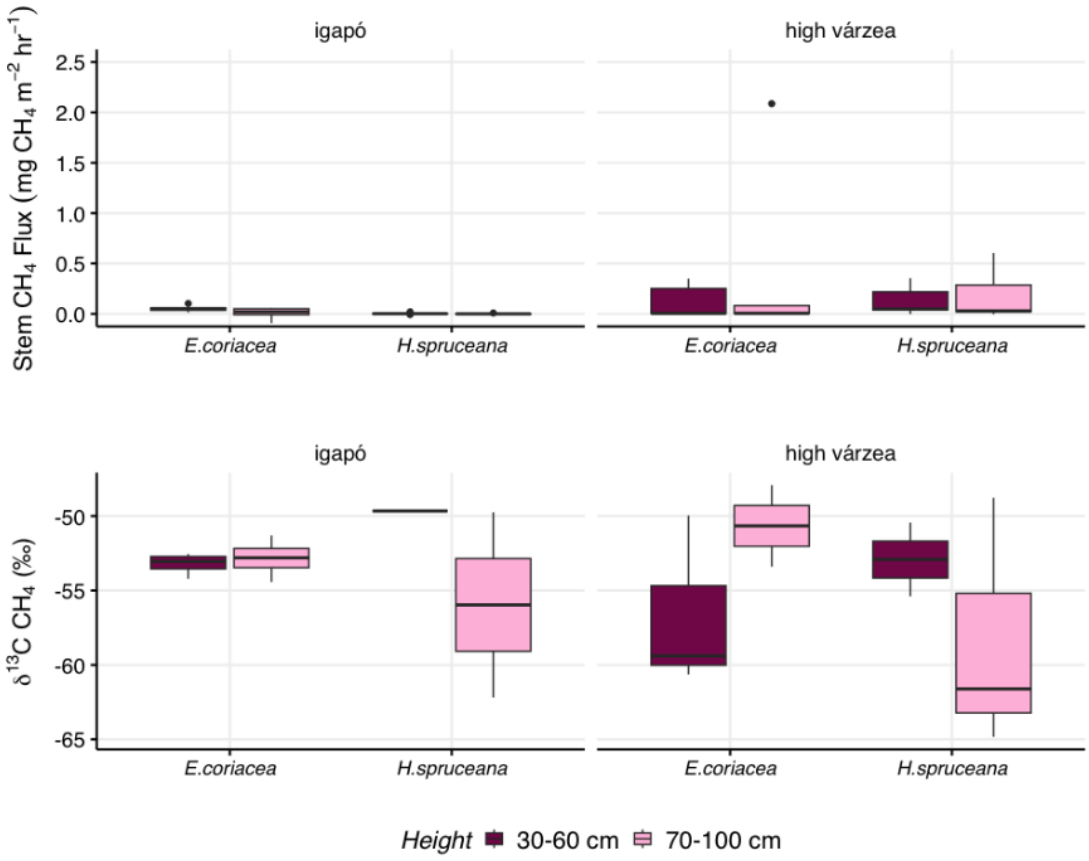

Figure 3.8 | Stem CH_4 fluxes (mg CH_4 m^{-2} hr^{-1}) and corresponding $\delta^{13}C$-CH_4 (‰) values measured during the dry season at two stem heights (30-60 cm and 70-100 cm above the soil surface) for *E. coriacea* and *H. spruceana* (n = 5 trees per species per plot) in igapó and high várzea plots.

During the dry season, CH_4 fluxes did not differ significantly by stem height or site in either species (Figure 3.8). No consistent relationship was observed between CH_4 flux and $\delta^{13}C$-CH_4. Isotopic signatures remained stable across heights and sites.

Across species and sites, CH_4 fluxes were generally higher in high várzea compared to igapó ($p < 0.05$). Within igapó, fluxes remained relatively stable up the stem for both species, although *E. coriacea* showed a slight decrease, while *H. spruceana* showed a small increase. In contrast, both species exhibited an average increase in emissions up the stem in high várzea. When comparing $\delta^{13}C$-CH_4 values with fluxes, there was no consistent pattern or statistically significant relationship. However, a general trend in isotopic shift was observed: For *H. spruceana*, $\delta^{13}C$-CH_4 values became slightly lower up the stem in high várzea (-2.2 ± 5.5‰) but remained relatively unchanged in igapó (-0.08‰). For *E. coriacea*, values became larger up the stem in high várzea (9.3 ± 2.9‰)

and were stable in igapó (0.3 ± 0.95‰). Sample sizes were small: 2 trees per species in high várzea and 1 (*H. spruceana)* and 5 (*E. coriacea*) trees in igapó. Despite trends, there were no significant differences in isotopic signature by species or site.

Seasonal Comparison

CH_4 fluxes in the dry season were, on average, 80 times lower than in the wet season across all plots and species. With a reduction in fluxes, $\delta^{13}C$-CH_4 values were larger during the dry season compared to the wet season ($p < 0.01$). For instance, in igapó, $\delta^{13}C$-CH_4 was -53.3 ± 3.4‰ during the dry season, compared to -68.3 ± 8.2‰ during the wet season. In high várzea, values were -55.2 ± 6.0‰ and -59.8 ± 6.6‰ for the dry and wet seasons, respectively. Similarly, $\delta^{2}H$-CH_4 values also increased from the wet to the dry season ($p < 0.01$). In igapó, $\delta^{2}H$-CH_4 was -130.7 ± 17.1‰ during the dry season and -250.9 ± 57.6‰ in the wet. In high várzea, a similar pattern occurred with values of -183.7 ± 49‰ in dry season and -248 ± 44.4‰ in the wet (SI Table 1).

3.5 Discussion

Our study demonstrates that CH_4 transported through stems of Amazonian floodplain trees undergoes partial oxidation during upward movement, reducing the amount emitted to the atmosphere. We observed patterns similar to those previously seen in subtropical wetland forests (Jeffrey, Maher, Tait, et al., 2021). This was evident during the flooded season, when stem CH_4 fluxes declined with increasing stem height (from 30-70 cm to 70-100 cm) and were accompanied by an increase in both $\delta^{13}C$-CH_4 and $\delta^{2}H$-CH_4 isotopic values (Figure 3.3). The positive correlation between $\delta^{13}C$-CH_4 and $\delta^{2}H$-CH_4, with species-level regression slopes of ~5.5, is consistent with isotopic shifts associated with microbial CH_4 oxidation (Coleman et al., 1981).

3.5.1 Variability in oxidation patterns

Compared with subtropical systems, CH_4 oxidation in Amazonian trees offset a smaller fraction of emissions and emitted substantially more CH_4 overall. Jeffrey, Maher, Tait, et al. (2021) reported that 16 to 69.2% of CH_4 was oxidised in tree stems of subtropical forests, whereas our estimates span 0 to 65%. Although the upper bounds are similar, 16% (n = 6 out of 36) of the trees we sampled showed no apparent isotopic change (i.e. lack of $\delta^{13}C$ enrichment), despite a decrease in CH_4 emissions up the stem. The

absence of $\delta^{13}C$ enrichment despite a decline in CH_4 concentrations up the stem suggests that CH_4 may be lost through non-fractionating physical pathways, such as diffusion or leakage via bark or lenticels, rather than via microbial oxidation. Alternatively, methanotrophic activity may be too low, absent, or inhibited due to limited oxygen availability, micronutrient constraints, or unfavourable stem microenvironments or simply may reflect the variability of methanotrophic communities in trees (Jeffrey, Maher, Tait, et al., 2021) or obscured isotopic signals from internal CH_4 production within stems (Epron et al., 2023; Vigano et al., 2009). Rapid CH_4 transport could also reduce residence time, limiting the extent of oxidation and associated isotopic fractionation. In some cases, internal CH_4 production within the stem may isotopically mask oxidation signals, although this would typically be accompanied by increased CH_4 concentrations. Notably, we observed signs of wood rot in some extracted wood cores, indicating the potential for in-stem CH_4 production via microbial decomposition processes in decayed xylem tissues.

Importantly, these patterns were not isolated to one species, indicating a broader ecosystem signal during the flooded season. During the dry season, patterns deviate from those observed in the wet season (Figure 3.8), which may reflect reduced CH_4 supply in soils (Gauci et al., 2022). Under these conditions, microbial communities may enter dormancy (Hanson & Hanson, 1996), or CH_4 oxidation may be dominated by low-affinity methanotrophs that are poorly adapted to trace CH_4 concentrations (Gauci et al., 2024).

When belowground CH_4 supply was high during the flooded season, evidence of CH_4 oxidation became more consistent across individuals and sites, with $\delta^{13}C$-CH_4 and $\delta^{2}H$-CH_4 values increasing up the stem across nearly all trees and no significant interspecific or site-level differences in the fraction oxidised. Nevertheless, substantial variability persisted likely reflecting microscale differences in stem environments. Wood porosity, oxygen availability, wood moisture content, and tree physiology are all known to influence methanotrophic communities and activity (Boddy & Rayner, 1983; Herbinger et al., 2005; Osunkoya et al., 2007; Sorz & Hietz, 2006; C. Wittmann & Pfanz, 2014), while variation in CH_4 transport pathways, such as diffusion versus advection, can influence isotopic enrichment by altering residence time (Baur et al., 2025; Li et al., 2025). In some cases, internal CH_4 production from decayed wood tissues may also isotopically mask oxidation signals (Vigano et al., 2009). These interacting factors likely explain the residual variation in $\delta^{13}C$ and $\delta^{2}H$ patterns, suggesting that anatomical and

microbial constraints can disrupt otherwise uniform oxidation patterns even under abundant substrate supply.

Oxidation patterns for *H. spruceana* vary significantly across floodplain ecosystems, averaging 35 ± 15% in igapó, 9 ± 3% in high várzea, and 10 ± 25% in low várzea (Table 3.2). This variability suggests that flood regimes may strongly influence oxidation. Igapó forests flood for shorter periods and at lower levels than both high and low várzea, which could drive distinct morphological adaptations across these habitats (Parolin et al., 2004). Such differences may alter stem porosity and, in turn, limit oxygen diffusion to methanotrophic communities, potentially explaining why large contrasts in oxidation are observed only in this species. This effect may be amplified by the comparatively lighter wood density of *H. spruceana* relative to *E. coriacea*, which can increase porosity (Jang & Kang, 2022) and thus sensitivity to environmental variation. *H. spruceana* also possesses lenticels, which can facilitate gas exchange and influence CH_4 diffusion (Pangala et al., 2013). Variation in lenticel density among ecosystems could therefore modify CH_4 residence times in stems and contribute to the observed patterns. Alternatively, differences in oxidation could highlight changes in internal CH_4 production across flooded environments which may obscure oxidation signals, further adding to the variability. Notably, these patterns are unique to *H. spruceana*; *E. coriacea*, measured across the same sites, shows no comparable variation in oxidation.

Contrasts between high and low várzea forests further underscore how hydrological regimes shape tree stem CH_4 fluxes and CH_4 oxidation capacity. The low várzea, which floods earlier and remains inundated longer, exhibited substantially higher fluxes than the high várzea, consistent with prolonged anoxia promoting methanogenesis (Rulík et al., 2023). However, the decline in CH_4 flux with stem height was less pronounced in the low várzea, despite comparable shifts in $\delta^{13}C$-CH_4 and $\delta^{2}H$-CH_4. One possible explanation for this observation is that stem methanotrophic communities may reach a saturation threshold beyond which additional CH_4 cannot be effectively oxidised (Bender & Conrad, 1992). Alternatively, the weaker flux decline could reflect additional CH_4 inputs from in-stem production, as evidenced by increasing fluxes and $\delta^{13}C$ depletion with height in some individuals (Figure 3.4). Recognition of such thresholds points to broader implications: while in-stem CH_4 oxidation exerts a strong control of net CH_4 emissions, it could be limited in its capacity to offset future increases in CH_4 production under shifting flood regimes and climate extremes (Fleischmann et al., 2023). Identifying

these thresholds, and which tree species host more resilient methanotrophic communities may help better constrain Amazonian CH_4 budgets in Earth system models.

3.5.2 Source of tree-emitted CH_4

Fluxes were substantially higher in the wet season than in the dry, reflecting greater CH_4 availability belowground and consistent with observations in other wetland systems (Covey & Megonigal, 2019). Typically, stem fluxes decline with height, reflecting diffusion or oxidation away from the soil source (Jeffrey, Maher, Tait, et al., 2021; Pangala et al., 2013). Yet fine-scale measurements revealed departures from this pattern: in *H. spruceana*, CH_4 emissions did not significantly decrease with stem height and were coupled to decreases in $\delta^{13}C$-CH_4 values (Figure 3.4). This pattern suggests an additional internal source of CH_4 capable of elevating fluxes and influencing $\delta^{13}C$-CH_4 to where oxidation patterns are no longer observed Previous work in Amazonian floodplain systems reported visible signs of decay in a small subset of Amazonian floodplain trees they sampled (Pangala et al., 2017). While such cases were limited (less than 4% of trees sampled), they highlight a possible mechanism for in-stem CH_4 production in flood-adapted species. Similar processes have been more clearly documented in upland ecosystems, where fungal infections and wet heartwood have been shown to support methanogenic activity and CH_4 accumulation within stems (Covey et al., 2012; Gorgolewski et al., 2023; Wang et al., 2016). Given that Amazonian floodplain trees are subjected to seasonal submersion for up to eight months, conditions conducive to wood decay, such as prolonged rainfall (Farias et al., 2025) and high humidity (Viitanen, 1997), are likely to arise. These findings suggest that wood rot, although underreported, may contribute to in-stem CH_4 production in tropical wetland systems and warrants targeted investigation in future studies.

By contrast with upland, free-draining systems, where stem emissions have been linked to roots accessing deep anoxic layers (Megonigal & Guenther, 2008; Plain & Epron, 2021), Amazonian floodplain trees receive a continuous supply of soil-derived CH_4 during inundation. Even under these conditions, however, our data show increases in stem fluxes with height alongside a decrease in $\delta^{13}C$-CH_4. Stem $\delta^{13}C$-CH_4 values were lower at 30 cm above flood waters than porewater $\delta^{13}C$-CH_4 at 30 cm depth below the soil surface (Figure 3.7). This additional isotopic shift is consistent with in-stem CH_4 production, superimposed on soil-derived inputs.

Species-specific contrasts further support this mechanism. From incremental flux measurements *H. spruceana* showed increasing fluxes with height and progressive decreases in $\delta^{13}C\text{-}CH_4$, while *E. coriacea* exhibited the expected pattern of declining fluxes and increasing $\delta^{13}C\text{-}CH_4$, consistent with soil-derived CH_4 transport and oxidation (Figure 3.4). The greater offset between porewater and stem $\delta^{13}C\text{-}CH_4$ in *H. spruceana* reinforces the likelihood of a stronger in-stem contribution (Figure 3.7). The species-specific differences in source contribution may be due to different functional traits between species (wood porosity, decay dynamics, and microbial communities) which can shape CH_4 production in stems(Covey et al., 2012; Gorgolewski et al., 2023; Sorz & Hietz, 2006). Through species-level resolution, we demonstrate that in-stem CH_4 production is likely to be unevenly distributed among Amazon tree species, but its relative contribution could be significant when upscaled across the stem.

Dry season data further supports variability in internal CH_4 production by species; *E. coriacea* displayed steady declines in fluxes and a shift to larger $\delta^{13}C\text{-}CH_4$ with stem height, consistent with active oxidation in the absence of inundation, whereas *H. spruceana* again showed elevated fluxes and lower $\delta^{13}C\text{-}CH_4$ values at upper stem positions. These dry-season patterns mirror wet-season deviations and parallel reports of in-stem production in upland forests (Covey et al., 2012; Wang et al., 2016). Together, these findings highlight that internal CH_4 sources, shaped by species-specific traits can disrupt expected flux-isotope relationships and contribute to the inconsistency of oxidation efficiency, making upscaling across forest stands challenging.

Dual-isotope data suggest that below-ground methanogenic pathways are site-specific across Amazonian floodplain types (Figure 3.5). In high várzea, $\delta^{13}C\text{-}CH_4$ and $\delta^{2}H\text{-}CH_4$ values were consistent with predominantly acetoclastic methanogenesis, which typically dominates in nutrient-rich, less acidic environments where acetate is abundant (Devol et al., 1988; Galand et al., 2005). This pattern aligns with known biogeochemical properties of whitewater várzea soils, including higher pH, and faster carbon turnover (De Souza Ferreira Neto et al., 2021; Junk & Piedade, 1997; Richey et al., 2002). In contrast, igapó exhibited a broader range in CH_4 isotopic composition, indicating both acetoclastic and hydrogenotrophic pathways – a characteristic of nutrient-poor, acidic blackwater systems where hydrogenotrophic methanogens are often favoured due to lower labile carbon availability (Galand et al., 2005; Le Mer & Roger, 2001; Sioli, 1984).

However, interpreting tree-emitted CH_4 solely through $\delta^{13}C$ and $\delta^{2}H$ remains challenging. Oxidation within stems can increase $\delta^{13}C$-CH_4, masking original production signatures and reducing the contrast between soil- and stem-derived CH_4 (Chanton et al., 2005; Jeffrey, Maher, Tait, et al., 2021; Whiticar, 1999). Moreover, if CH_4 is produced internally under strongly reducing microsites (e.g. in wood rot or water-saturated xylem), the isotopic signal may be more depleted than observed, especially if oxidation occurs during upward transport. This could obscure the contribution of in-stem production in dual-isotope datasets. Previous studies have shown that even high internal CH_4 concentrations may not manifest isotopically if microbial oxidation is partial and diffusive transport dominates (Covey et al., 2012; Martinez et al., 2022). Furthermore, end-member values for $\delta^{2}H$-CH_4 vary more across ecosystems and microbial communities than $\delta^{13}C$-CH_4, introducing additional uncertainty (Teh et al., 2005; Thauer et al., 2008). Together, these factors limit the resolution of isotope-based partitioning, especially where production and oxidation occur concurrently within stems.

Although isotopic approaches alone cannot fully disentangle CH_4 sources, the presence of internal production during periods dominated by soil fluxes highlights its potential to modulate overall emissions. Potential substrates include decaying wood tissues (Covey et al., 2012; Gorgolewski et al., 2023; Mochidome et al., 2025), which are abundant in Amazonian floodplain trees and increase during the rainy season (Farias et al., 2025). However, distinguishing biogenic CH_4 isotopically remains challenging, as both soil- and stem-derived CH_4 share microbial origins.

3.5.3 Diffusion as an unquantified egress pathway of CH_4

Throughout this study we interpret shifts in the stable isotopic composition of stem CH_4 as evidence of oxidation, but acknowledge that diffusion can also influence isotopic ratios. Diffusive transport likely still plays a role in CH_4 movement through tree stems, potentially interacting with oxidation and in-stem production. Diffusion-driven isotopic fractionation could modulate residence time, affecting the degree of microbial processing, while also providing a physical egress route for CH_4 not subject to enzymatic fractionation. Diffusion-driven fractionation of ^{13}C and ^{2}H has been documented in other systems (e.g. landfill soils; de Visscher et al., 2004; Mahieu et al., 2008) but its magnitude is typically small ($\leq$ ~2‰ change in $\delta^{13}C$-CH_4), far less than the isotopic shifts we measured (Table 3.2). This makes diffusion alone an unlikely explanation for our results.

In addition to the magnitude of isotopic shifts, Additional evidence also supports oxidation as the dominant process: (1) CH_4 concentrations within tree stems have been reported to reach hundreds of ppm in upland trees, even when external fluxes remain modest (Covey et al., 2012; Martinez et al., 2022). This discrepancy suggests substantial in-stem CH_4 consumption prior to emission, (2) microbial communities capable of oxidising CH_4 have been identified not only on bark surface but also within the stem, where they may act as filters of residual CH_4 (Arnold et al., 2025; Jeffrey, Maher, Chiri, et al., 2021); and (3) Our data suggest that in-stem CH_4 production may introduce additional isotopically light CH_4, potentially masking oxidation signals or offsetting enrichment caused by microbial activity. The combined effect of these processes (diffusion, oxidation, and internal production) creates a complex isotopic signal in tree-emitted CH_4 that cannot be attributed to any single pathway.

3.6 Conclusion

This study provides strong evidence that CH_4 oxidation occurs within Amazonian floodplain trees, demonstrating that stems are not passive conduits of soil-derived CH_4 but active sites of microbial processing. Like upland trees (Gauci et al., 2024), these floodplain species can host in-stem sinks that alter both the magnitude and isotopic composition of CH_4 emissions (Gauci et al., 2024; Jeffrey, Maher, Tait, et al., 2021), thereby partially mitigating atmospheric CH_4 release. Oxidation was evident across sites and species, yet efficiency varied, and oxidation did not always correspond with proportional reductions in fluxes, pointing to complex interactions with in-stem CH_4 production, transport, and emission pathways.

We present evidence for in-stem CH_4 production, likely species-dependent and occurring at a scale detectable even when soil remains the dominant source. This dual role of stems as both sinks and sources of CH_4 adds a previously underappreciated layer of complexity to tropical wetland carbon cycling. Understanding the capacity and limitations of in-stem oxidation, alongside the conditions that promote internal production, is critical to refining wetland methane budgets. Incorporating these processes into scaling frameworks and models will be essential for improving predictions of methane emissions under changing climate and shifting hydrological regimes.

3.7 Acknowledgements

This research was funded by a Royal Society Research Grant (RGF\R1\180042) awarded to SRP. Holly Blincow was supported by a studentship associated with this grant. SRP acknowledges support from the Royal Society Dorothy Hodgkin research fellowship (DH160111) and Royal Society enhancement award (RGF\EA\180042). The authors would like to thank the Mamirauá Institute for Sustainable Development for support throughout the study. We thank M.Castro, J.Castro, A.Silva J.Carvalho and E.Martins for all their fieldwork support and guidance.

3.8 Supporting Information

SI Table 3.1 | Mean ± SD of fluxes, δ^{13}C-CH4 and δ^{2}H-CH_4 for tree species sampled, grouped by site and season.

Site	Season	Species	Mean δ^{13}C-CH_4	Mean δ^{2}H-CH_4	Mean Flux ±SD
Igapó	Dry	*E. coriacea*	-53 ± 1	-135.4 ± 16.5	0.03 ± 0.1
Igapó	Dry	*H. spruceana*	-53.9 ± 7.2	-114.3 ± 1.2	0.001 ± 0.01
Igapó	Wet	*E. coriacea*	-64.3 ± 8.6	-269.5 ± 62.2	1.9 ± 2.9
Igapó	Wet	*H. spruceana*	-71.5 ± 6.5	-222.9 ± 42.2	0.6 ± 0.5
High várzea	Dry	*E. coriacea*	-54.3 ± 5.6	-199.7 ± 70.3	0.3 ± 0.6
High várzea	Dry	*H. spruceana*	-56.2 ± 6.9	-170.5 ± 19.6	0.2 ± 0.2
High várzea	Wet	*E. coriacea*	-54.6 ± 5.4	-231.2 ± 55.1	5.1 ± 8
High várzea	Wet	*H. spruceana*	-65 ± 1.8	-267 ± 16.5	5.9 ± 3.6

Chapter 4 - Wood rot as an alternative source of in-stem methane production in flooded Amazonian forests

4.1 Abstract

Methane (CH_4) emissions from tree stems represent a significant yet underexplored component of tropical CH_4 budgets. While these emissions are often attributed to CH_4 transported from soil, emerging evidence points to in-stem CH_4 production. We examine CH_4 emissions from Amazonian floodplain trees (várzea and igapó forests) during both wet and dry seasons, combining stem and soil flux measurements, radiocarbon (^{14}C) signatures and sonic time-of-flight tomography to test whether wood decay contributes to internal CH_4 sources.

Our results show that dry-season stem CH_4 fluxes were substantially lower than wet-season fluxes. However, net CH_4 emissions were detected up to 6 m along stems even when soils acted as an overall sink (-7.41 to 8.2 µg CH_4 m^{-2} hr^{-1} from 39 soil flux measurements vs. -91.8 to 2087 µg CH_4 m^{-2} hr^{-1} from 218 tree flux measurements), providing evidence for an additional, non-soil CH_4 source. Radiocarbon analysis revealed that stem-emitted CH_4 carried an older carbon signature than soil-derived CH_4, with CH_4 age increasing alongside the presence and extent of wood decay, as identified by sonic tomography. These patterns suggest microbial activity linked to wood decay may contribute to in-stem CH_4 production. Yet, we found no consistent correlation between peak CH_4 emissions and wood decay severity, emphasizing the complexity of methane dynamics within stems.

Overall, our findings highlight wood decay as a potential alternative source of CH_4 in Amazonian floodplain trees and underscores the importance of source partitioning for refining estimates of biogenic CH_4 emissions in tropical systems.

4.2 Introduction

Methane (CH_4) emissions from tree stems have emerged as a significant and sometimes underestimated component of the global CH_4 budget, particularly in tropical wetland ecosystems. In these regions, stem-mediated emissions are estimated to contribute 50-95% to the ecosystem scale budget (Pangala et al., 2013, 2017) and in

Amazonian lowlands, at a regional scale they are estimated to contribute up to 21.2 ± 2.5 Tg CH_4 per year (Pangala et al., 2017), representing a substantial portion of the global wetland CH_4 budget which is currently estimated to be 159-165 Tg CH_4 yr^{-1} (Saunois et al., 2025). Such emissions have been attributed largely to CH_4 produced in saturated, anoxic soils, which is then transported upward through trees via various gas exchange pathways (Rusch & Rennenberg, 1998; Vainio et al., 2022). However, emerging evidence suggests trees may not merely transport CH_4 from the soil but also produce it internally in the stem (Covey et al., 2012; Epron et al., 2023; Wang et al., 2016), though the magnitude and drivers remain unclear (Covey et al., 2012; Epron et al., 2023; Wang et al., 2016), particularly in the tropics where in-stem CH_4 production is largely unexplored and the relative contribution from soil and stems remains poorly constrained.

In-stem CH_4 emissions can occur at varying heights up stems (Epron et al., 2023; Mochidome et al., 2025), even in systems where surrounding soils act as a CH_4 sink (Daniel et al., 2023). Recent studies have identified methanogenic archaea in both heartwood and sapwood (Feng et al., 2022; Smits et al., 2022; Yip et al., 2019) as a possible source, while tree physiology such as water content and sap flow have also been seen to impact stem CH_4 emissions (Huang et al., 2022; Wang et al., 2016, 2017). Among possible causes, wood decay and wetwood have received particular attention, with rotting heartwood producing CH_4 under laboratory conditions (Covey et al., 2012; Schink & Ward, 1984; Zeikus & Ward, 1974), and wetwood contributing to emissions in situ (Covey et al., 2012; Schink et al., 1981). Additionally, fungi have been shown to generate CH_4 (Lenhart et al., 2012), with higher internal concentrations reported in trees colonised by white-rot fungi compared to those without (Hietala et al., 2015).

Correlating wood decay with observed CH_4 peaks, and with interspecific variation in decay, could help explain emission hotspots. However, this relationship is complex: in-stem CH_4 concentrations do not always directly correspond to net fluxes (Covey et al., 2012; Epron et al., 2023), and concurrent in-stem oxidation can further alter emission patterns (Jeffrey, Maher, Chiri, et al., 2021; Jeffrey, Maher, Tait, et al., 2021).

In-stem quantification of CH_4 production can be challenging as sources of CH_4 are heterogenous, both up the stem and radially and therefore greater understanding of its variability across the stem is required. Wood decay has previously been measured through invasive techniques such as using borers, which can be impractical when wanting to

sample multiple heights as these techniques create holes, increasing the possibility of decay fungi causing sapwood rot (Toole & Gammage, 1959; Wagener & Davidson, 1954), which limits repeat sampling. However, new techniques are emerging such as sonic tomography which provides an alternative, non-destructive method for analysing wood decay (Soge et al., 2021). This method has been used extensively for measuring internal stem defects associated with wood decay (Karlinasari et al., 2018; Qin et al., 2018; Son et al., 2021) and is based on the principle of stress-wave propagation whereby soundwaves travel at a lower velocity in decayed and degraded wood compared to sound wood (Soge et al., 2021). When used in tandem with CH_4 flux measurements, this method can provide an opportunity to understand the relationship between emitted CH_4 and wood decay as a possible tree-derived sources of CH_4 production along the stem – something that has not been done on living tree stems before. However, to accurately attribute fluxes to wood decay, partitioning soil-derived and tree-derived CH_4 is required.

Previous work has shown that tree-mediated CH_4 emissions can arise from both soil transport and in-stem production (Barba, Poyatos, et al., 2019; Covey et al., 2012; Mochidome et al., 2025; Mochidome & Epron, 2024; Pangala et al., 2017; Wang et al., 2016). However, separating these sources remains a challenge, particularly in wetland systems where soil signatures dominate (Jeffrey et al., 2023; Pangala et al., 2017; Sjögersten et al., 2020). Stable carbon isotopes ($\delta^{13}C$-CH_4) have limited diagnostic power because biogenic sources overlap in isotopic values (Conrad, 2005; Whiticar, 1999), and can be easily affected by oxidation or transport processes (Epron et al., 2023; Jeffrey et al., 2023; Mahieu et al., 2008). Radiocarbon (^{14}C) provides a more powerful tracer. Unlike $\delta^{13}C$, it is unaffected by oxidation, and differences in ^{14}C signatures between soils and tree biomass can be used to infer the age and origin of emitted CH_4 (Fichtler et al., 2003; Garnett et al., 2020; Horwath et al., 1994; Moguel et al., 2022; Trumbore, 2009). In wetlands, most soil methanogenesis is fuelled by recent, labile carbon, notably root exudates and fresh DOC, so CH_4 produced in soils typically carries a modern ^{14}C signature reflecting contemporary photosynthate (e.g. Dean et al., 2017; Garnett et al. 2012, 2020). When soil-derived CH_4 is transported into and emitted from tree stems, its ^{14}C remains comparatively young. By contrast, in-stem production draws on carbon pools within the tree, including older heartwood reserves whose apparent age scales with tree age and carbon turnover; CH_4 generated from these substrates therefore may exhibit older ^{14}C signatures (Horwath et al., 1994). The resulting age contrast between soil-transported

and stem-produced CH_4 underpins a radiocarbon partitioning approach that allows for separating and, with sufficient sampling, quantifying their respective contributions to net stem flux (Moguel et al., 2022; Vihermaa et al., 2014). In Amazon ecosystems, ^{14}C has been applied to determine the timing of carbon fixation in soils (Chanca et al., 2025) and in trees (Linares et al., 2017). By comparing ^{14}C signatures across sources, this approach can reveal the pathways through which carbon is released (Vihermaa et al., 2014). However, it has not yet been applied to tree-mediated CH_4 emissions, despite its potential to distinguish soil-derived from tree-derived contributions, particularly in systems where wood decay or fungal activity may obscure $\delta^{13}C$ interpretations (Schroll et al., 2020).

In this study, we aim to explore the role of wood decay as a potential source of CH_4 within Amazonian floodplain trees by integrating ^{14}C source partitioning approaches (from porewater, wood cores and tree chambers), CH_4 flux measurements and wood decay assessments using sonic tomography. This approach enables us to quantify the contribution of tree-derived CH_4, an overlooked CH_4 production pathway, and to refine our understanding of CH_4 production mechanisms in these high-CH_4 emitting environments.

We hypothesise that Amazonian floodplain trees emit CH_4 from both soil-derived and in-stem CH_4 sources, with internal wood decay facilitating in-stem CH_4 production. Consequently, stem emissions will persist through the dry season, even where adjacent soils are a net CH_4 sink and trees exhibiting greater decay (quantified by sonic time-of-flight tomography) will exhibit higher stem CH_4 fluxes in the dry season. We further hypothesise that radiocarbon (^{14}C) can resolve these sources: stem-emitted CH_4 will display older ^{14}C than porewater CH_4 derived from modern, labile soil carbon, the apparent ^{14}C age of stem CH_4 will increase with the extent of decay.

4.3 Methods

4.3.1 Study site

The study was conducted in the central Amazonian floodplain of Brazil, approximately 500 km west of Manaus within two sustainable development reserves: Amanã Sustainable Development Reserve (ASDR) and Mamirauá Sustainable Development Reserve (MSDR). The first plot, an igapó forest, was located in ASDR, at the South of Amanã Lake (S2° 38.598' W64° 39.980'). This catchment encompasses two

hydrologically different river systems, the Solimões, Japurá and Negro River, with the Japurá dominating the south of Amanã Lake in the dry season and the Negro River dominating in the flooded season. It is therefore classed as a blackwater system, meaning it is characterised by nutrient-poor water systems (Prance, 1979) with acidic waters ranging from 4.6-5.2 pH (Schmidt, 1972). Flood waters in this site reach ~1.5 m.

The second and third plot was in the MSDR, a várzea forest bounded by the Solimões, Japurá, and Auati Paraná Rivers. These plots represented a high várzea forest (S2° 48.916' W65° 05.192') and a low várzea forest (S 2°49′56.20″, W 65°00′14.35″), both located close to the Japurá river along a smaller river channel. High and low várzea forests are seasonally flooded by whitewater rivers and are known for their higher nutrient levels (Prance 1979), lower oxygen concentrations (Junk and Piedade, 1997) and near neutral pH (Wittmann et al. 2022). Where they contrast is that high várzea experiences an average flood level of 2-3 m for <50 days a year, whilst low várzea experiences flooding of ~5 m for >50 days a year.

These plots were chosen to reflect the contrasting hydrology of the Amazon and collectively, they represent a large area of the floodplain; high and low várzea forests span 456,000 km^2 whilst igapó forests span 302,000 km^2 (Melack & Hess, 2010), comprising nearly 85% of the 900,000 km^2 of the floodplain basin (Hess et al., 2015). For this study, sampling was conducted in both the wet and dry seasons in the low várzea plot whereas in high várzea and igapó, sampling was only observed in the dry season.

4.3.2 Sampling regime

Measurements were conducted during both the wet (May 2024) and dry (November 2024) seasons. In the dry season, we conducted stem and soil flux measurements, $\delta^{13}C\text{-}CH_4$ sampling, and wood decay assessments on trees at multiple stem heights across igapó, high várzea, and low várzea habitats. During the wet season, we measured stem CH_4 flux from 30-70 cm stem heights above the floodline and measured wood decay at the same height. ^{14}C samples from porewater, wood cores, and tree chambers were also collected in low várzea. All ^{14}C samples were collected from our low várzea plot only as both the high várzea and igapó plot did not flood in May 2024 due to the El Niño event. ^{14}C analysis requires relatively large volumes of CH_4 (3 ml CH_4; Garnett et al. 2019). At sites where soils remained dry, CH_4 availability was below this threshold, making $^{14}C\text{-}CH_4$ analysis unfeasible. Consequently, all ^{14}C sampling was

concentrated in the wet season in the low várzea plot which was flooded and subsequently, had high concentrations of CH_4. To compensate for the loss of replication across sites and to improve the robustness of source partitioning, the number of trees sampled in low várzea was doubled (from five to ten individuals per species). Increasing replication in this way not only maximised the probability of obtaining sufficient CH_4 for analysis but also captured a broader range of tree ages and stem conditions, thereby enhancing the likelihood of resolving variability in ^{14}C signatures between porewater and stem-derived CH_4. This design strengthened our ability to partition the sources of CH_4 contributing to tree emissions.

4.3.3 Stem and soil flux measurements

Tree stem CH_4 fluxes were measured in May 2024 and November 2024 to reflect the wet and dry seasons of the Amazon floodplain, using previously established chamber designs (Pangala et al., 2017).

Fluxes were measured in the wet season in low várzea 30-60 cm above the floodline. In the dry season, fluxes were measured from all three plots (igapó, low and high várzea) at multiple heights. These heights comprised of two samples taken at the lower portion of the tree at 30-60 cm and 70-100 cm to capture fluxes from areas of trees that are seasonally inundated. The second two chambers were affixed 30 cm above the average floodline of each plot. For igapó, this was 130 cm and 170 cm, in high várzea it was 230 cm and 270 cm and in low várzea, it was 180 cm and 220 cm. The final two chambers were affixed 1 m above the floodline where the stem has never been inundated. For igapó this was 230 cm and 270 cm, in high várzea it was 330 cm and 370 cm and in low várzea, it was 530 cm and 570 cm. Chamber heights were selected to represent the area of the tree consistently submerged during inundation as well as to capture the section of the tree that is sampled during the wet season (above the floodline) and then finally, to capture flux dynamics where there has been little to no flooding. This was to understand the impact of flooding on the tree fluxes and wood decay.

Soil CH_4 fluxes were measured in November 2024 during the dry season, by positioning a soil chamber within 1 m of each sampled tree, with loose leaf fall removed from the top of the soil. The soil chamber (16 cm internal diameter × 25 cm height) was built from a metal cylinder with a transparent airtight lid and sampling ports, inserted 5

cm into the soil. Fluxes from both the soil and the stem were calculated using the same methods ascribed to tree stem fluxes, outline in chapter 2 and 3.

Trees studied in chapter 2 and 3 were resampled for this study (*E. Coriacea* and *H. spruceana*). In igapó and high várzea, 5 trees of each species were sampled and in low várzea, 10 trees of each species were sampled.

4. 3. 4. Internal stem CH_4 concentrations

Internal CH_4 concentrations were captured at 1m height by attaching a syringe onto a wood borer, fitted with rubber tubing for a gas tight connection. A 3-way valve was opened to the borer and once the borer reached the centre of the tree, the syringe was pulled back and then locked. Any gas that had been drawn up along the borer was the captured and needled into Exertainer vials (Labco, UK) for GC analysis. In some cases where gas content in the stem was high, the syringe filled automatically.

4.3.5 Wood decay analysis

Wood decay was measured using Time-of-flight (ToF) sonic tomography in low várzea during the flooded season (May 2024) and again in the wet season (November 2024) across all three plots. Wood decay was measured using a Microsecond timer (Fakopp Kft, Hungary) from a cross section of 30 trees (N-S and E-W) by inserting a pin ~2 cm deep into the tree stem, attached to a transducer box. Measurements were taken North-South and then East-West across all trees to account for climatic conditions which could impact wood decay potential through increased sun exposure and moisture conditions. For example, wind movement from NE to SE could systematically expose areas of the stem to increased moisture and sun rising and setting could impact sun exposure, which when coupled with increased moisture, could increase the prevalence of wood decay.

The pin is then tapped on one side with a metal hammer, and a soundwave is sent to the corresponding pin. The method is designed to detect the length of time for the soundwave to travel through the wood which will take longer depending on the amount of decay or hollowness present inside the tree. Sound moves slower through wood decay than it does through undisturbed wood. Therefore, by understanding the time taken for a

soundwave to move through a non-rotted tree, a calculation can be made to measure the amount of decay in a tree using the diameter of a tree:

$$\%decay = (100 - \left(\left(\frac{T_T}{T_A}\right) \times 100\right)/100$$

Whereby T_A is the average time measured between the two pins over 10 repeat measurements (expressed as µs). And T_T is the target time if no decay is present:

$$T_T(\mu s) = \left(\frac{distance\ between\ sensors(cm)}{Reference\ velocity\ in\ m/s}\right) \times\ 10{,}000$$

T_T is calculated by creating a reference velocity for each species sampled by making a wood decay measurement at the cross section of a tree and then coring the tree to visually inspect for signs of decay. This is then converted into a reference velocity:

$$Reference\ velocity\ (ms) = \frac{Distance\ (cm)}{A_T\ [\mu s]} \times\ 10{,}000$$

Whereby A_T is the average time measured between the two pins over 10 repeat measurements of a non-rotted tree. Three reference velocities were created for each tree species and averaged per species.

Sonic tomography is a new method in the context of tree stem CH_4 emissions, and as such, we tested two time-of-flight instruments against one another. Wood decay was measured by both instruments at the same point on the stem of two trees for comparison, and no significant differences were observed. In addition, we assessed whether hammer strike strength influenced results by tapping the pin both lightly and firmly. No changes were observed but to ensure consistency, the hammer was tapped using a swinging motion and not hard enough to push the pins into the tree as decreasing the distance between the pins unexpectedly can result in an incorrect measurement of decay.

To align sonic tomography with stem CH_4 flux measurements, we first assessed decay at three heights corresponding to the bottom, middle, and top of the chamber placement. No significant differences in decay were detected among these heights. Therefore, all subsequent measurements were taken at the midpoint of the flux chamber height, ensuring that decay assessments corresponded directly with the location of chamber-based flux measurements and allowing comparability between decay and CH_4 emission data.

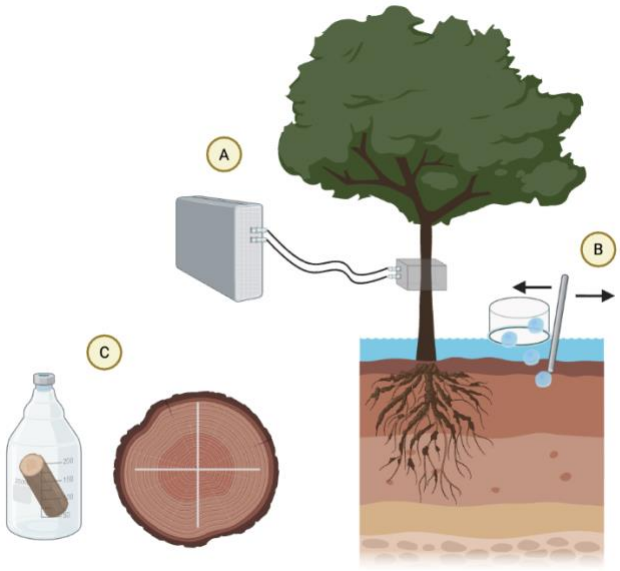

Figure 4.1 | Sampling techniques for ^{14}C analysis. A) Tree stem chamber measurements. B) Porewater measurements from disturbance-induced ebullition. C) Cross-sectional wood core incubation.

4.3.6 $\delta^{13}C$-CH_4 stable isotopes

Isotope samples were collected for $\delta^{13}C$-CH_4 analysis from tree chambers during a single field campaign in the November 2024 dry season, immediately following a 5-minute flux measurement. Sampling and analysis followed the procedures outlined in Chapter 3. In total, 218 tree samples and 39 soil measurements were collected across three plots, corresponding to flux measurements at different heights.

At the high-várzea site, isotope sampling was restricted to the lower two heights (1-2) and the upper two heights (5-6), consistent with the original design, which contrasted fluxes below and above the floodline. At the other sites, intermediate stem heights (3-4) were also included to capture vertical variation in $\delta^{13}C$-CH_4 signatures. Consequently, isotope data from high várzea does not include these intermediate positions.

4.3.7 ^{14}C radiocarbon isotopes

All ^{14}C samples were collected from our low várzea plot only as both the high várzea and igapó plot did not flood in May 2024. As ^{14}C requires a large quantity of CH_4 for analysis, these sites could not be sampled from. As such, all sampling was moved to

low várzea where the number of trees sampled doubled from 5 of each species to 10. ^{14}C in CH_4 was collected from porewater and tree chambers as quantities of CH_4 could be sufficiently captured, but ^{14}C sampling of wood cores was conducted using molecular sieves to capture CO_2 (Garnett et al., 2020). This approach was warranted due to logistical constraints in the remote Amazon, where gas cylinders required for flushing wood core incubations were unavailable. Instead, CO_2 was used as a proxy for CH_4 under the assumption that CO_2 is a by-product of methanogenesis, particularly if várzea forests predominantly produce CH_4 via acetoclastic pathways (Blincow et al., Chapter 3).

Radiocarbon samples were collected from stem CH_4 flux, porewater and wood cores to compare ^{14}C sources of CH_4 to stem emitted CH_4 (Figure 4.1). ^{14}C signatures from the tree chamber were collected by attaching our flux chamber to the tree 30 cm above the floodline. Chambers were left on the tree to allow an accumulation of CH_4 great enough for radiocarbon analysis (1.5 ml of CH_4, as outlined by Garnett et al. 2019). The length of time required to capture the sample was dependant on the strength of the output of each tree and therefore varied from 20 minutes to 24 hours. The size of the sample collected was also dependant on the concentration. For example, in order to obtain 1.5ml CH_4 in a 3 L sample bag, a minimum concentration of 500 ppm is required or the number of litres of sample was increased if CH_4 could not accumulate to the required concentration.

Porewater signatures were captured by disturbance-induced ebullition from the soil. Gas bubbles were generated by disturbing the soil to a depth of 20 cm and capturing the gas bubbles generated using an aquatic chamber (see Bastviken et al., 2004 for chamber design). The sample from both tree chambers and porewater were collected via a syringe and injected into foil gas bags provided by the National Environmental Isotope Facility (NEIF) via a sample port (Garnett et al., 2012). These bags were 5 L and only ever filled to 3 L to allow for gas expansion during sample transit from the field sites to the NEIF isotope facility in Scotland. To reduce the capacity for leakages, CPC coupling were used to attach the syringe to the bag (Tom Parker, UK). Two Food bag clips (WeLoc clips) were also attached to the sampling port tubing to ensure a tight seal.

To capture ^{14}C from wood cores, a 5 mm increment borer was used to extract a radial sample of each tree (Haglof, Sweden). These were placed into sealed sample bags in the field and then transported into 1 L duran bottles on the same day. The bottles were sealed with a rubber bung with an inlet and outlet. At the beginning of the incubation, the

samples were scrubbed of atmospheric CO_2 using soda lime traps and a pump provided by NEIF. A starting concentration was noted and the ports were closed with a CPC coupling and clips, with samples were left to incubate until enough CO_2 had been generated for ^{14}C analysis (2 ml of CO_2). The timeframe was between 24 and 48 hrs. When CO_2 concentrations reached a sufficient level, a cartridge containing CO_2-absorbing zeolite molecular sieve was attached via a sampling line and a pump to extract the sample from the incubation vessel (Garnett & Murray, 2013). The cartridge was then sealed with clips before uncoupling from the sample line.

All samples were sent to NEIF where they were analysed according to their source. Firstly CO_2 samples from wood cores were scrubbed of atmospheric ^{14}C contamination and $\delta^{13}C$-normalized using previously tested methods (Garnett et al., 2012, 2019; Garnett & Murray, 2013). The CO_2 was released from the molecular sieve by heating it to 500 ^oC and the gas was purified cryogenically. In addition, CH_4 from porewater and tree chambers samples were first isolated by removing CO_2 using soda lime and zeolite molecular sieves. The purified CH_4 was then combusted over heated platinum–alumina catalysts (950 °C) to generate CH_4-derived CO_2, which was cryogenically purified. This CO_2 was split for $\delta^{13}C$ and ^{14}C analysis. All samples were graphitized and passed to the Scottish Universities Environmental Research Centre (SUERC) for analysis on their Accelerator Mass Spectrometry (AMS) for ^{14}C analysis and are subsequently expressed as %modern.

4.3.8 Statistical analysis

The difference between soil and stem emissions were analysed with a linear mixed effect model. The global model included flux as the dependent variable and tree species, site, sample source (tree vs stem) and their interactions as the independent variables. Tree identity was included as a random effect to account for repeat sampling.

To assess the impact of wood decay on CH_4 emissions from tree stems, linear mixed effect models were run including wood decay, site, species and height as fixed effects, and with tree ID as a random effect. Sonic velocity occasionally exceeded that of the calibration reference tree, resulting in negative decay estimates. Because wood decay values cannot be biologically negative, these values were interpreted as representing no detectable decay and reflect calibration and wood property differences rather than true 'negative' rot. As a result, negative decay <0 were truncated at zero rather than removing

them from the dataset. One data point was also excluded due to considerably high rot, causing skewness. A linear model was also constructed to investigate how wood decay varied across species, sites and different stem heights.

To investigate changes in stable isotope ratios across the stem, linear mixed effect models were used to compare ^{13}C CH_4 across tree and soil sources, as well as across sites and species, with tree ID as a random effect. Site and species were retained in the best model.

To understand whether ^{14}C can be used to resolve the source of CH_4 production, the ^{14}C age from tree cores, porewater and tree chambers were compared using a one-way anova.. Tukey's Honest Significant Difference (HSD) test was then used to determine whether mean values differed significantly among sample types.

To determine the influence of wood rot on tree-derived CH_4 production, the effect of wood decay on ^{14}C age from tree chambers was assessed using a linear model. Species and stem diameter were also included as interactions to account for their potential effect on ^{14}C age. Further, to understand how CH_4 sources varied between species, we compared the radiocarbon age of tree stem emissions and wood cores from *E. coriacea* and *H. spruceana*.

All statistical analyses were conducted using R software (v12.0). All linear models were refined using backward step selection and final models retained only predictors with a *p*-value of <0.05.

4.4 Results

4.4.1 Dry season measurements

Tree stem and soil CH_4 flux

CH_4 fluxes from tree stems in the dry season were significantly greater than soil CH_4 fluxes ($p = 0.026$) and both were highly variable across all three sites ($p < 0.001$) (Figure 4.2). Soils were an average sink of CH_4 in igapó and low várzea (-5.8 ± 1.1 and -0.8 ± 2.7 µg m^{-2}, hr^{-1} respectively), but an average source in high várzea (1.3 ± 6.1 µg m^{-2}, hr^{-1}), with large variability. In comparison, tree stems were an average source of CH_4 across all tree species, heights and forest plots. In igapó, the mean flux was 76.7 ± 126 and 5.38 ± 9.91µg m^{-2}, hr^{-1} across all measured heights for *E.coriacea* and *H.spruceana*

respectively. In high várzea, the mean flux was 129 ± 384 for *E. coriacea* and 126 ± 151 µg m^{-2}, hr^{-1} for *H. spruceana*. In low várzea, the mean flux was 24.9 ± 42.7 and 16.9 ± 39.5 µg m^{-2}, hr^{-1} for E.coriacea and *H.spruceana*. Comparing fluxes between species within plots, species only differed significantly in igapó ($p < 0.01$) but high and low várzea sites did not.

Stem height did not have a significant effect on stem CH_4 fluxes (Figure 4.4) and emissions remained highly variable. Only 4 of the 112 *E. coriacea* stems showed CH_4 uptake, compared with 14 of the 106 *H. spruceana* samples (Figure 4.4). *E.coriacea* demonstrated the largest average uptake (-26 ± 43.9 µg m^{-2}, hr^{-1}) compared to *H.spruceana* (-2.25 ± 2.01 µg m^{-2}, hr^{-1}).

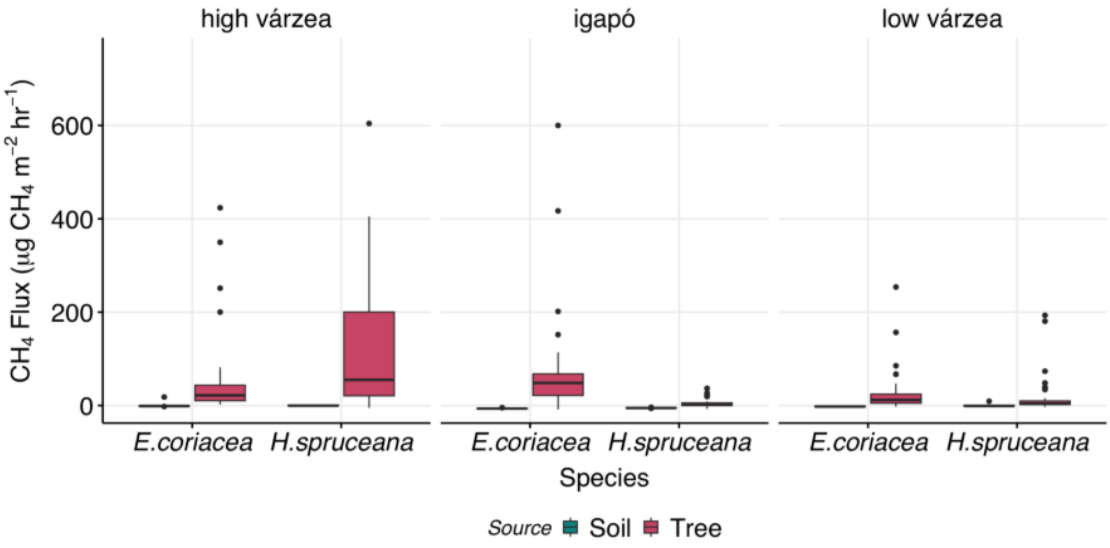

Figure 4.2 | Dry season tree and soil CH_4 flux expressed as µg m^{-2}, hr^{-1} across 3 sites and two species. In igapó and várzea a total of 10 trees were sampled in each plot. 20 trees were sampled in low várzea. Measurements taken at heights ranging from 30 cm to 6.8 m (igapó, *E.coriacea* n= 32, *H.spruceana* n= 30, high várzea *E.coriacea* n= 30, *H.spruceana* n= 30, and low várzea *E.coriacea* n= 50, *H.spruceana* n= 46). Soil samples taken adjacent to each tree sampled (igapó n = 10, high várzea n = 10 and low várzea n = 19). One extreme value for stem flux was outside the plotted y-axis range (≈2000 µg CH_4 m^{-2} hr^{-1}, *E.coriacea* in high várzea) but was retained in all analyses.

Fluxes were highly variable across all plots ranging from -91.8 to 2087 µg m^{-2}, hr^{-1}. High várzea had the highest average fluxes at 94.1 ± 134.59 from both tree species whilst igapó had an average of 43.6 ± 98.2 and low várzea had 21.1 ± 41.2 µg m^{-2}, hr^{-1}.

Although high várzea had the greatest average, it had the largest variation, with igapó and low várzea having slightly smaller standard deviations (SD). (Figure 4.2).

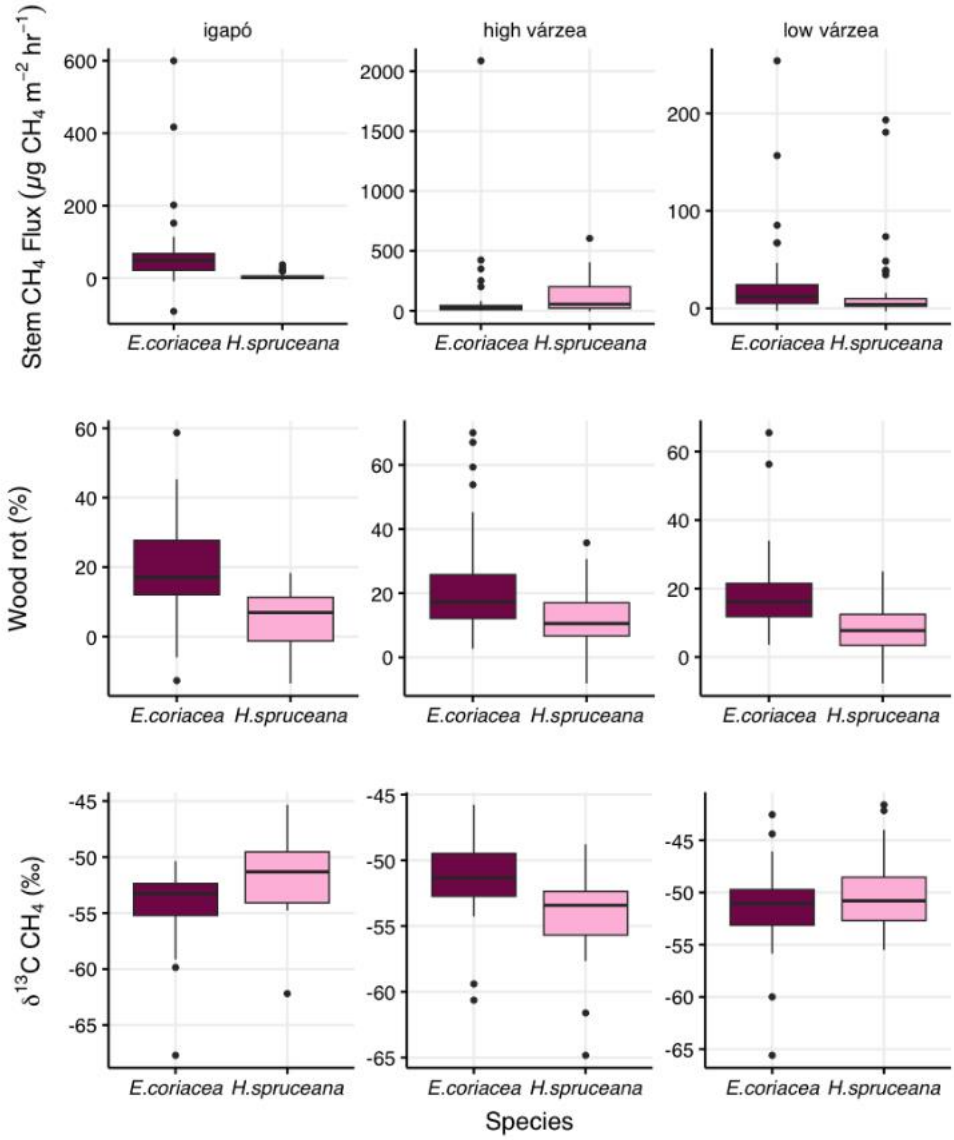

Figure 4.3 | Dry season fluxes, wood decay and stable isotope signature across three plots, coloured by species. Fluxes and wood decay sampled at 6 heights up each tree (See Table S4.1 for sample size).

Wood decay measurements

Stem CH_4 flux increased significantly with wood rot within a tree ($p < 0.01$). However, only 9 of 40 trees showed a positive relationship, and slope estimates varied considerably among trees.

The percentage of wood decay in trees differed significantly between species ($p < 0.001$). Wood decay was, on average, greater in *E. coriacea* in all plots compared to *H.*

spruceana (p <0.001) (Figure 4.3). In *E. coriacea*, wood decay averaged 20 ± 14 % in igapó, 22 ± 16 % in high várzea and 18 ± 11% in low várzea across all stem heights. In *H. spruceana*, wood decay averaged 4 ± 10 %, 12 ± 10 % and 8 ± 8 % in igapó, high várzea and low várzea respectively. Stem height did not have a significant effect on wood decay in either species (Figure 4.5). There was no significant difference in wood decay among plots that experienced different durations of flooding (17 ± 12 %, 19 ± 15 % and 15 ± 1-0 % for igapó, high várzea and low várzea respectively).

$\delta^{13}C$-CH_4 Stable isotopes

$\delta^{13}C$-CH_4 values did not differ significantly between species or heights, but tended to correlate with stem CH_4 fluxes, although this relationship was not statistically significant (p = 0.09). In igapó and low várzea, where *E. coriacea* exhibited higher stem CH_4 fluxes, the corresponding $\delta^{13}C$-CH_4 values were more depleted than those of *H. spruceana* (-54.0 ± 3.5‰ vs. -51.7 ± 3.6‰ in igapó; -51.3 ± 3.6‰ vs. -50.2 ± 3.2‰ in low várzea). Conversely, in high várzea, where *H. spruceana* was the higher emitter, its $\delta^{13}C$-CH_4 values were more depleted relative to *E. coriacea* (-54.5 ± 4.2‰ vs. -51.7 ± 4.1‰).

$\delta^{13}C$-CH_4 values differed significantly between soils and tree stems (p <0.01), with stem emitted $\delta^{13}C$-CH_4 ~1.7% more depleted than soils. $\delta^{13}C$-CH_4 varied across sites (p <0.001), in particular, low várzea was ~2.1‰ more enriched than igapó, whilst there was very little difference between high várzea and igapó.

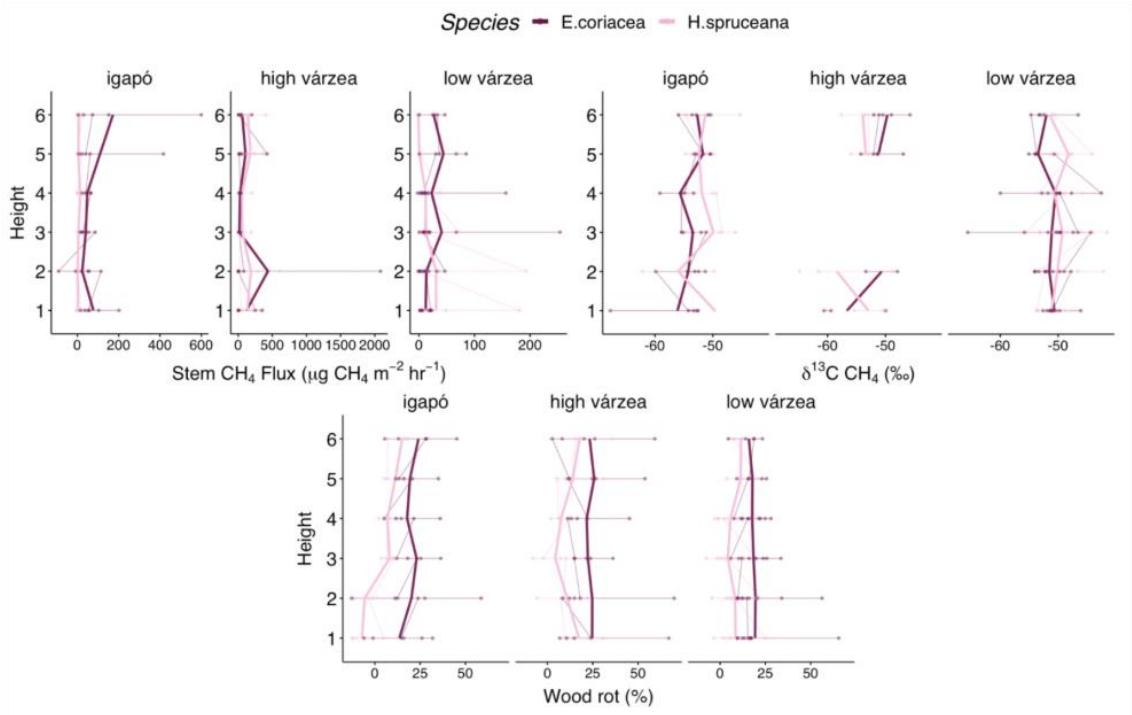

Figure 4.4 | Stem fluxes, wood decay and $\delta^{13}C$-CH_4 measurements at multiple heights relative to the floodline (See SI Table 1 for sample size). Heights 1 and 2 are below the floodline, heights 3 and 4 are located directly above the average floodline for the plot, and heights 5 and 6 are 1 m above the floodline. The floodline for each plot differs, with igapó's average floodline at 1.5 m, high várzea's at 3 m, and low várzea's at 4 m (See Table S4.1 for sample size).

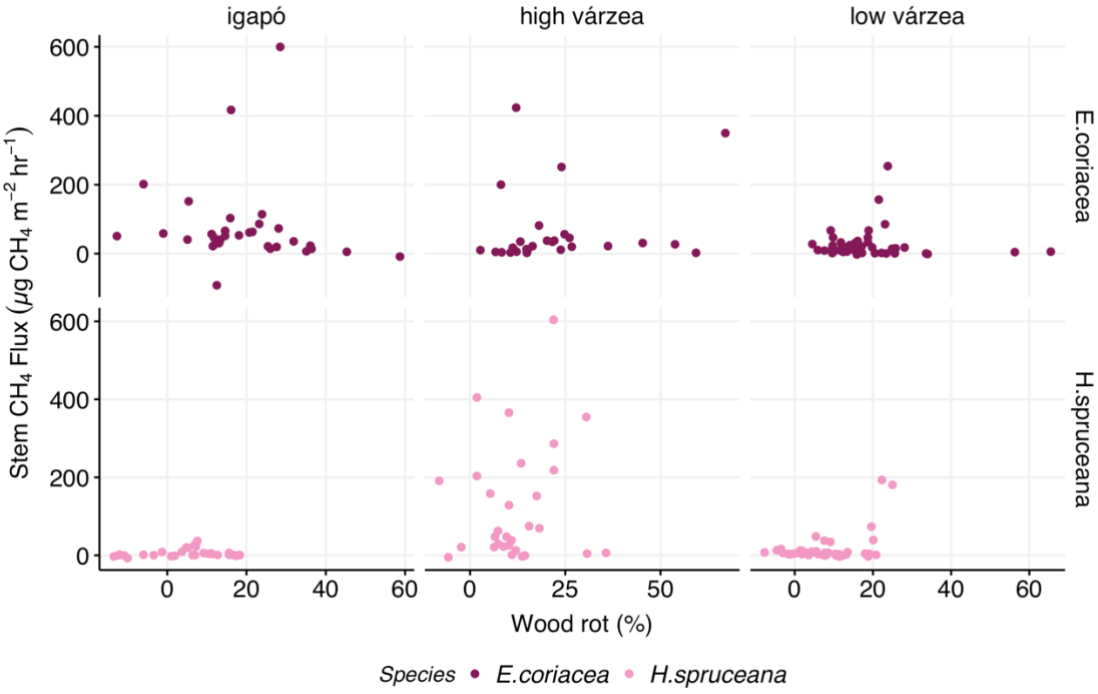

Figure 4.5 | Wood decay (%) correlated with stem CH_4 flux across all stem heights for *E. coriacea* (igapó n=32, high várzea n=29, low várzea n= 50) and *H.spruceana* (igapó n = 30, high várzea n = 30, low várzea n = 46) in all three forest plots.

4.4.2 Wet season ^{14}C age and wood decay measurements

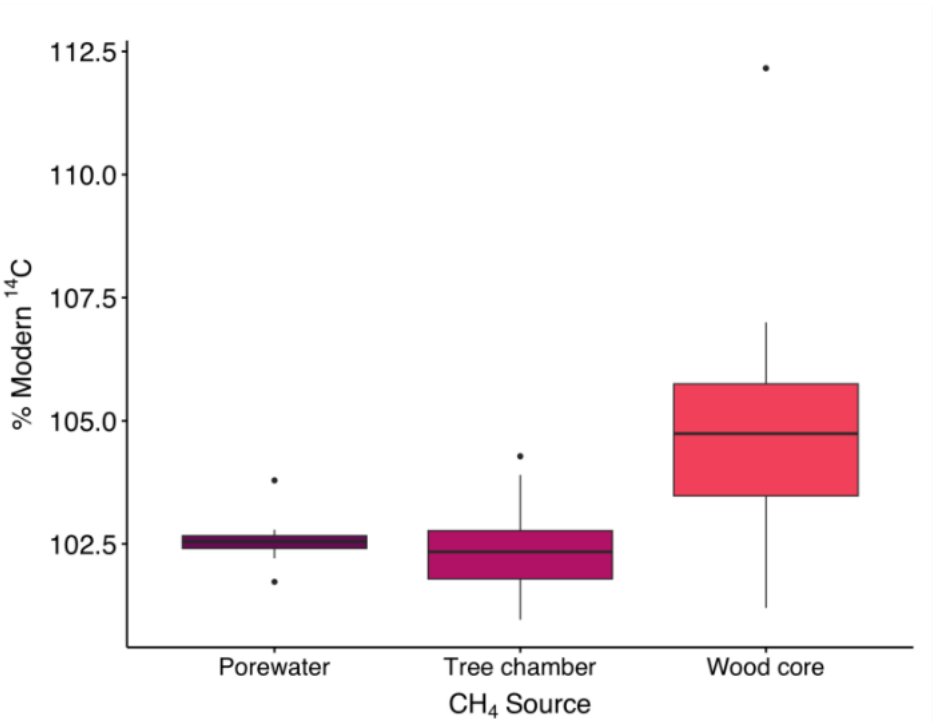

Figure 4.6 | ^{14}C signature from porewater (n = 11), wood cores (n = 19) and tree chambers (n = 21) across both *H. spruceana* and *E.coriacea*, expressed as % Modern ^{14}C. Calculated from CALIBomb (Reimer & Reimer, 2026)

Radiocarbon (^{14}C) age differed between porewater, wood cores, and tree stem chamber CH_4 samples (Figure 4.6). Specifically, the ^{14}C age of wood cores was higher than porewater samples ($p < 0.001$), indicating an older carbon source. There was no significant difference between porewater and tree chamber ^{14}C values, but tree chamber samples differed significantly from the wood core ^{14}C, as confirmed by Tukey post hoc tests.

The percentage of wood decay showed no significant effect on the radiocarbon age of wood cores. The strength of association between wood decay and ^{14}C differed between species (Figure 4.7). In *H. spruceana*, decay explained a substantial proportion of the variance in ^{14}C ($R^2 = 0.30$, n = 11), but not in *E. coriacea* ($R^2 = 0.04$, n = 10).

Wood incubation experiments yielded an average ^{14}C value of 105 ± 2.8% for H. *spruceana* and 104 ± 1.7% for *E. coriacea*. In contrast, tree chamber samples had lower values, with H. *spruceana* averaging 102 ± 0.5% and *E. coriacea* 103 ± 0.8%.

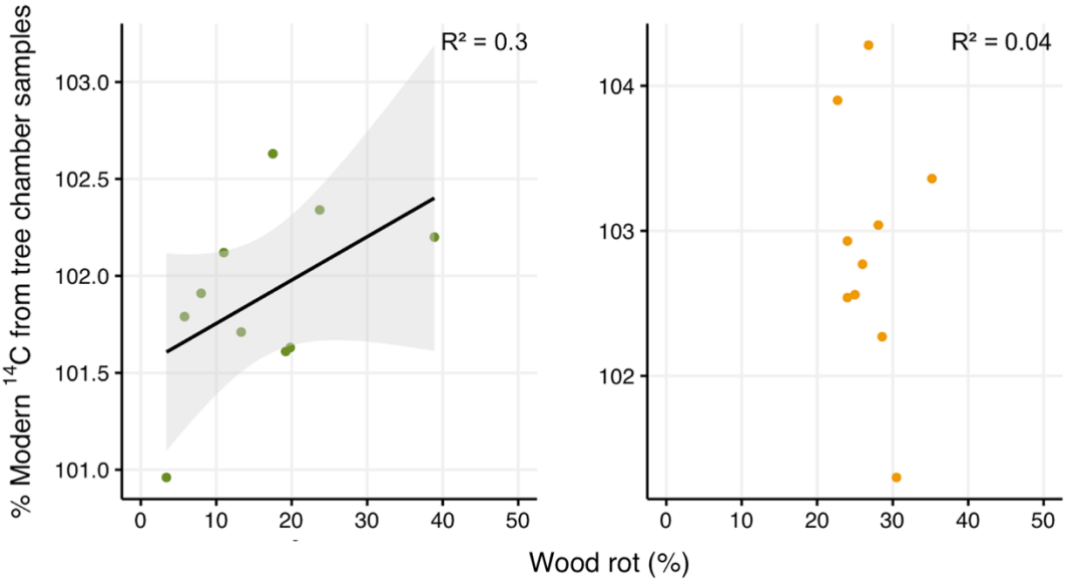

Figure 4.7 | Relationship between wood decay and %modern radiocarbon ($F^{14}C$) from tree chambers of *H. spruceana* (n = 11) and *E. coriacea* (n = 10).

The ^{14}C age of CH_4 from wood incubations and tree chambers, differed significantly for *H. spruceana* ($p < 0.01$) but not *E. coriacea* (Figure 4.8). The ^{14}C age from the tree chambers differed significantly between *E.coriacea* and *H.spruceana* ($p < 0.01$), but not from wood incubations.

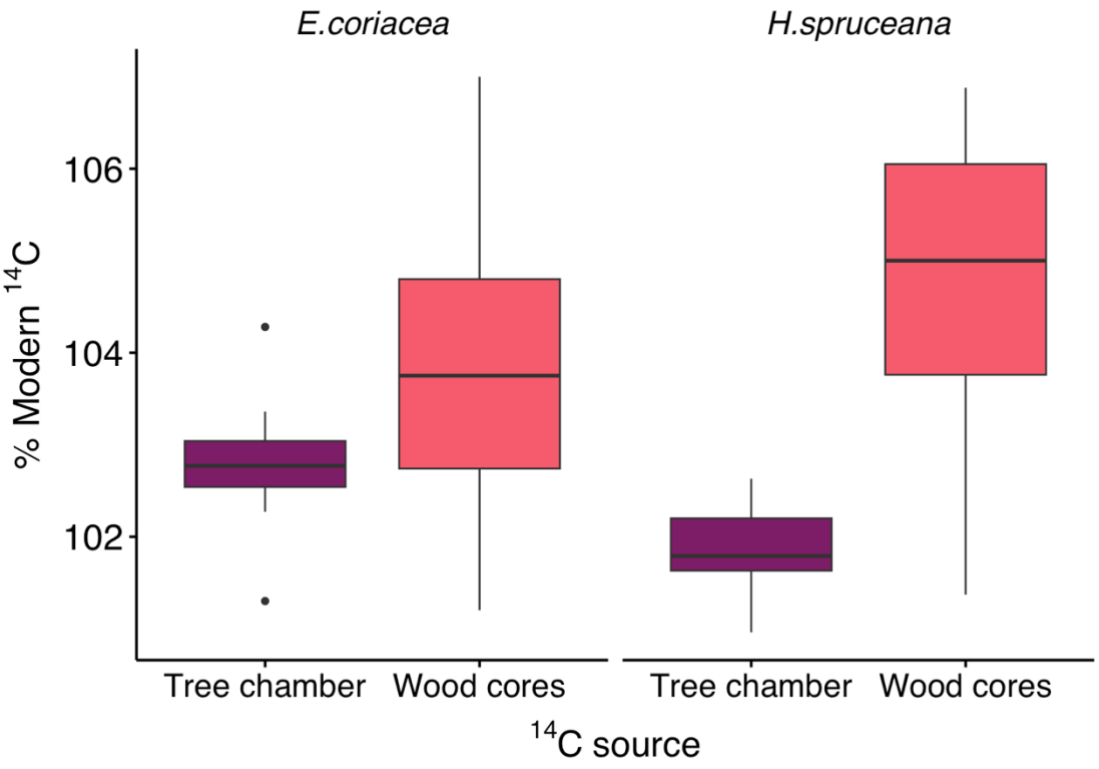

Figure 4.8 | Comparison %modern ^{14}C values from wood cores and tree chambers of *E.coriacea* and *H.spruceana* (n = 9 per species for each measurement type).

4.5 Discussion

4.5.1 In-tree CH_4 production

Our results demonstrate that tree stem CH_4 emissions from Amazon floodplain forests are likely the result of both soil-derived and stem-derived production. Trees continued to emit CH_4 up to 6 m along the stem even in the dry season, when adjacent soils were a net sink (Figure 4.2). This uncoupling between stem and soil fluxes mirrors patterns reported in other tropical forest systems (Daniel et al., 2023). The absence of a vertical decline in stem CH_4 emissions with increasing stem height during the dry season, together with soil uptake, indicates a shift in the dominant source from soil-derived CH_4 (Pangala et al., 2013, 2014; Pitz et al., 2018; Wang et al., 2016) to within stem produced CH_4 (Epron et al., 2023; Mochidome et al., 2025; Wang et al., 2017) and demonstrates that floodplain trees can remain a CH_4 source independent of soil supply. Wet-season ^{14}C data supports an in-stem CH_4 contribution: stem-emitted ^{14}C ages did not align/match with porewater ^{14}C ages (Fig. 4.6), suggesting an internally derived CH_4 source,

supported by previous evidence that Amazon floodplain trees can produce CH_4 in situ, albeit at lower proportions (Pangala et al., 2017). Further, internal stem CH_4 concentrations, although variable, can be considerably high (Table S4.2) and are unlikely to be derived from the soil where dissolved concentrations, even in the wet season (Chapter 2) are much lower.

By capturing stem CH_4 emissions up to 6 m in height during the dry season, our data provides a more comprehensive picture of stem CH_4 flux dynamics in the Amazon floodplain and highlights in-stem CH_4 production as an additional source of CH_4, mirroring free-draining upland systems in temperate regions (Epron et al., 2023; Mochidome et al., 2025). Furthermore, high emissions at upper stem heights suggest in-stem CH_4 production is the most likely source (Mochidome et al., 2025). These findings can help refine previous emission estimates for flooded forest systems which only attributed CH_4 emissions to wet season conditions (Pangala et al., 2017) and non-flooded riparian forests (Gauci et al., 2022). Instead, we suggest floodplain forests are a source of CH_4 year-round, even when forests are not inundated.

4.5.2 Site- and species-level variation in stem-produced CH_4

Stem CH_4 fluxes varied by more than an order of magnitude across sites, exceeding wet-season variability (Chapter 3) and indicating that in-stem production is not spatially uniform. If flooding were the dominant driver, emissions should peak in low várzea, where flood depth and duration are greatest and anoxia promotes methanogenesis (Wagner, 2017). Instead, the highest average fluxes occurred in high várzea, and no differences were observed above versus below the floodline. This pattern suggests that soils are no longer the primary source of CH_4 once floodwaters recede, contrasting with the wet season when emissions tracked soil biogeochemistry and flood dynamics (Chapters 2 and 3). A more likely explanation is that floodplain tree species differ in how they adapt to local hydrological regimes (Fontes et al., 2020), creating contrasting internal conditions for CH_4 production. The species-specific results support this view: *E. coriacea* dominated emissions in igapó and low várzea, whereas *H. spruceana* was the main emitter in high várzea. Such patterns point to site × species interactions, where physiological traits and morphological adaptations mediate fluxes more strongly than flood regime alone.

Within species, fluxes also varied substantially, with some stem regions acting as emission hotspots while others functioned as sinks. This fine-scale heterogeneity implies that emissions are not governed solely by species physiology but also by localised stem processes. Potential drivers include lenticel density, radial transport pathways, and microbial communities capable of methanogenesis (Anttila et al., 2024; Covey et al., 2012; Pangala et al., 2013), or external injury and infection (Gorgolewski et al., 2023). Therefore, attributing CH_4 fluxes solely to species-level functional traits risks oversimplifying CH_4 cycling and obscuring the microscale controls that regulate CH_4 production and transport within individual stems.

Wood decay provides additional insight into in-stem processes. Decay was observed across nearly all trees but did not vary significantly between forest types (igapó =12.5 ± 14.4%, high várzea =17.8 ± 15.6%, and low várzea =13.2 ± 10.9%) (Figure 4.3), indicating that site-level factors such as flood duration is not a dominant control of wood decay, supported by the lack of decay variability between submerged and non-submerged stem portions. Species-level differences, however, were pronounced: *E. coriacea* consistently exhibited greater decay than *H. spruceana*. Moreover, decay was distributed uniformly along the stem, contrasting with butt rot patterns typically concentrated near the base (Gilbert et al., 2016). Tree cores extracted confirmed systemic decay in *E. coriacea*, revealing high water content and heartwood degradation. These traits may reflect altered wetwood dynamics associated with flood tolerance (Parolin, 2012), predisposing this species to internal degradation (F. Wittmann, Schöngart, Parolin, et al., 2006). Such intrinsic traits could both sustain decay and enhance conditions for in-stem CH_4 production.

Our results highlight that the relationship between decay and CH_4 dynamics appears complex; comparisons of decay extent with radiocarbon signatures showed that increased decay was associated with older CH_4 ages, aligning more closely with wood core values, but only in *H. spruceana*. This supports the interpretation that decay facilitates internal CH_4 production (Hietala et al., 2015; Lenhart et al., 2012) and aligns with recent evidence that trees emit CH_4 produced within stems (Epron et al., 2023; Martinez et al., 2022; Mochidome et al., 2025). Yet, this pattern was not consistent across species and although statistically significant, fluxes did not consistently scale with decay across plots and species (Figure 4.5). One explanation is that internally produced CH_4 is

often cycled within stems rather than emitted directly: high internal concentrations do not always correspond to high surface fluxes (Covey et al., 2012; Epron et al., 2023). Oxidation further complicates this relationship, as $\delta^{13}C$-CH_4 signatures became enriched when fluxes were low, consistent with microbial consumption before emission (Jeffrey, Maher, Tait, et al., 2021; Chapter 3).Decay may therefore influence not only CH_4 production but also its transport and oxidation, since increased permeability to oxygen (Sorz & Hietz, 2006) could enhance methanotrophy and reduce net flux.

Different decay types may also play distinct roles in CH_4 cycling. Both decayed wood and wetwood can support CH_4 production (Covey et al., 2012; Zeikus & Ward, 1974), but fungal colonisation may either stimulate or suppress emissions depending on conditions (Hietala et al., 2015). Environmental factors such as oxygen and temperature strongly mediate these effects (Schroll et al., 2024), with CH_4 being produced by fungi in aerobic or low O_2 conditions (Highley et al., 1983; Schroll et al., 2024). Floodplain forests in particular promote fungal growth relative to terra firme (López-Quintero et al., 2012), much of it saprotrophic (Farias et al., 2025), suggesting a potential but understudied contribution to CH_4 cycling in Amazonian wetlands.

Species-level contrasts in radiocarbon signatures reinforce the role of in-stem production. In *H. spruceana*, chamber ^{14}C ages were younger than wood cores (102 ± 0.5% vs. 105 ± 1.7%), consistent with stronger soil-derived contributions, despite a higher correlation in increased CH_4 fluxes with increased wood decay. In *E. coriacea*, chamber and wood incubation ages were closely aligned (103 ± 0.9% vs. 104 ± 1.7%), pointing to greater in-stem CH_4 production, but increased wood decay stem fluxes did not correlate to increased stem fluxes.

Species-level contrasts in radiocarbon signatures reinforce differing controls on methane production pathways. In H. spruceana, chamber ^{14}C ages were younger than wood cores (102 ± 0.5% vs. 105 ± 1.7%), consistent with a stronger soil-derived contribution to emitted CH_4. Despite this, stem fluxes increased with increasing wood decay, suggesting that decay intensity modulates CH_4 transport or in-stem production even where soil-derived inputs are substantial. In contrast, *E. coriacea* exhibited closely aligned chamber and wood incubation radiocarbon ages (103 ± 0.9% vs. 104 ± 1.7%), pointing toward a dominant in-stem production pathway. However, variation in wood decay did not explain flux variability. This likely reflects the constitutive nature of decay

in this species: wood rot was consistently present across individuals (as examined through wood cores), potentially establishing a persistent methanogenic niche that elevates baseline CH_4 production. Under such conditions, decay severity may no longer be the primary limiting factor, and flux variability may instead be governed by transport dynamics, stem aeration, or oxidation processes. Thus, while decay appears to regulate flux variability in *H. spruceana*, it may function as a species-level trait rather than an individual-level driver in *E. coriacea.*

This interpretation helps explain why *E. coriacea*, despite having greater wood density, was consistently a higher emitter across both wet and dry seasons (Chapter 3). If internal methanogenesis represents a dominant and persistent source, elevated emissions may reflect sustained in-stem production rather than structural constraints imposed by wood density. Moreover, stem-based processes are inherently heterogeneous, varying with internal redox conditions, microbial community structure, and decay architecture. Such internal variability may account for the greater inter-individual flux variation observed in *E. coriacea* compared to species more strongly influenced by soil-derived inputs. Although decay was not a universal predictor of flux magnitude, its prevalence in *E. coriacea*, and the coincidence of the highest fluxes also occurring in this species underscores its likely role as a likely source for microbial CH_4 production. Together, these findings suggest that in-stem CH_4 production is strongly species-dependent, with decay acting either as a regulator (as in *H. spruceana*) or as a structural feature that elevates baseline emissions (as in *E. coriacea*). This interaction between decay processes, microbial communities, and species-specific wood traits warrants closer mechanistic investigation.

4.5.3 Sonic tomography as a tool for identifying wood decay

Sonic tomography detected internal wood decay across individuals and sites and resolved clear species contrasts (greater decay in *E. coriacea* than *H. spruceana*). Decay percentages co-varied with radiocarbon evidence for an internal source: where decay was higher, stem ^{14}C ages shifted towards wood-core values, indicating a larger tree-derived contribution to emitted CH_4 under flooded conditions. By contrast, net stem fluxes showed no clear relationship with decay across plots, consistent with the dampening effects of within-stem oxidation and transport constraints (also supported by enrichment of $\delta^{13}C$ at lower fluxes; Chapter 3). Tomography thus supplied the structural context

needed to interpret why trees with similar external appearance diverged in isotopic source signatures and flux behaviour. It was also a practical and non-invasive method to assess internal wood decay.

To our knowledge, this is the first use of ToF tomography in conjunction with stem CH_4 fluxes and ^{14}C partitioning in Amazon floodplain forests. The technique was relatively quick to implement in the field, required no destructive sampling, and did not necessitate laboratory processing, making it well-suited for large-scale surveys in inaccessible regions such as Amazonian floodplains (Zhang & Khoshelham, 2020). Importantly, this efficiency means that data on decay can be collected across many individuals and sites, providing opportunities for upscaling decay estimates to better understand its role in tree-mediated CH_4 emissions.

Internal wood decay can influence net stem CH_4 in multiple ways: production (creation of anoxic, microbially active niches), transport (altered porosity and gas pathways), and consumption (enhanced O_2 ingress promoting methanotrophy). Tomography provides a field-ready proxy for these internal conditions and therefore complements flux and isotope measurements, closing the gap between external emissions and within-stem processes (e.g. Covey et al., 2012; Epron et al., 2023; Sorz & Hietz, 2006). Furthermore, two-dimensional ToF tomography is most sensitive to advanced decay and may under-detect early-stage or near-surface degradation (Johnstone et al., 2010; Li et al., 2012; Qiu et al., 2019) and therefore may underestimate subtle processes that could still influence gas production or transport. 2D sonic tomography has been shown to detect decay at magnitudes similar to destructive methods, although at reduced sensitivity to early-stage decay (Li et al., 2012) when validated against other non-invasive techniques. Geometric assumption is to treat tree trunks as cylindrical and to assume that the cross-section is circular, which can bias estimates and potentially lead to misinterpretation of decay extent in buttressed or irregular stems common in floodplains (Burcham et al., 2023; Feng et al., 2014). Tomograms also do not distinguish decay type (fungal rot, bacterial wetwood, cavities) and is insensitive to decay occurring near the surface (Johnstone et al., 2010; Qiu et al., 2019). Moreover, ultrasonic sound waves cannot reliably differentiate between voids and actively decaying tissue (Kazemi-Najafi et al., 2009), which is particularly relevant in larger trees where hollowing and internal voids are common. Therefore, biochemical interpretation requires ancillary data; inability

to separate voids from actively decaying tissue can persist (Kazemi-Najafi et al., 2009). These factors help explain the observed decay-flux decoupling: tomography quantifies extent, whereas net flux reflects the balance between production, transport and oxidation. Looking ahead, three-dimensional sonic tomography, ones that use 8-16 sensors across the stem improving precision and potentially reducing overestimations of decay and pairing tomography with internal stem gas profiling (CH_4, O_2) and microbial/fungal assays would reduce geometric bias, help identify decay types and more tightly connect stem structure to CH_4 cycling.

4.5.4 Radiocarbon as a tool for source-portioning

In this study, ^{14}C enabled source partitioning of tree-mediated CH_4 in Amazonian floodplains. Radiocarbon has been applied successfully in a range of ecosystems to trace CH_4 sources, (Garnett et al., 2012; Moguel et al., 2022) and for characterising porewater CH_4 emissions (Dean et al., 2017) and dating tree carbon ages (Chanca et al., 2025). However, to our knowledge, it has not previously been applied to tree stem CH_4 emissions. Our results therefore provide an important first demonstration that this approach is feasible in tree-mediated systems. We observed differences in apparent ^{14}C ages between the two species examined, indicating that the technique can resolve contributions from contrasting carbon pools, even though substantial overlaps in radiocarbon signatures were also present. These overlaps highlight the challenge of fully disentangling and quantifying contributions from soil- versus stem-derived CH_4, particularly in a dynamic ecosystem where tree age, regeneration after flooding, and stress responses are likely to influence internal carbon cycling. Nonetheless, the critical outcome is that radiocarbon measurements provide an absolute indicator of in-stem CH_4 production, rather than relying solely on $\delta^{13}C$-based partitioning, and our findings confirm that such production is occurring.

Radiocarbon provides a powerful means of source partitioning because, unlike $\delta^{13}C$, it is not as strongly influenced by oxidation processes (Whiticar et al., 1986) or fractionation during transport (Conrad, 2005). This makes it particularly valuable for tree-mediated CH_4 systems, where multiple production and transport pathways can complicate stable isotope interpretations (Covey et al., 2012; Jeffrey, Maher, Tait, et al., 2021). In systems where internal wood decay or saprotrophic fungal activity may generate CH_4,

$\delta^{13}C$ values often overlap with those of soil-derived CH_4 (Schroll et al., 2020), limiting their capacity to distinguish between sources.

In this study, radiocarbon sampling of wood cores was conducted using CO_2 rather than CH_4 due to logistical constraints of flushing incubation vessels in the remote Amazon. Instead, CO_2 was used as a proxy for CH_4 under the assumption that CO_2 is a by-product of methanogenesis, particularly if várzea forests predominantly produce CH_4 via acetoclastic pathways (Blincow et al., Chapter 3). We acknowledge, however, that the radiocarbon age of CO_2 in tree stems may not correlate exactly to CH_4, and future studies should aim to directly capture CH_4 from wood cores to resolve this uncertainty.

A further limitation of radiocarbon analysis lies in the requirement for relatively high CH_4 concentrations to obtain robust measurements. To achieve a ^{14}C signature free from atmospheric interference, samples must contain at least ~1 mL of CH_4, which is difficult to collect in systems with low fluxes, such as temperate wetlands or non-flooded forests (Gauci et al., 2010; Machacova et al., 2016). In addition, the high cost of radiocarbon measurements restricts the number of samples that can feasibly be analysed, limiting spatial and temporal resolution. These challenges highlight the need for methodological advances to broaden the application of radiocarbon partitioning, particularly in diverse and low-emitting forest systems.

4.6 Conclusion

To our knowledge, this is the first study to provide direct evidence of in-tree CH_4 production in Amazonian floodplain forests. By combining three complementary approaches (CH_4 flux measurements, wood decay analysis, and radiocarbon values), we demonstrate that tree stems are not merely conduits for soil-derived CH_4 but can also act as sites of in-stem CH_4 production. Importantly, our data show that during the dry season, stem fluxes persist to at least 6 m stem height even when adjacent soils are a CH_4 sink, consistent with an internal production source. Given that the dry season in this region lasts up to 8 months, these findings indicate that stem-derived CH_4 is not negligible and may account for a significant amount of dry season CH_4 emissions.

While our results suggest factors such as decay extent, species-specific traits, and internal oxidation may influence in-stem CH_4 production, no consistent patterns emerged

across sites or species. Nevertheless, evidence from fluxes, wood decay, and ^{14}C analyses provides strong support that in-stem production occurs and that its contribution is significant. Based on observations from just two tree species, in-stem CH_4 production was substantial, implying that broader taxonomic and size-class coverage would likely increase the in-stem component. Future research should expand to include a broader diversity of species and tree ages, alongside refined assessments of wood decay using 3D imaging techniques. Complementary measurements such as internal CH_4/O_2 profiling, microbial and fungal community assays, and integrated ^{14}C measurement will be essential to unravel the underlying mechanisms of in-stem CH_4 production. Explicit inclusion of in-stem production in regional CH_4 budgets is therefore warranted, particularly for seasonally flooded forests where it may sustain CH_4 emissions beyond the wet season.

4.7 Supplementary Information

Table S5.1 | Sample sizes for wood decay, $\delta^{13}C$-CH_4 and Stem CH_4 flux

Species	*Site*	*n (wood decay)*	*n ($\delta^{13}C$-CH_4)*	*n (Stem CH_4 flux)*
E. coriacea	igapó	32	30	32
E. coriacea	high várzea	30	15	30
E. coriacea	low várzea	48	50	50
H. spruceana	igapó	29	22	30
H. spruceana	high várzea	30	15	30
H. spruceana	low várzea	46	46	46

Table S6.2 | Internal concentrations of CH_4, sampled from increment borers at 1m stem height during the dry season of November 2024.

Species	*Site*	*Average internal concentration (ppm)*	*±SD*	*n*
E. coriacea	igapó	610.58	786.48	7
E. coriacea	high várzea	558.31	1125.89	7

E. coriacea	low várzea	20833.70	66859.6	11
H. spruceana	igapó	684.90	1011.96	7
H. spruceana	high várzea	49268.73	97107.92	7
H. spruceana	low várzea	9.46	9.73	6

Chapter 5 - General discussion

5.1 Study objectives and conclusions

This section summarises the research objectives and how they addressed the knowledge gaps identified in chapter 1.

Obj. 1. To assess how soil biogeochemical properties influence stem CH_4 emissions across contrasting Amazonian floodplain ecosystems.

Conclusion 1: Soil biogeochemistry in Amazonian floodplain forests exerts a stronger control on stem CH_4 emissions than tree species identity. In várzea forest, elevated electrical conductivity, near-neutral pH, low oxygen concentrations, and high CH_4 production potential in the upper 50 cm of soil were positively correlated with stem CH_4 fluxes, especially in *E.coriacea*. Fine root biomass in this zone also showed a significant relationship with emissions, suggesting that rhizosphere activity enhances CH_4 availability and transport. In contrast, igapó forests (characterised by acidic, oxygenated, and nutrient-poor conditions), exhibited lower CH_4 fluxes and weaker correlations with below-ground variables. Despite examining species with contrasting wood density, there was no strong variability in emissions across species, but there was large variability inter-species. However, biogeochemistry did not explain the variability in CH_4 emissions within sites or among species, indicating that additional tree-level controls may be at play. These findings highlight the importance of biogeochemical context in shaping ecosystem-level emission patterns, while also underscoring the need to investigate species-specific traits and internal stem processes to better understand the drivers of CH_4 flux variability.

Obj.2. To investigate the potential for CH_4 oxidation within Amazonian floodplain tree stems.

Conclusion 2: Tropical Amazonian floodplain trees actively oxidise CH_4 within their stems. Isotopic shifts in $\delta^{13}C$-CH_4 and $\delta^{2}H$-CH_4 along the stem profile were consistent with oxidation and aligned with reductions in stem CH_4 flux. However, oxidation did not consistently scale with flux magnitude, indicating complex interactions

between CH_4 production, transport, and consumption within the stem. In some cases, reversed isotopic gradients or elevated fluxes occurred despite high oxidation fractions, suggesting that in-stem CH_4 production may obscure oxidation signals.

Oxidation patterns varied considerably between individual trees. Some showed no isotopic evidence of oxidation despite declining fluxes, further supporting the influence of internal CH_4 production. While no strong species-level trends were observed, intra-species differences may contribute to emission variability. These findings highlight the need for broader investigation into stem oxidation across diverse floodplain species to better understand its role in regulating ecosystem-level CH_4 emissions.

Obj.3. To determine the relative contribution of soil-derived CH_4 versus in-stem CH_4 production to overall stem emissions.

Conclusion 3*:* Our data confirm that stem-emitted CH_4 in Amazonian trees originates from multiple sources:

- Soil-derived CH_4 transported via roots and stem tissues.
- Internal CH_4 production within stem tissues

Stable isotope analysis ($\delta^{13}C$-CH_4 and $\delta^{2}H$- CH_4) and radiocarbon signatures (^{14}C) support this multi-source framework. Radiocarbon data revealed that CH_4 emitted from stems sometimes had a different age profile than surrounding porewater, suggesting internal production from older carbon pools. Furthermore, our data suggests the amount of CH_4 derived from individual sources likely varies across tree species. Seasonal measurements further indicate that the dominant CH_4 source may shift from soil-derived CH_4 during the wet season, to internal in-stem CH_4 production in the dry season. This seasonal decoupling has important implications for upscaling emissions, particularly if the dominant CH_4 emitting species changes seasonally.

Obj.4. To evaluate whether wood decay contributes to CH_4 production and influences stem CH_4 flux variability.

Conclusion 4: Fine-scale flux measurements suggest that in-stem CH_4 production occurs in Amazonian floodplain trees, consistent with findings from other forest systems (Epron et al., 2023). High levels of wood decay observed in these trees may contribute to

internal CH_4 generation, as previously demonstrated in temperate forests (Lenhart et al., 2012). Radiocarbon analysis revealed that trees with greater wood rot percentages tended to emit CH_4 with older ^{14}C signatures, supporting the idea of in-situ production from decayed tissues.

However, the role of wood decay in driving stem flux variability remains complex and difficult to quantify. Direct correlations between decay severity and CH_4 flux were inconsistent across sites and species, likely due to several confounding factors:

- limitations in decay detection methods (e.g., sonic tomography's sensitivity to cavities over diffuse decay),
- challenges in isolating decay-driven CH_4 from other internal sources, and the possibility that not all decay leads to CH_4 production.
- Oxidation within stems may mask production signals, further complicating interpretation.

Despite these uncertainties, the presence of wet heartwood and microbial communities capable of methanogenesis within decayed tissues (Wang et al., 2017; Zeikus & Ward, 1974) reinforces the hypothesis that wood rot is a viable source of CH_4. Future research should focus on improving decay quantification techniques and assessing the prevalence and impact of decay-driven CH_4 production across species and floodplain ecosystems.

5.2 General Discussion

Our study demonstrates that Amazonian trees play a central role in transporting CH_4, with substantial variability across floodplain ecosystems, tree species, and seasons. Below, we discuss the general conclusions of this thesis and identify future recommendations for research.

5.2.1 The influence of soil biogeochemistry on stem CH_4 emissions

Our study highlights that soil biogeochemistry exerts a stronger control on stem CH_4 emissions than tree species identity in Amazonian floodplain systems (Chapter 2). In particular, the availability of CH_4 belowground appears to be a dominant driver of stem

emissions, outweighing differences in species' capacity to transport or emit CH_4. Várzea soils, characterized by high alluvium (Prance, 1979) and a pH of 6.9-7.4 (Schmidt, 1972), provide more favourable conditions for CH_4 production and in contrast, igapó soils promote greater rhizospheric oxidation with lower pH (Schmidt, 1972) and increased dissolved oxygen, reducing the availability of CH_4 to stems. Although we cannot account for the impact of flood duration which could enhance microbial activity and CH_4 production, the longer flood duration and high flood levels in várzea forests could influence CH_4 availability through increased anoxia, more conducive to methanogenesis. These patterns point to soil processes as a key regulator of aboveground fluxes.

The water table is understood to be one of the key drivers of CH_4 production and has been suggested to play a central role in driving variability in stem emissions in some ecosystems showing stem emissions increasing with increasing water table depth (Gauci et al., 2022; Terazawa et al., 2015), however in the flooded forests of the Amazon the biogeochemistry of an ecosystem may be a more useful indicator that flood water level in understanding tree stem CH_4 emissions. Once floodplain forests are inundated, the water table ceases to be a meaningful predictor (Gauci et al., 2022; Jeffrey et al., 2023), since all flooded soils are expected to support methanogenesis under anoxic conditions (Conrad, 2009). Under these conditions, the biogeochemical environment of the flooded soils becomes the dominant control of CH_4 production and, consequently, on stem CH_4 emissions. This highlights an overlooked complexity in flooded systems: although all sites are capable of producing CH_4 when inundated, species-level and site-level variability in emissions must be understood alongside biogeochemistry rather than hydrology alone.

In Chapter 4, we examined tree stem CH_4 fluxes under dry season conditions and found no strong relationship between emissions and site-level differences. This contrasts with wet season findings (Chapter 2), where soil biogeochemistry emerged as a dominant regulator of CH_4 variability across sites. During the dry season, oxic conditions make soils less favourable for CH_4 production. Although soil chemistry was not measured in this study, it is likely a weaker influence on stem emissions at this time. Localized microsites of CH_4 production may persist, but their contribution appears far smaller than the strong soil-derived signal observed in the wet season. This suggests that the primary source of CH_4 shifts from belowground (soil) to in-stem processes during the dry season. This interpretation is supported by evidence of internal CH_4 production presented in

Chapter 3 and aligns with patterns observed in free-draining systems (Covey & Megonigal, 2019; Wang et al., 2017) as well as by non-uniform decrease in emissions up the stem (Chapter 3 and 4). Although sub-surface biogeochemical data was not collected during the dry season for this study, future studies should look to incorporate belowground sampling during dry periods to build on these findings, helping to clarify how ecosystem variability influences CH_4 production and availability in non-inundated floodplain trees. Together, these chapters suggest a seasonal shift in CH_4 regulation, from external biogeochemical controls during inundation to internal tree-level processes during drawdown, highlighting the need for integrated approaches that consider both soil and stem dynamics across hydrological phases.

5.2.2 The role of tree species in controlling stem CH_4 emissions

This study represents an important step toward integrating tree species identity into the growing body of research on tropical stem CH_4 emissions (Gauci et al., 2022; Pangala et al., 2013, 2017; Sjögersten et al., 2020; van Haren et al., 2021). By focusing on two floodplain species—*Eschweilera coriacea* and *Hevea spruceana*—we were able to explore species-specific patterns in CH_4 fluxes both within and across ecosystems. Although overall fluxes did not differ significantly between species at the ecosystem scale, *E. coriacea* consistently emitted more CH_4 than *H. spruceana*, despite having higher wood density (Chapter 2). This finding reinforces previous observations from Panama (Sjögersten et al., 2020) that wood density alone is not a reliable predictor of stem CH_4 emissions.

Examining species-level patterns in more detail revealed further distinctions. *E. coriacea* showed a stronger correlation between stem flux and near-surface soil geochemistry, whereas *H. spruceana* exhibited weaker relationships. Fluxes also declined more steeply with stem height in *E. coriacea*, suggesting species-specific differences in permeability, vessel connectivity, and basal degassing that influence axial CH_4 transport (Covey & Megonigal, 2019; Mochidome & Epron, 2024). Interestingly, despite these differences in flux profiles, CH_4 oxidation rates appeared similar across both species (Chapter 3), raising the possibility that *E. coriacea* may lose CH_4 through axial diffusion, though this remains to be tested.

Oxidation measured in Chapter 3 did not significantly vary between species, consistent with findings from subtropical forests (Jeffrey, Maher, Tait, et al., 2021). However, $\delta^{13}C\text{-}CH_4$ values measured along the stem did not always reflect oxidation, even when fluxes declined, contrasting with subtropical trees where isotopic enrichment consistently indicated oxidation (Jeffrey, Maher, Tait, et al., 2021). We suggest that internal CH_4 production may be influencing $\delta^{13}C\text{-}CH_4$ values, potentially elevating isotope ratios (Chanton, 2005) and masking oxidation signals. These findings underscore the complexity of interpreting isotopic data in systems where multiple CH_4 processes co-occur.

When investigating in-stem CH_4 production, we found higher levels of wood decay in *E. coriacea*, and radiocarbon data indicated that this species emitted a greater proportion of CH_4 from internal sources compared to *H. spruceana* (Chapter 4). This has important implications for annual CH_4 budgets: trees with active internal production may continue emitting CH_4 year-round, even outside the flooded season, potentially contributing to the non-inundated CH_4 budget of the Amazon (Gauci et al., 2022). However, our dry season measurements suggest these patterns are not easily predictable. Across sites, *E. coriacea* was not consistently the highest emitter despite its higher levels of wood decay, indicating that in-stem CH_4 production may vary with site conditions and affect species differently.

Together, these findings suggest that species-level contributions to stem CH_4 emissions go far beyond simple flux comparisons. They highlight how physiological traits, decay dynamics, and interactions with soil geochemistry shape emission patterns in distinct ways. While our study begins to unravel the influence of species on CH_4 variability, it also underscores the complexity of this relationship and the need for broader investigation.

To advance this understanding, collaboration with tree physiologists will be essential. Identifying the morphological and physiological traits that govern CH_4 transport and production, such as vessel architecture, aerenchyma development, and decay susceptibility could help explain both spatial and temporal variability in emissions. Expanding species coverage is particularly important, as microbial communities and their CH_4-related functions may shift under climate warming (Tveit et al., 2025), potentially altering the role of trees as CH_4 sources or sinks. Yet, studies on species adaptation in

Amazonian floodplains remain scarce (Parolin et al., 2004; Wittmann et al., 2022), and addressing this gap will be critical for interpreting CH_4 flux dynamics and refining ecosystem-scale emission models.

5.2.3 Sources of CH_4 from amazonian floodplain trees

Stem CH_4 emissions in wetland forests are widely understood to originate predominantly from below-ground soil sources (Gauci et al., 2010; Pangala et al., 2013; Terazawa et al., 2007). Our data supports this view: sites with higher dissolved CH_4 concentrations in porewater exhibited higher stem fluxes, suggesting that CH_4 availability belowground is a key driver of emissions. In the várzea forest plot, porewater CH_4 concentrations were substantially higher than in the igapó plot, and this was reflected in consistently elevated stem fluxes – even when comparing the same species across forest types. These findings indicate that the top 50 cm of floodplain soil, where root density and dissolved CH_4 are greatest, likely serves as the dominant source of CH_4 transported through stems. Radiocarbon analysis further supports this, with emitted CH_4 signatures closely matching those of porewater CH_4.

Our results also provide insight into the methanogenic pathways operating in these soils. In the várzea forest, dual isotope values ($\delta^{13}C$- CH_4 and $\delta^{2}H$-CH_4) were consistent with predominantly acetoclastic methanogenesis, while in the igapó forest, CH_4 composition suggested a mix of acetoclastic and hydrogenotrophic pathways. Although oxidation within stems can complicate interpretation, these site-level differences highlight that the CH_4 available to trees varies not only in concentration but also in origin.

Despite strong evidence for soil-derived CH_4 as the primary source of stem emissions, our data also points to a secondary source: in-stem CH_4 production. This is supported by $\delta^{13}C$ stable isotope shifts, radiocarbon signatures, and stem flux patterns (Chapter 4). For example, in the wet season, CH_4 concentrations often declined up the stem, but $\delta^{13}C$ values did not always reflect oxidation. In some trees, $\delta^{13}C$-CH_4 became more depleted with height, suggestive of in-stem CH_4 production rather than oxidation. During the dry season, we observed increases in CH_4 fluxes up the stem accompanied by decreasing $\delta^{13}C$ values, further supporting the likelihood of internal CH_4 generation (Chapter 4). These patterns were evident even when soil remained the dominant source during inundation (Chapter 3).

Radiocarbon measurements, when considered alongside observations of wood decay, suggest that decayed tissues may act as a potential source of CH_4 within stems (Figure 4.8). Several studies have demonstrated that microbial activity in decaying wood can produce CH_4 (Covey et al., 2012; Schink et al., 1981; Zeikus & Ward, 1974), but establishing a direct link between decay severity and stem CH_4 flux remains challenging. This complexity arises because CH_4 production within stems occurs alongside other processes. Oxidation can reduce the amount of CH_4 available for emission (Chapter 3), and uncertainties around internal transport pathways (Vroom et al., 2022) suggest that CH_4 may be redistributed vertically rather than emitted directly at decay sites. As a result, peaks in stem CH_4 flux may not correspond neatly with localized decay (Covey et al., 2012; Mochidome et al., 2025).

Together, these findings indicate that while soil remains the dominant CH_4 source for Amazonian floodplain trees, internal production, likely linked to wood decay, also contributes to emissions. Understanding the balance between these sources is essential for refining CH_4 budgets and predicting how emissions may shift under changing environmental conditions.

5.2.4 Seasonal changes in stem CH_4 patterns

Our study provides evidence that tropical floodplain forests emit CH_4 during both the wet and dry seasons, but the dominant source of stem CH_4 likely shifts with seasonal hydrology. During the wet season, when forests are inundated, soils act as the primary CH_4 source. This is supported by our observations of decreasing CH_4 concentrations with stem height – consistent with patterns reported in other studies (Pangala et al., 2013, 2015; Sjögersten et al., 2020). In contrast, our dry season measurements (Chapter 3) suggest that in-stem CH_4 production becomes the dominant source, particularly in species with higher wood decay and internal microbial activity.

By examining CH_4 fluxes at the species level, we reveal that seasonal shifts in CH_4 sources are not uniform across tree species. For example, *E. coriacea* is a larger emitter in low várzea and igapó in the dry season, but *H. spruceana* is the dominant emitter in high várzea. This variability means that high-emitting trees in the wet season are not necessarily high emitters consistently in the dry season. Understanding the source

of CH_4 for individual species at an ecosystem level, is therefore critical for predicting their contribution to seasonal fluxes.

Current estimates of dry-season CH_4 emissions from non-flooded Amazonian forests remain highly uncertain (2.2-3.6 Tg CH_4 yr^{-1}; Gauci et al., 2022) and are thought to be driven primarily by belowground sources. However, Gauci et al. (2022) reported negligible stem fluxes under low water table conditions, without assessing emissions higher up the stem. In contrast, our flux measurements, captured up to 6 m up the stem, reveal detectable stem emissions during the dry season, suggesting that trees themselves may represent an additional CH_4 source when the water table is low. When scaled vertically, these emissions could contribute meaningfully to basin-wide budgets of seasonally flooded forests. Importantly, our data also show strong species-level variability. If only a few species emit disproportionately large amounts of CH_4 yet occupy a relatively small fraction of forest area, upscaling without accounting for this heterogeneity could lead to significant overestimation. Incorporating species-specific emission profiles across wider spatial scales will therefore be essential for refining seasonal CH_4 budgets.

Understanding seasonal CH_4 patterns is especially important in the context of climate change. Fleischmann et al. (2023) report that maximum annual flood extent in the central Amazon basin has increased by ~26% since the 1980s, alongside longer flood durations. Notably, seven of the ten highest annual water levels recorded in the past 119 years have occurred since 2009. These trends suggest that floodplain forests will experience more prolonged and extensive inundation, potentially altering seasonal CH_4 emission dynamics. Integrating species-level insights with seasonal patterns will be essential for predicting future CH_4 emissions under changing hydrological regimes.

5.2.5 How our work contributes to refining upscaling CH_4 emission estimates in the Amazon

Upscaling CH_4 fluxes from tropical wetland forests remains a major challenge due to the complexity and variability of tree CH_4 emissions. While previous studies have attempted to estimate CH_4 contributions from wetland systems (Table 5.1), our findings highlight several critical factors that must be considered before reliable upscaling can be achieved.

Our data reveals interspecies variability in stem CH_4 (Chapter 2), and species-specific oxidation patterns (Chapter 3) may influence net fluxes, particularly under changing environmental conditions. Understanding these internal and external controls on CH_4 oxidation is essential before extrapolating fluxes across diverse forest types. Importantly, we show that the relative contribution of tree versus soil CH_4 emissions can vary by species, which has implications for seasonal flux dynamics and source attribution (Chapter 4). Further, if certain species contribute disproportionately to CH_4 emissions, then changes in forest composition (whether due to climate-driven mortality or successional dynamics) could significantly alter regional fluxes.

Given the Amazon's extraordinary tree diversity, the inclusion of only two species in our study underscores the need for broader sampling. Most published studies have focused on a narrow subset of species (Gauci et al., 2010; Jeffrey, Maher, Tait, et al., 2021) or do not account for species (Pangala et al., 2017), limiting our understanding of how stem fluxes scale across forest plots. Future research should incorporate tools such as LiDAR or aerial drone surveys to quantify species abundance and canopy structure, enabling more accurate estimates of forest-level CH_4 emissions.

Table 7.1| Summary of published estimates of tree-mediated CH_4 fluxes across a range of wetland forest types. Fluxes are reported as daily emissions per hectare (nmol CH_4 ha^{-1} d^{-1}), alongside the proportion of total wetland CH_4 emissions attributed to trees in each study. The table also includes the percentage of tree coverage within the surveyed area, where available, to provide context for the relative contribution of stem emissions.

Wetland forest type	*Tree CH_4 flux (μg CH_4 ha^{-1} d^{-1})*	*Proportion wetland net emission flux*	*Publication*	*Tree coverage of surveyed area*
Peatland (Borneo)	6.7 to 30.1	67 to 87%	Pangala et al. 2013	n/a
Temperate (UK)	0.61 to 5.7	9 to 27%	Pangala et al. 2015	2%
Floodplain (Amazon)	47.2 to 456.8	50 %	Pangala et al. 2017	0.8%
Mangrove (Australia)	0.35 to 2.8	3 to 26 %	Jeffrey et al 2019	0.3%

Melaleuca (Australia)	278.8	10%	Jeffrey et al. 2020	2.1%
Peatland (Panama)	48.1 to 348.8	30%	Sjogersten et al. 2020	1%
Lealeuca (Australia)	19 to 606.3	28 to 68%	Jeffrey et al. 2023	2.2%

Our study spans both igapó and várzea floodplain systems, which differ in hydrology, flood duration, and water chemistry (Chapter 2). These differences appear to drive variation in CH_4 production and transport, with implications for stem emissions. Such plot-level variability reinforces the need for caution when upscaling across floodplain areas. As shown in Table 5.1, published flux estimates vary widely across wetland forest types and measurements taken only cover only a small proportion of the floodplain. Understanding the variability across these wetland systems may help reduce the uncertainty in upscaling estimates.

Whilst seasonally inundated forests are recognised contributors to ecosystem CH_4 emissions, our data underscore the importance of site-specific hydrology and floodwater composition in shaping subsurface CH_4 dynamics and, consequently, stem emissions. Caution should be taken when upscaling emissions from one tropical forest to another as hydrological regimes differ markedly across the tropics (Lee et al., 2011).

Seasonal inundation plays a key role in shaping CH_4 dynamics. Our results suggest that different tree species may dominate as CH_4 emitters across wet and dry seasons (Chapter 3), with shifts in source contribution between soil and stem, potentially driving seasonal variability. This underscores the importance of understanding not just emission rates, but also the underlying sources and their temporal dynamics.

Furthermore, tree stem CH_4 emissions are not currently considered as a separate source in the global methane budget (Saunois et al., 2025). Our work suggests that this omission may lead to underestimation of wetland CH_4 emissions, especially in forested systems where tree-mediated fluxes can be substantial.

5.3 Summary and conclusions

5.3.1 Recommendation for future work

Several mechanistic questions emerge from our findings. The dominant production sources of CH_4 within stems, and their variation across species and seasons, remain unresolved. It is unclear whether internal processes alone can explain the peaks in stem CH_4 fluxes observed in some individuals, or what the oxidation capacity "tipping point" might be – beyond which trees can no longer sufficiently oxidise CH_4 before it is emitted. As our study measured oxidation patterns in only two species, future work should expand the range of species investigated to capture broader variability in CH_4 regulation across floodplain forests. Additionally, identifying methanotrophic communities could further support an increased understanding of oxidation patterns (Jeffrey, Maher, Tait, et al., 2021), particularly across species and ecosystems.

Fine-scale measurements from small incremental chambers revealed mixed emission patterns along stems and suggest that certain species may produce CH_4 internally. Supporting this, our isotopic data showed a clear contrast between porewater and stem values, pointing to an in-stem production source that remains unaccounted for. Future research should therefore aim to disentangle the relative contributions of soil- and stem-derived CH_4 and examine how these vary across species, seasons, and floodplain systems. Stable isotope tracers offer a promising tool. For example, introducing ^{13}C-labelled CH_4 into soils and tracking its signal up stems could help identify the height at which soil-derived CH_4 is attenuated, either through oxidation or dilution with in-stem production, meaning any residual CH_4 detected is sourced from in-stem CH_4 production. Complementary use of ^{14}C-CH_4 in mesocosm experiments would allow more precise tracing of CH_4, helping to separate transport, oxidation, and internal production pathways under controlled conditions. Together, such tracer approaches applied in both field and laboratory settings could provide a more mechanistic understanding of CH_4 cycling within Amazonian trees.

The role of wood decay in contributing to stem CH_4 flux also requires closer investigation. Addressing this will involve both clarifying the contribution of in-stem CH_4 production and accurately assessing the prevalence of decay in trees, so that flux estimates can be reliably upscaled. In our work, we introduced radiocarbon measurements as a technique to partition CH_4 sources between soil and stem production. This approach offers a way to quantify the relative contributions of each source; however, further refinement is needed. In particular, obtaining ^{14}C data from older trees would help to more

clearly distinguish tree-derived CH_4 from soil-derived emissions. Incubating wood cores under anoxic conditions may also help produce CH_4 in the quantities required to analyse CH_4 in wood stems for a more accurate comparison for source attribution. In addition, sonic tomography provides a promising method for rapidly assessing wood decay across spatial scales, but decay-quantification techniques still require development to allow accurate estimation of its prevalence and impact on CH_4 flux. Finally, future studies should investigate stem CH_4 transport to determine the extent to which emission hotspots can be attributed to decay processes.

Looking ahead, broadening the species range examined will be key to understanding how both oxidation and in-stem production regulate emissions at the forest scale. Developing functional trait groupings that explain interspecific variability in CH_4 fluxes would provide a framework for generalising findings. Scaling species-level processes to the landscape will also require integrating detailed field measurements with remote sensing and drone-based approaches, enabling refinement of forest-scale CH_4 budgets. Ultimately, embedding species-specific and process-based parameters (e.g. in-stem CH_4 production potential, oxidation capacity, and wood decay prevalence) into ecosystem carbon models will strengthen predictions of CH_4 emissions from wetlands and floodplains under future climate and hydrological change.

5.4 Conclusion

The findings that have emerged from this thesis contribute to a growing understanding of CH_4 production and movement within stems, across species, ecosystems and seasons. The studies included demonstrate how tree stem CH_4 is strongly regulated by ecosystem level biogeochemistry whilst also being moderated by internal stem oxidation and production. Separating sources of CH_4 from soil-derived and stem-derived is intricate and will be aided with an increased understanding of how stem-derived CH_4 is produced.

6. References

Anttila, J., Tikkasalo, O. P., Hölttä, T., Lintunen, A., Vainio, E., Leppä, K., Haikarainen, I., Koivula, H., Ghasemi Falk, H., Kohl, L., Launiainen, S., & Pihlatie, M. (2024). Model of methane transport in tree stems: Case study of sap flow and radial diffusion. *Plant, Cell & Environment*, *47*(1), 140–155. https://doi.org/10.1111/PCE.14718

Arnold, W., Gewirtzman, J., Raymond, P. A., Duguid, M. C., Brodersen, C. R., Brown, C., Norbraten, N., T'ika, Q., Wood, V., Bradford, M. A., Peccia, J., & Gewirtzman, J. (2025). A diverse and distinct microbiome inside living trees. *Nature*, *644*. https://doi.org/10.1038/s41586-025-09316-0

Aulakh, M. S., Wassmann, R., Bueno, C., & Rennenberg, H. (2001). Impact of root exudates of different cultivars and plant development stages of rice (Oryza sativa L.) on methane production in a paddy soil. *Plant and Soil*, *230*(1), 77–86.

Barba, J., Bradford, M. A., Brewer, P. E., Bruhn, D., Covey, K., van Haren, J., Megonigal, J. P., Mikkelsen, T. N., Pangala, S. R., Pihlatie, M., & Poulter, B. (2019). Viewpoints Methane emissions from tree stems: A new frontier in the global carbon cycle. *New Phytologist*, *222*(1), 18–28.

Barba, J., Poyatos, R., & Vargas, R. (2019). Automated measurements of greenhouse gases fluxes from tree stems and soils: Magnitudes, patterns and drivers. *Scientific Reports*, *9*(1). https://doi.org/10.1038/s41598-019-39663-8

Barbosa, P. M., Melack, J. M., Amaral, J. H. F., Linkhorst, A., & Forsberg, B. R. (2021). Large Seasonal and Habitat Differences in Methane Ebullition on the Amazon

Floodplain. *Journal of Geophysical Research: Biogeosciences*, *126*(7), e2020JG005911. https://doi.org/10.1029/2020JG005911

Barbosa, P. M., Melack, J. M., Farjalla, V. F., Amaral, J. H. F., Scofield, V., & Forsberg, B. R. (2016). Diffusive methane fluxes from Negro, Solimões and Madeira rivers and fringing lakes in the Amazon basin. *Limnology and Oceanography*, *61*(S1), S221–S237. https://doi.org/10.1002/LNO.10358

Bastviken, D., Cole, J., Pace, M., & Tranvik, L. (2004). Methane emissions from lakes: Dependence of lake characteristics, two regional assessments, and a global estimate. *Global Biogeochemical Cycles*, *18*(4), 1–12. https://doi.org/10.1029/2004GB002238

Baur, P. A., Rodrigues-Oliveira, T., Hager, K., Luo, Z.-H., Schleper, C., & Glatzel, S. (2025). Temporal dynamics of CH_4 emission pathways in the subsaline reed wetland of Lake Neusiedl. *Biogeosciences*, *22*(17), 4467–4490. https://doi.org/10.5194/bg-22-4467-2025

Bloemen, J., Mcguire, M. A., Aubrey, D. P., Teskey, R. O., & Steppe, K. (2013). Transport of root-respired CO2 via the transpiration stream affects aboveground carbon assimilation and CO2 efflux in trees. *New Phytologist*, *197*(2), 555–565. https://doi.org/10.1111/j.1469-8137.2012.04366.x

Bloom, A. A., Bowman, W. K., Lee, M., Turner, J. A., Schroeder, R., Worden, R. J., Weidner, R., McDonald, C. K., & Jacob, J. D. (2017). A global wetland methane emissions and uncertainty dataset for atmospheric chemical transport models (WetCHARTs version 1.0). *Geoscientific Model Development*, *10*(6), 2141–2156. https://doi.org/10.5194/gmd-10-2141-2017

Bloom, A. A., Palmer, P. I., Fraser, A., & Reay, D. S. (2021). Seasonal variability of tropical wetland CH 4 emissions: The role of the methanogen-available carbon pool. *Biogeosciences*, *9*. https://doi.org/10.5194/bg-9-2821-2012

Boddy, L., & Rayner, A. D. M. (1983). Origins of Decay in Living Deciduous Trees: The Role of Moisture Content and a Re-Appraisal of the Expanded Concept of Tree Decay. *New Phytologist*, *94*(4), 623–641. https://doi.org/10.1111/j.1469-8137.1983.tb04871.x

Bréchet, L. M., Salomón, R. L., Machacova, K., Stahl, C., Burban, B., Goret, J. Y., Steppe, K., Bonal, D., & Janssens, I. A. (2025). Insights into the subdaily variations in methane, nitrous oxide and carbon dioxide fluxes from upland tropical tree stems. *New Phytologist*, *245*(6), 2451–2466. https://doi.org/10.1111/nph.20401

Bridgham, S. D., Cadillo-Quiroz, H., Keller, J. K., & Zhuang, Q. (2013). Methane emissions from wetlands: Biogeochemical, microbial, and modeling perspectives from local to global scales. *Global Change Biology*, *19*(5), 1325–1346. https://doi.org/10.1111/gcb.12131

Bubier, J., Moore, T., Savage, K., & Crill, P. (2005). A comparison of methane flux in a boreal landscape between a dry and a wet year. *Global Biogeochemical Cycles*, *19*(1), 1–11. https://doi.org/10.1029/2004GB002351

Burcham, D. C., Brazee, N. J., Marra, R. E., & Kane, B. (2023). Geometry matters for sonic tomography of trees. *Trees - Structure and Function*, *37*(3), 837–848. https://doi.org/10.1007/S00468-023-02387-4

Camargo, M., Giarrizzo, T., & Jesus, Ajs. (2015). Effect of seasonal flooding cycle on litterfall production in alluvial rainforest on the middle Xingu River (Amazon

basin, Brazil). *Brazilian Journal of Biology*, *75*(3 suppl 1), 250–256. https://doi.org/10.1590/1519-6984.00514BM

Cawley, K., Goodman, K., Weintraub, S., & Parker, S. (2020). Neon user guide to dissolved gases in surface water. In *neonDissGas package*.

Chanca, I., Levin, I., Trumbore, S., Macario, K., Lavric, J., Quesada, C. A., Araújo, A. C. D., Júnior, C. Q. D., Asperen, H. V., Hammer, S., & Sierra, C. A. (2025). How long does carbon stay in a near-pristine central Amazon forest? An empirical estimate with radiocarbon. *Biogeosciences*, *22*(2), 455–472. https://doi.org/10.5194/bg-22-455-2025

Chanton, J., Chaser, L., Glasser, P., & Siegel, D. (2005). Carbon and Hydrogen Isotopic Effects in Microbial Methane from Terrestrial Environments. In L. B. Flanagan, J. R. Ehleringer, & D. E. Pataki (Eds), *Stable Isotopes and Biosphere—Atmosger Interactions. Processes and Biological Controls* (pp. 85–105). Elsevier Academic Press.

Chanton, J. P. (2005). The effect of gas transport on the isotope signature of methane in wetlands. *Organic Geochemistry*, *36*(5), 753–768. https://doi.org/10.1016/j.orggeochem.2004.10.007

Chanton, J. P., & Whiting, G. (1995). Ebullition and transport by plants. In *Biogenic Trace Gases: Measuring Emissions from Soil and Water* (p. 98).

Chave, J., Coomes, D., Jansen, S., Lewis, S. L., Swenson, N. G., & Zanne, A. E. (2009). Towards a worldwide wood economics spectrum. *Ecology Letters*, *12*(4), 351–366. https://doi.org/10.1111/j.1461-0248.2009.01285.x

Coleman, D. D., Risatti, J. B., & Schoell, M. (1981). Fractionation of carbon and hydrogen isotopes by methane-oxidizing bacteria. *Geochimica et Cosmochimica Acta*, *45*(7), 1033–1037. https://doi.org/10.1016/0016-7037(81)90129-0

Conrad, R. (1989). Control of methane production in terrestrial ecosystems. *Exchange of Trace Gases between Terrestrial Ecosystems and the Atmosphere*, 39–58.

Conrad, R. (2005). Quantification of methanogenic pathways using stable carbon isotopic signatures: A review and a proposal. *Organic Geochemistry*, *36*(5), 739–752. https://doi.org/10.1016/J.ORGGEOCHEM.2004.09.006

Conrad, R. (2007). Microbial Ecology of Methanogens and Methanotrophs. *Advances in Agronomy*, *96*, 1–63. https://doi.org/10.1016/S0065-2113(07)96005-8

Conrad, R. (2009). The global methane cycle: Recent advances in understanding the microbial processes involved. *Environmental Microbiology Reports*, *1*(5), 285–292. https://doi.org/10.1111/j.1758-2229.2009.00038.x

Cook, S., Peacock, M., Evans, C. D., Page, S. E., Whelan, M., Gauci, V., & Khoon, K. L. (2016). *Open Research Online Cold storage as a method for the long-term preservation of tropical dissolved organic carbon (DOC)*. *18*, 1–8. https://doi.org/10.19189/MaP.2016.OMB.249

Covey, K. R., & Megonigal, J. P. (2019). Methane production and emissions in trees and forests. *New Phytologist*, *222*(1), 35–51. https://doi.org/10.1111/NPH.15624

Covey, K. R., Wood, S. A., Warren, R. J., Lee, X., & Bradford, M. A. (2012). Elevated methane concentrations in trees of an upland forest. *Geophysical Research Letters*, *39*(15). https://doi.org/10.1029/2012GL052361

Cristina, A. C., Struyf, E., Roland, M., Gielen, B., Vincke, C., & Janssens, I. A. (2022). Two types of installation of 3D-printed zero tension lysimeter for soil leaching

and water bucket model validation. *European Journal of Soil Science*, *73*(4). https://doi.org/10.1111/EJSS.13295

Cugler, G., Figueiredo, V., Gauci, V., Stauffer, T., Peixoto, R. B., Rao Pangala, S., & Enrich-Prast, A. (2024). Analysis of CH4 and N2O Fluxes in the Dry Season: Influence of Soils and Vegetation Types in the Pantanal. *Forests*, *15*(12). https://doi.org/10.3390/f15122224

da Silva Marinho, T. A., Piedade, M. T. F., & Wittmann, F. (2010). Distribution and population structure of four Central Amazonian high-várzea timber species. *Wetlands Ecology and Management*, *18*(6), 665–677. https://doi.org/10.1007/s11273-010-9186-y

Daniel, W., Stahl, C., Burban, B., Goret, J. Y., Cazal, J., Richter, A., Janssens, I. A., & Bréchet, L. M. (2023). Tree stem and soil methane and nitrous oxide fluxes, but not carbon dioxide fluxes, switch sign along a topographic gradient in a tropical forest. *Plant and Soil*, *488*(1–2), 533–549. https://doi.org/10.1007/S11104-023-05991-Y/FIGURES/4

De Souza Ferreira Neto, G., Baccaro, F. B., Quesada, C. A. N., Figueiredo, A. S., Oliveira, R., Gomes, E., Spironello, W. R., & Barnett, A. A. (2021). Sedimental Journey: Soil Fertility of Fluvial Islands Increases with Proximity to An Amazonian White-Water River. *Wetlands*, *41*(8), 104. https://doi.org/10.1007/s13157-021-01506-6

de Visscher, A., de Pourcq, I., & Chanton, J. (2004). Isotope fractionation effects by diffusion and methane oxidation in landfill cover soils. *Journal of Geophysical Research: Atmospheres*, *109*(D18), 18111–18111. https://doi.org/10.1029/2004JD004857

Dean, J. F., Billett, M. F., Murray, C., & Garnett, M. H. (2017). Ancient dissolved methane in inland waters revealed by a new collection method at low field concentrations for radiocarbon (14C) analysis. *Water Research*, *115*, 236–244. https://doi.org/10.1016/J.WATRES.2017.03.009

Delwiche, K. B., Knox, S. H., Malhotra, A., Fluet-Chouinard, E., McNicol, G., Feron, S., Ouyang, Z., Papale, D., Trotta, C., Canfora, E., Cheah, Y. W., Christianson, D., Alberto, M. C. R., Alekseychik, P., Aurela, M., Baldocchi, D., Bansal, S., Billesbach, D. P., Bohrer, G., … Jackson, R. B. (2021). FLUXNET-CH4: A global, multi-ecosystem dataset and analysis of methane seasonality from freshwater wetlands. *Earth System Science Data*, *13*(7), 3607–3689. https://doi.org/10.5194/essd-13-3607-2021

Devol, A. H., Richey, J. E., Clark, W. A., King, S. L., & Martinelli, L. A. (1988). Methane emissions to the troposphere from the Amazon floodplain. *Journal of Geophysical Research: Atmospheres*, *93*(D2), 1583–1592. https://doi.org/10.1029/JD093iD02p01583

Engle, D., & Melack, J. M. (2000). Methane emissions from an Amazon floodplain lake: Enhanced release during episodic mixing and during falling water. *Biogeochemistry*, *51*(1), 71–90. https://doi.org/10.1023/A:1006389124823/METRICS

Epron, D., Mochidome, T., Tanabe, T., Dannoura, M., & Sakabe, A. (2023). Variability in Stem Methane Emissions and Wood Methane Production of Different Tree Species in a Cold Temperate Mountain Forest. *Ecosystems*, *26*(4), 784–799. https://doi.org/10.1007/S10021-022-00795-0/FIGURES/7

Etminan, M., Myhre, G., Highwood, E. J., & Shine, K. P. (2016). Radiative forcing of carbon dioxide, methane, and nitrous oxide: A significant revision of the methane radiative forcing. *Geophysical Research Letters*, *43*(24), 12,614-12,623. https://doi.org/10.1002/2016GL071930

Evans, D. E. (2004). Aerenchyma formation. *New Phytologist*, *161*(1), 35–49. https://doi.org/10.1046/j.1469-8137.2003.00907.x

Farias, V. P., Vilhena, M. do P. S. P., Gondim-Vieira, A. W., Mendes-Freire, R. B., Pacheco, R. D., Silva, B. S. F. da, & Soares, A. M. da S. (2025). Distribution Patterns of Wood-Decay Macrofungi (Agaricomycetes) in Floodplain Forest Islands of the Eastern Amazon. *Journal of Fungi*, *11*(4). https://doi.org/10.3390/JOF11040288,

Feng, H., Guo, J., Ma, X., Han, M., Kneeshaw, D., Sun, H., Malghani, S., Chen, H., & Wang, W. (2022). Methane emissions may be driven by hydrogenotrophic methanogens inhabiting the stem tissues of poplar. *New Phytologist*, *233*(1), 182–193. https://doi.org/10.1111/NPH.17778

Feng, H., Li, G., Fu, S., & Wang, X. (2014). *Tomographic Image Reconstruction Using an Interpolation Method for Tree Decay Detection*.

Fichtler, E., Clark, D. A., & Worbes, M. (2003). Age and Long-term Growth of Trees in an Old-growth Tropical Rain Forest, Based on Analyses of Tree Rings and 14C1. *Biotropica*, *35*(3), 306–317. https://doi.org/10.1111/J.1744-7429.2003.TB00585.X

Fleischmann, A. S., Papa, F., Hamilton, S. K., Fassoni-Andrade, A., Wongchuig, S., Espinoza, J.-C., D Paiva, R. C., Melack, J. M., Fluet-Chouinard, E., Castello, L., Almeida, R. M., Bonnet, M.-P., Alves, L. G., Moreira, D., Yamazaki, D., Revel,

M., & Collischonn, W. (2023). Increased floodplain inundation in the Amazon since 1980. *Environ. Res. Lett*, *18*, 34024–34024. https://doi.org/10.1088/1748-9326/acb9a7

Flores, B. M., Montoya, E., Sakschewski, B., Nascimento, N., Staal, A., Betts, R. A., Levis, C., Lapola, D. M., Esquível-Muelbert, A., Jakovac, C., Nobre, C. A., Oliveira, R. S., Borma, L. S., Nian, D., Boers, N., Hecht, S. B., Steege, H. ter, Arieira, J., Lucas, I. L., … Hirota, M. (2024). Critical transitions in the Amazon forest system. *Nature 2024 626:7999*, *626*(7999), 555–564. https://doi.org/10.1038/s41586-023-06970-0

Fontes, C. G., Fine, P. V. A., Wittmann, F., Bittencourt, P. R. L., Piedade, M. T. F., Higuchi, N., Chambers, J. Q., & Dawson, T. E. (2020). Convergent evolution of tree hydraulic traits in Amazonian habitats: Implications for community assemblage and vulnerability to drought. *New Phytologist*, *228*(1), 106–120. https://doi.org/10.1111/NPH.16675

Forster, P., Storelvmo, T., Armour, K., Collins, W., Dufresne, J.-L., Lunt, D. J., Mauritsen, T., Palmer, M. D., Watanabe, M., Wild, M., & Zhang, H. (2023). The Earth's Energy Budget, Climate Feedbacks and Climate Sensitivity. In V. Massob-Delmotte, P. Zhai, A. Pirani, S. L. Connors, C. Péan, S. Berger, N. Caud, Y. Chen, L. Goldfarb, M. I. Gomis, M. Huang, K. Leitzell, E. Lonnoy, J. B. R. Matthrews, T. K. Maycock, T. Waterfield, O. Yelekçi, R. Yu, & B. Zhou (Eds), *Climate Change 2021 – The Physical Science Basis* (pp. 923–1054). Cambridge University Press. https://doi.org/10.1017/9781009157896.009

Furch, K. (1997). Chemistry of Varzea and Igapo Soils and Nutrient Inventory of Their Floodplain Forests. In *The central Amazon floodplain: Ecology of a pulsing system* (pp. 47–67). Springer Berlin Heidelberg.

Furch, K., & Junk, W. (1997). Physicochemical Conditions in Floodplains. In J. Wolfgang (Ed.), *The central Amazon floodplain. Ecology of a Pulsing System* (Vol. 126, pp. 69–107). Springer.

Furch, K., & Wolfgang, J. (1997). Physicochemical conditions in the floodplains. In *The central Amazon floodplain: Ecology of a pulsing system* (pp. 69–108). (Original work published Springer Berlin Heidelberg)

Galand, P. E., Fritze, H., Conrad, R., & Yrjälä, K. (2005). Pathways for methanogenesis and diversity of methanogenic archaea in three boreal peatland ecosystems. *Applied and Environmental Microbiology*, *71*(4), 2195–2198. https://doi.org/10.1128/AEM.71.4.2195-2198.2005/FORMAT/EPUB

Garnett, M. H., Gulliver, P., & Billett, M. F. (2016). A rapid method to collect methane from peatland streams for radiocarbon analysis. *Ecohydrology*, *9*(1), 113–121. https://doi.org/10.1002/eco.1617

Garnett, M. H., Hardie, S. M. L., & Murray, C. (2012). Radiocarbon analysis of methane emitted from the surface of a raised peat bog. *Soil Biology and Biochemistry*, *50*, 158–163. https://doi.org/10.1016/j.soilbio.2012.03.018

Garnett, M. H., Hardie, S. M. L., & Murray, C. (2020). Radiocarbon analysis reveals that vegetation facilitates the release of old methane in a temperate raised bog. *Biogeochemistry*, *148*(1), 1–17. https://doi.org/10.1007/s10533-020-00638-x

Garnett, M. H., Murray, C., Gulliver, P., & Ascough, P. L. (2019). Radiocarbon Analysis of Methane at the NERC Radiocarbon Facility (East Kilbride). *Radiocarbon*, *61*(5), 1477–1487. https://doi.org/10.1017/rdc.2019.3

Garnett, M., & Murray, C. (2013). Processing of CO2 samples collected using zeolite molecular sieve for 14C analysis at the NERC radiocarbon facilty (East Kilbride, UK). *Radiocarbon*, *55*(2), 410–415.

Gauci, V., Figueiredo, V., Gedney, N., Pangala, S. R., Stauffer, T., Weedon, G. P., & Enrich-Prast, A. (2022). Non-flooded riparian Amazon trees are a regionally significant methane source. *Philosophical Transactions of the Royal Society A: Mathematical, Physical and Engineering Sciences*, *380*(2215). https://doi.org/10.1098/rsta.2020.0446

Gauci, V., Gowing, D. J. G., Hornibrook, E. R. C., Davis, J. M., & Dise, N. B. (2010). Woody stem methane emission in mature wetland alder trees. *Atmospheric Environment*, *44*(17), 2157–2160. https://doi.org/10.1016/j.atmosenv.2010.02.034

Gauci, V., Pangala, S. R., Shenkin, A., Barba, J., Bastviken, D., Figueiredo, V., Gomez, C., Enrich-Prast, A., Sayer, E., Stauffer, T., Welch, B., Elias, D., McNamara, N., Allen, M., & Malhi, Y. (2024). Global atmospheric methane uptake by upland tree woody surfaces. *Nature*, *631*(8022), 796–800. https://doi.org/10.1038/s41586-024-07592-w

Gedney, N., Rudorff, C., & Betts, R. A. (2024). Future amazon basin wetland hydrology under projected climate change. *PLOS Water*, *3*(9), e0000225. https://doi.org/10.1371/JOURNAL.PWAT.0000225

Gilbert, G. S., Ballesteros, J. O., Barrios-Rodriguez, C. A., Bonadies, E. F., Cedeño-Sánchez, M. L., Fossatti-Caballero, N. J., Trejos-Rodríguez, M. M., Pérez-Suñiga, J. M., Holub-Young, K. S., Henn, L. A. W., Thompson, J. B., García-López, C. G., Romo, A. C., Johnston, D. C., Barrick, P. P., Jordan, F. A., Hershcovich, S., Russo, N., Sánchez, J. D., … Hubbell, S. P. (2016). Use of sonic tomography to detect and quantify wood decay in living trees. *Applications in Plant Sciences*, *4*(12). https://doi.org/10.3732/apps.1600060

Girkin, N. T., Vane, C. H., Turner, B. L., Ostle, N. J., & Sjögersten, S. (2020). Root oxygen mitigates methane fluxes in tropical peatlands. *Environmental Research Letters*, *15*(6), 064013–064013. https://doi.org/10.1088/1748-9326/AB8495

Gorgolewski, A. S., Caspersen, J. P., Vantellingen, J., Thomas, S. C., & Daniels, J. H. (2023). Tree Foliage is a Methane Sink in Upland Temperate Forests. *Ecosystems*, *26*. https://doi.org/10.1007/s10021-022-0075

Hanson, R. S., & Hanson, T. E. (1996). Methanotrophic bacteria. *Microbiological Reviews*, *60*(2), 439–471. https://doi.org/10.1128/MR.60.2.439-471.1996,

Herbinger, K., Then, C., Löw, M., Haberer, K., Alexou, M., Koch, N., Remele, K., Heerdt, C., Grill, D., Rennenberg, H., Häberle, K. H., Matyssek, R., Tausz, M., & Wieser, G. (2005). Tree age dependence and within-canopy variation of leaf gas exchange and antioxidative defence in Fagus sylvatica under experimental free-air ozone exposure. *Environmental Pollution*, *137*(3), 476–482. https://doi.org/10.1016/J.ENVPOL.2005.01.034

Hess, L. L., Melack, J. M., Affonso, A. G., Barbosa, C., Gastil-Buhl, M., & Novo, E. M. L. M. (2015). Wetlands of the Lowland Amazon Basin: Extent, Vegetative Cover,

and Dual-season Inundated Area as Mapped with JERS-1 Synthetic Aperture Radar. *Wetlands*, *35*, 745–756. https://doi.org/10.1007/s13157-015-0666-y

Heuertz, M., Caron, H., Scotti-Saintagne, C., Pétronelli, P., Engel, J., Tysklind, N., Miloudi, S., Gaiotto, F. A., Chave, J., Molino, J.-F., Sabatier, D., Loureiro, J., & Budde, K. B. (2020). The hyperdominant tropical tree Eschweilera coriacea (Lecythidaceae) shows higher genetic heterogeneity than sympatric Eschweilera species in French Guiana. *Plant Ecology and Evolution*, *153*(1), 67–81. https://doi.org/10.5091/plecevo.2020.1565

Hietala, A. M., Dörsch, P., Kvaalen, H., & Solheim, H. (2015). Carbon dioxide and methane formation in norway spruce stems infected by white-rot fungi. *Forests*, *6*(9), 3304–3325. https://doi.org/10.3390/f6093304

Highley, T. L., Bar-Lev, S. S., Kirk, T. K., & Larsen, M. J. (1983). Influence of O2 and CO2 on wood decay by heartrot and saprot fungi. *Phytopathology*, *73*, 630–633.

Horwath, W. R., Pregitzer, K. S., & Paul, E. A. (1994). 4C Allocation in tree-soil systems. In *Tree Physiology* (Vol. 14, pp. 1163–1176). Heron Publishing-Victoriu. http://treephys.oxfordjournals.org/

Huang, X., Liu, X., Xue, Y., Pan, B., Xiao, L., Wang, S., Lever, M. A., Hinrichs, K.-U., Inagaki, F., & Liu, C. (2022). Methane Production by Facultative Anaerobic Wood-Rot Fungi via a New Halomethane-Dependent Pathway. *Microbiology Spectrum*, *10*(5). https://doi.org/10.1128/spectrum.01700-22

Inubushi, K., Otake, S., Furukawa, Y., Shibasaki, N., Ali, M., Itang, A. M., & Tsuruta, H. (2005). Factors influencing methane emission from peat soils: Comparison of tropical and temperate wetlands. *Nutrient Cycling in Agroecosystems*, *71*(1), 93–99. https://doi.org/10.1007/s10705-004-5283-8

Jang, E. S., & Kang, C. W. (2022). Porosity analysis of three types of balsa (Ochroma pyramidale) wood depending on density. *Journal of Wood Science*, *68*(1), 1–6. https://doi.org/10.1186/S10086-022-02037-2/TABLES/2

Jeffrey, L. C., Maher, D. T., Chiri, E., Leung, P. M., Nauer, P. A., Arndt, S. K., Tait, D. R., Greening, C., & Johnston, S. G. (2021). Bark-dwelling methanotrophic bacteria decrease methane emissions from trees. *Nature Communications*, *12*(1), 1–8. https://doi.org/10.1038/S41467-021-22333-7;TECHMETA

Jeffrey, L. C., Maher, D. T., Tait, D. R., Reading, M. J., Chiri, E., Greening, C., & Johnston, S. G. (2021). Isotopic evidence for axial tree stem methane oxidation within subtropical lowland forests. *New Phytologist*, *230*, 2200–2212. https://doi.org/10.1111/nph.17343

Jeffrey, L. C., Moras, C. A., Tait, D. R., Johnston, S. G., Call, M., Sippo, J. Z., Jeffrey, N. C., Laicher-Edwards, D., & Maher, D. T. (2023). Large Methane Emissions From Tree Stems Complicate the Wetland Methane Budget. *Journal of Geophysical Research: Biogeosciences*, *128*(12). https://doi.org/10.1029/2023JG007679

Jeffrey, L. C., Reithmaier, G., Sippo, J. Z., Johnston, S. G., Tait, D. R., Harada, Y., & Maher, D. T. (2019). Are methane emissions from mangrove stems a cryptic carbon loss pathway? Insights from a catastrophic forest mortality. *New Phytologist*, *224*(1), 146–154. https://doi.org/10.1111/nph.15995

Ji, Y., Angel, R., Klose, M., Claus, P., Marotta, H., Pinho, L., Enrich-Prast, A., & Conrad, R. (2016). Structure and function of methanogenic microbial communities in sediments of Amazonian lakes with different water types. *Environmental Microbiology*, *18*(12), 5082–5100. https://doi.org/10.1111/1462-2920.13491

Johnstone, D., Moore, G., Tausz, M., & Nicolas, M. (2010). The Measurement of Wood Decay in Landscape Trees. *Arboriculture & Urban Forestry*, *36*(3), 121–127.

Junk, W. J., & Piedade, M. T. F. (1997). *Plant Life in the Floodplain with Special Reference to Herbaceous Plants*. 147–185. https://doi.org/10.1007/978-3-662-03416-3_8

Junk, W. J., Piedade, M. T. F., Schöngart, J., Cohn-Haft, M., Adeney, J. M., & Wittmann, F. (2011). A classification of major naturally-occurring amazonian lowland wetlands. *Wetlands*, *31*(4), 623–640. https://doi.org/10.1007/s13157-011-0190-7

Junk, W. J., Wittmann, F., Schöngart, J., & Piedade, M. T. F. (2015). A classification of the major habitats of Amazonian black-water river floodplains and a comparison with their white-water counterparts. *Springer*, *23*(4), 677–693. https://doi.org/10.1007/S11273-015-9412-8

Karlinasari, L., Lestari, A. T., Nababan, M. Y. S., Siregar, I. Z., & Nandika, D. (2018). Assessment of urban tree condition using sonic tomography technology. *IOP Conference Series: Earth and Environmental Science*, *203*(1). https://doi.org/10.1088/1755-1315/203/1/012030

Kazemi-Najafi, S., Shalbafan, A., & Ebrahimi, G. (2009). Internal decay assessment in standing beech trees using ultrasonic velocity measurement. *European Journal of Forest Research*, *128*(4), 345–350. https://doi.org/10.1007/s10342-009-0269-3

Knief, C. (2015). Diversity and habitat preferences of cultivated and uncultivated aerobic methanotrophic bacteria evaluated based on pmoA as molecular marker. *Frontiers in Microbiology*, *6*(DEC), 170928. https://doi.org/10.3389/FMICB.2015.01346/FULL

Laanbroek, H. J. (2010). Methane emission from natural wetlands: Interplay between emergent macrophytes and soil microbial processes. A mini-review. *Annals of Botany*, *105*(1), 141–153. https://doi.org/10.1093/AOB/MCP201

Lan, X., Thoning, K. W., & Dlugokencky, E. J. (2025, June). Trends in globally-averaged CH4, N2O, and SF6 determined from NOAA Global Monitoring Laboratory measurements. In *Https://doi.org/10.15138/P8XG-AA10*.

Le Mer, J., & Roger, P. (2001). *Production, oxidation, emission and consumption of methane by soils: A review*.

Lee, H., Beighley, R. E., Alsdorf, D., Jung, H. C., Shum, C. K., Duan, J., Guo, J., Yamazaki, D., & Andreadis, K. (2011). Characterization of terrestrial water dynamics in the Congo Basin using GRACE and satellite radar altimetry. *Remote Sensing of Environment*, *115*(12), 3530–3538. https://doi.org/10.1016/J.RSE.2011.08.015

Lehner, B., Anand, M., Fluet-Chouinard, E., Tan, F., Aires, F., Allen, G. H., Bousquet, P., Canadell, J. G., Davidson, N., Ding, M., Finlayson, C. M., Gumbricht, T., Hilarides, L., Hugelius, G., Jackson, R. B., Korver, M. C., Liu, L., McIntyre, P. B., Nagy, S., … Thieme, M. (2025). Mapping the world's inland surface waters: An upgrade to the Global Lakes and Wetlands Database (GLWD v2). *Earth System Science Data*, *17*(6), 2277–2329. https://doi.org/10.5194/ESSD-17-2277-2025

Lenhart, K., Bunge, M., Ratering, S., Neu, T. R., Schüttmann, I., Greule, M., Kammann, C., Schnell, S., Müller, C., Zorn, H., & Keppler, F. (2012). Evidence for methane production by saprotrophic fungi. *Nature Communications*, *3*. https://doi.org/10.1038/ncomms2049

Lenth, R. V., & Piaskowski, J. (2017). *emmeans: Estimated Marginal Means, aka Least-Squares Means* (p. 2.0.1) [Data set]. https://doi.org/10.32614/CRAN.package.emmeans

Li, H. L., Zhang, X. M., Deng, F. D., Han, X. G., Xiao, C. W., Han, S. J., & Wang, Z. P. (2020). Microbial methane production is affected by secondary metabolites in the heartwood of living trees in upland forests. *Trees - Structure and Function*, *34*(1), 243–254. https://doi.org/10.1007/S00468-019-01914-6/METRICS

Li, L., Wang, X., Wang, L., Allison, • R. Bruce, Li, L., Wang, · L., Wang, X., & Allison, R. B. (2012). *Acoustic tomography in relation to 2D ultrasonic velocity and hardness mappings*. *46*, 551–561. https://doi.org/10.1007/s00226-011-0426-y

Li, Z., Shang, Y., Wang, C., Wang, J., Liu, X., Li, F., Chen, G., Cheng, H., Zou, J., & Liu, S. (2025). Generally Reduced Sink Capacity of Upland Soils for Atmospheric Methane Over the Past Three Decades (1993–2022). *Global Change Biology*, *31*(5), e70248. https://doi.org/10.1111/gcb.70248

Limpert, K. E., Carnell, P. E., Trevathan-Tackett, S. M., & Macreadie, P. I. (2020). Reducing Emissions From Degraded Floodplain Wetlands. *Frontiers in Environmental Science*, *8*. https://doi.org/10.3389/fenvs.2020.00008

Linares, R., Santos, H. C., Brandes, A. F. N., Barros, C. F., Lisi, C. S., Balieiro, F. C., & Faria, S. M. D. (2017). Exploring the 14C Bomb Peak with Tree Rings of Tropical Species from the Amazon Forest. *Radiocarbon*, *59*(2), 303–313. https://doi.org/10.1017/RDC.2017.10

Liptay, K., Chanton, J., Czepiel, P., & Mosher, B. (1998). Use of stable isotopes to determine methane oxidation in landfill cover soils. *Journal of Geophysical*

Research: Atmospheres, *103*(D7), 8243–8250. https://doi.org/10.1029/97JD02630

Liu, D., Ding, W., Jia, Z., & Cai, Z. (2012). The impact of dissolved organic carbon on the spatial variability of methanogenic archaea communities in natural wetland ecosystems across China. *Applied Microbiology and Biotechnology*, *96*(1), 253–263. https://doi.org/10.1007/s00253-011-3842-x

López-Quintero, C. A., Straatsma, G., Franco-Molano, A. E., & Boekhout, T. (2012). Macrofungal diversity in Colombian Amazon forests varies with regions and regimes of disturbance. *Biodiversity and Conservation*, *21*(9), 2221–2243. https://doi.org/10.1007/s10531-012-0280-8

Määttä, T., & Malhotra, A. (2024). The hidden roots of wetland methane emissions. *Global Change Biology*, *30*(2). https://doi.org/10.1111/gcb.17127

Machacova, K., Bäck, J., Vanhatalo, A., Halmeenmäki, E., Kolari, P., Mammarella, I., Pumpanen, J., Acosta, M., Urban, O., & Pihlatie, M. (2016). Pinus sylvestris as a missing source of nitrous oxide and methane in boreal forest OPEN. *Nature*. https://doi.org/10.1038/srep23410

Machacova, K., Warlo, H., Svobodová, K., Agyei, T., Uchytilová, T., Horáček, P., & Lang, F. (2023). Methane emission from stems of European beech (Fagus sylvatica) offsets as much as half of methane oxidation in soil. *New Phytologist*, *238*(2), 584–597. https://doi.org/10.1111/NPH.18726

Mahieu, K., De Visscher, A., Vanrolleghem, P. A., & Van Cleemput, O. (2008). Modelling of stable isotope fractionation by methane oxidation and diffusion in landfill cover soils. *Waste Management*, *28*(9), 1535–1542. https://doi.org/10.1016/j.wasman.2007.06.003

Maier, M., Machacova, K., Lang, F., Svobodova, K., & Urban, O. (2018). Combining soil and tree-stem flux measurements and soil gas profiles to understand CH4 pathways in Fagus sylvatica forests. *Journal of Plant Nutrition and Soil Science*, *181*(1), 31–35. https://doi.org/10.1002/JPLN.201600405

Malhi, Y., Wood, D., Baker, T. R., Wright, J., Phillips, O. L., Cochrane, T., Meir, P., Chave, J., Almeida, S., Arroyo, L., Higuchi, N., Killeen, T. J., Laurance, S. G., Laurance, W. F., Lewis, S. L., Monteagudo, A., Neill, D. A., Vargas, P. N., Pitman, N. C. A., … Vinceti, B. (2006). The regional variation of aboveground live biomass in old-growth Amazonian forests. *Global Change Biology*, *12*(7), 1107–1138. https://doi.org/10.1111/j.1365-2486.2006.01120.x

Martinez, M., Ardon, M., & Carmichael, M. J. (2022). Identifying Sources and Oxidation of Methane in Standing Dead Trees in Freshwater Forested Wetlands. *Frontiers in Environmental Science*, 701–701.

Megonigal, J. P., & Guenther, A. B. (2008). Methane emissions from upland forest soils and vegetation. *Tree Physiology*, *28*(4), 491–498. https://doi.org/10.1093/treephys/28.4.491

Melack, J. M., & Forsberg, B. R. (2001). Biogeochemistry of Amazon floodplain. In *The Biogeochemistry of the Amazon Basin* (1st edn, pp. 235–274). Oxford University Press.

Melack, J. M., & Hess, L. L. (2010). *Remote Sensing of the Distribution and Extent of Wetlands in the Amazon Basin*. 43–59. https://doi.org/10.1007/978-90-481-8725-6_3

Mochidome, T., & Epron, D. (2024). Drivers of intra-individual spatial variability in methane emissions from tree trunks in upland forest. *Trees*. https://doi.org/10.1007/s00468-024-02501-0

Mochidome, T., Hölttä, T., Asakawa, S., Watanabe, T., Dannoura, M., & Epron, D. (2025). Local methanogenesis drives significant methane emissions from upper tree trunks in a cool-temperate upland forest. *New Phytologist*. https://doi.org/10.1111/nph.70331

Moguel, R. G., Vogel, F., Ars, S., Schaefer, H., Turnbull, J. C., & Douglas, P. M. J. (2022). Using carbon-14 and carbon-13 measurements for source attribution of atmospheric methane in the Athabasca oil sands region. *Atmospheric Chemistry and Physics*, *22*(3), 2121–2133. https://doi.org/10.5194/ACP-22-2121-2022,

Moisan, M. A., Lajoie, G., Constant, P., Martineau, C., & Maire, V. (2024). How tree traits modulate tree methane fluxes: A review. *Science of the Total Environment*, *940*. https://doi.org/10.1016/j.scitotenv.2024.173730

Murguia-Flores, F., Jaramillo, V. J., & Gallego-Sala, A. (2023, September). Assessing Methane Emissions From Tropical Wetlands: Uncertainties From Natural Variability and Drivers at the Global Scale. In *Global Biogeochemical Cycles* (Vol. 37, Issue 9). John Wiley and Sons Inc. https://doi.org/10.1029/2022GB007601

Osunkoya, O. O., Sheng, T. K., Mahmud, N. A., & Damit, N. (2007). Variation in wood density, wood water content, stem growth and mortality among twenty-seven tree species in a tropical rainforest on Borneo Island. *Austral Ecology*, *32*(2), 191–201. https://doi.org/10.1111/J.1442-9993.2007.01678.X

Pangala, S. R., Enrich-Prast, A., Basso, L. S., Peixoto, R. B., Bastviken, D., Hornibrook, E. R. C., Gatti, L. V., Marotta, H., Calazans, L. S. B., Sakuragui, C. M., Bastos, W. R., Malm, O., Gloor, E., Miller, J. B., & Gauci, V. (2017). Large emissions from floodplain trees close the Amazon methane budget. *Nature*, *552*(7684), 230–234. https://doi.org/10.1038/nature24639

Pangala, S. R., Gowing, D. J., Hornibrook, E. R. C., & Gauci, V. (2014). Controls on methane emissions from Alnus glutinosa saplings. *New Phytologist*, *201*(3), 887–896. https://doi.org/10.1111/NPH.12561

Pangala, S. R., Hornibrook, E. R. C., Gowing, D. J., & Gauci, V. (2015). The contribution of trees to ecosystem methane emissions in a temperate forested wetland. *Global Change Biology*, *21*, 2642–2654. https://doi.org/10.1111/gcb.12891

Pangala, S. R., Moore, S., Hornibrook, E. R. C., & Gauci, V. (2013). Trees are major conduits for methane egress from tropical forested wetlands. *New Phytologist*, *197*(2), 524–531. https://doi.org/10.1111/NPH.12031

Parolin, P. (2012). Diversity of adaptations to flooding in trees of Amazonian floodplains. *Pesquisas Botanica*, *63*, 7–28.

Parolin, P., De Simone, 0, Haase, K., Waldhoff, D., Rottenberger, S., Kuhn, U., Kesselmeier, J., Kleiss, B., Schmidt, W., P1edade, M. T. F., & Junk, W. J. (2004). *Central Amazonian Floodplain Forests: Tree Adaptations in a Pulsing System* (The Botanical Review, Vol. 70, Issue 3, pp. 357–380).

Pitz, S., & Megonigal, J. P. (2017). Rapid reports Temperate forest methane sink diminished by tree emissions. *New Phytologist*, *214*, 1432–1439. https://doi.org/10.1111/nph.14559

Pitz, S., Megonigal, J. P., Chang, C.-H., & Szlávecz, K. (2018). Methane fluxes from tree stems and soils along a habitat gradient. *Biogeochemistry*, *137*(3), 307–320. https://doi.org/10.1007/s10533-017-0400-3

Plain, C., & Epron, D. (2021). Pulse labelling of deep soil layers in forest with 13CH4: Testing a new method for tracing methane in the upper horizons, understorey vegetation and tree stems using laser-based spectrometry. *Biogeochemistry*, *153*(2), 215–222. https://doi.org/10.1007/s10533-021-00775-x

Poorter, L., McDonald, I., Alarcón, A., Fichtler, E., Licona, J., Peña-Claros, M., Sterck, F., Villegas, Z., & Sass-Klaassen, U. (2010). The importance of wood traits and hydraulic conductance for the performance and life history strategies of 42 rainforest tree species. *New Phytologist*, *185*(2), 481–492. https://doi.org/10.1111/j.1469-8137.2009.03092.x

Prance, Ghiliean. T. (1979). Notes on the vegetation of Amazonia III. The terminology of Amazonian forest types subject to inundation. *Brittonia*, *31*, 26–38.

Qin, R., Qiu, Q., Lam, J. H. M., Tang, A. M. C., Leung, M. W. K., & Lau, D. (2018). Health assessment of tree trunk by using acoustic-laser technique and sonic tomography. *Wood Science and Technology*, *52*(4), 1113–1132. https://doi.org/10.1007/S00226-018-1016-Z/TABLES/5

Qiu, Q., Qin, R., Lam, J. H. M., Tang, A. M. C., Leung, M. W. K., & Lau, D. (2019). An innovative tomographic technique integrated with acoustic-laser approach for detecting defects in tree trunk. *Computers and Electronics in Agriculture*, *156*, 129–137. https://doi.org/10.1016/J.COMPAG.2018.11.017

Reimer, R. W., & Reimer, P. J. (2026). *CALIBomb*. http://calib.org

Richey, J. E., Melack, J. M., Aufdenkampe, A. K., Ballester, V. M., & Hess, L. L. (2002). Outgassing from Amazonian rivers and wetlands as a large tropical source of atmospheric CO2. *Nature*, *416*(6881), 617–620. https://doi.org/10.1038/416617a

Rosenqvist, Å., Forsberg, B. R., Pimentel, T., Rauste, Y. A., & Richey, J. E. (2002). The use of spaceborne radar data to model inundation patterns and trace gas emissions in the central Amazon floodplain. *International Journal of Remote Sensing*, *23*(7), 1303–1328. https://doi.org/10.1080/01431160110092911

Rulík, M., Weber, L., Min, S., & Šmíd, R. (2023). CO2 and CH4 fluxes from inundated floodplain ponds: Role of diel variability and duration of inundation. *Frontiers in Environmental Science*, *11*. https://doi.org/10.3389/fenvs.2023.1006988

Rusch, H., & Rennenberg, H. (1998). *Black alder (Alnus Glutinosa (L.) Gaertn.) trees mediate methane and nitrous oxide emission from the soil to the atmosphere* (Plant and Soil, Vol. 201, pp. 1–7).

Sakabe, A., Takahashi, K., Azuma, W., Itoh, M., Tateishi, M., & Kosugi, Y. (2021). Controlling Factors of Seasonal Variation of Stem Methane Emissions From Alnus japonica in a Riparian Wetland of a Temperate Forest. *Journal of Geophysical Research: Biogeosciences*, *126*(10). https://doi.org/10.1029/2021JG006326

Saunois, M., Martinez, A., Poulter, B., Zhang, Z., Raymond, P. A., Regnier, P., Canadell, J. G., Jackson, R. B., Patra, P. K., Bousquet, P., Ciais, P., Dlugokencky, E. J., Lan, X., Allen, G. H., Bastviken, D., Beerling, D. J., Belikov, D. A., Blake, D. R., Castaldi, S., … Zhuang, Q. (2025). Global Methane Budget 2000–2020. *Earth System Science Data*, *17*(5), 1873–1958. https://doi.org/10.5194/essd-17-1873-2025

Saunois, M., R. Stavert, A., Poulter, B., Bousquet, P., G. Canadell, J., B. Jackson, R., A. Raymond, P., J. Dlugokencky, E., Houweling, S., K. Patra, P., Ciais, P., K. Arora, V., Bastviken, D., Bergamaschi, P., R. Blake, D., Brailsford, G., Bruhwiler, L., M. Carlson, K., Carrol, M., … Zhuang, Q. (2020). The global methane budget 2000-2017. *Earth System Science Data*, *12*(3), 1561–1623. https://doi.org/10.5194/ESSD-12-1561-2020

Schink, B., & Ward, J. C. (1984). Microaerobic and Anaerobic Bacterial Activities Involved in Formation of Wetwood and Discoloured Wood. *IAWA Journal*, *5*(2), 105–109. https://doi.org/10.1163/22941932-90000872

Schink, B., Ward, J. C., & Zeikus, J. G. (1981). Microbiology of Wetwood: Role of Anaerobic Bacterial Populations in Living Trees. *Microbiology*, *123*(2), 313–322. https://doi.org/10.1099/00221287-123-2-313

Schmidt, G. W. (1972). Amounts of suspended solids and dissolved substances in the middle reaches of the Amazon over the course of one year (August, 1969—July, 1970). *Amazoniana: Limnologia et Oecologia Regionalis Systematis Fluminis Amazonas*, *3*(2), 208–223.

Schöngart, J., & Wittmann, F. (2010). *Biomass and Net Primary Production of Central Amazonian Floodplain Forests* (pp. 347–388). https://doi.org/10.1007/978-90-481-8725-6_18

Schroll, M., Keppler, F., Greule, M., Eckhardt, C., Zorn, H., & Lenhart, K. (2020). The stable carbon isotope signature of methane produced by saprotrophic fungi. *Biogeosciences*, *17*(14), 3891–3901. https://doi.org/10.5194/bg-17-3891-2020

Schroll, M., Lenhart, K., Bender, T., Hötten, P., Rudolph, A., Sörensen, S., & Keppler, F. (2024). Fungal Methane Production Controlled by Oxygen Levels and Temperature. *Methane*, *3*(2), 257–275. https://doi.org/10.3390/methane3020015

Segers, R. (1998). *Methane Production and Methane Consumption: A Review of Processes Underlying Wetland Methane Fluxes* (Vol. 41, Issue 1, pp. 23–51). https://www.jstor.org/stable/1469307?seq=1&cid=pdf-

Silver, W. L., Lugo, A. E., & Keller, M. (1999). *Soil Oxygen Availability and Biogeochemistry along Rainfall and Topographic Gradients in Upland Wet Tropical Forest Soils* (Vol. 44, Issue 3, pp. 301–328). https://about.jstor.org/terms

Sioli, H. (1984). The Amazon and its main affluents: Hydrography, morphology of the river courses, and river types. In H. Sioli (Ed.), *The Amazon: Limnology and landscape ecology of a mighty tropical river and its basin* (pp. 127–165). Springer Netherlands. https://doi.org/10.1007/978-94-009-6542-3_5

Sjögersten, S., Siegenthaler, A., Lopez, O. R., Aplin, P., Turner, B., & Gauci, V. (2020). Methane emissions from tree stems in neotropical peatlands. *New Phytologist*, *225*(2), 769–781. https://doi.org/10.1111/NPH.16178

Smits, K. M., Grant, D. S., Johnston, S. E., Bogard, M. J., Rood, S. B., Selinger, L. B., & Flanagan, L. B. (2022). Riparian Cottonwood Trees and Adjacent River Sediments Have Different Microbial Communities and Produce Methane With Contrasting Carbon Isotope Compositions. *Journal of Geophysical Research: Biogeosciences*, *127*(1). https://doi.org/10.1029/2021jg006699

Soge, A. O., Popoola, O. I., & Adetoyinbo, A. A. (2021). Detection of wood decay and cavities in living trees: A review. *Canadian Journal of Forest Research*, *51*(7),

937–947. https://doi.org/10.1139/CJFR-2020-0340/ASSET/IMAGES/CJFR-2020-0340TAB1.GIF

Son, J., Lee, G., & Shin, J. (2021). Reliability of Noninvasive Sonic Tomography for the Detection of Internal Defects in Old, Large Trees of Abies holophylla Maxim. *Forests 2021, Vol. 12, Page 1131*, *12*(8), 1131. https://doi.org/10.3390/F12081131

Soosaar, K., Schindler, T., Machacova, K., Pärn, J., Fachín-Malaverri, L. M., Rengifo-Marin, J. E., Alegría-Muñoz, W., Jibaja-Aspajo, J. L., Negron-Juarez, R., Zárate-Gómez, R., Garay-Dinis, D. J., Arista-Oversluijs, A. G., Tello-Espinoza, R., Pacheco-Gómez, T., & Mander, Ü. (2022). High Methane Emission From Palm Stems and Nitrous Oxide Emission From the Soil in a Peruvian Amazon Peat Swamp Forest. *Frontiers in Forests and Global Change*, *5*, 849186–849186. https://doi.org/10.3389/FFGC.2022.849186/BIBTEX

Sorz, J., & Hietz, P. (2006). Gas diffusion through wood: Implications for oxygen supply. *Trees - Structure and Function*, *20*(1), 34–41. https://doi.org/10.1007/s00468-005-0010-x

Steege, H. T., Pitman, N. C. A., Sabatier, D., Baraloto, C., Salomão, R. P., Guevara, J. E., Phillips, O. L., Castilho, C. V., Magnusson, W. E., Molino, J. F., Monteagudo, A., Vargas, P. N., Montero, J. C., Feldpausch, T. R., Coronado, E. N. H., Killeen, T. J., Mostacedo, B., Vasquez, R., Assis, R. L., … Silman, M. R. (2013). Hyperdominance in the Amazonian tree flora. *Science*, *342*(6156). https://doi.org/10.1126/science.1243092

Takahashi, K., Sakabe, A., Azuma, W. A., Itoh, M., Imai, T., Matsumura, Y., Tateishi, M., & Kosugi, Y. (2022). Insights into the mechanism of diurnal variations in

methane emission from the stem surfaces of Alnus japonica. *New Phytologist*, *235*(5), 1757–1766. https://doi.org/10.1111/nph.18283

Teh, Y. A., Silver, W. L., & Conrad, M. E. (2005). Oxygen effects on methane production and oxidation in humid tropical forest soils. *Global Change Biology*, *11*(8), 1283–1297. https://doi.org/10.1111/J.1365-2486.2005.00983.X

Ter Steege, H., Mota De Oliveira, S., Pitman, N. C. A., Sabatier, D., Antonelli, A., Guevara Andino, J. E., Aymard, G. A., & Salomão, R. P. (2019). Towards a dynamic list of Amazonian tree species. *Scientific Reports*. https://doi.org/10.1038/s41598-019-40101-y

Terazawa, K., Ishizuka, S., Sakata, T., Yamada, K., & Takahashi, M. (2007). Methane emissions from stems of Fraxinus mandshurica var. Japonica trees in a floodplain forest. *Soil Biology and Biochemistry*, *39*(10), 2689–2692. https://doi.org/10.1016/J.SOILBIO.2007.05.013

Terazawa, K., Yamada, K., Ohno, Y., Sakata, T., & Ishizuka, S. (2015). Spatial and temporal variability in methane emissions from tree stems of Fraxinus mandshurica in a cool-temperate floodplain forest. *Biogeochemistry*, *123*(3), 349–362. https://doi.org/10.1007/S10533-015-0070-Y/METRICS

Thauer, R. K., Kaster, A.-K., Seedorf, H., Buckel, W., & Hedderich, R. (2008). Methanogenic archaea: Ecologically relevant differences in energy conservation. *Nature Reviews Microbiology*, *6*(8), 579–591. https://doi.org/10.1038/nrmicro1931

Toole, R. E., & Gammage, J. L. (1959). Damage From Increment Borings in Bottomland Hardwoods. *OF FORESTI Y*, *57*(2), 909–910.

Trumbore, S. (2009, May). Radiocarbon and soil carbon dynamics. In *Annual Review of Earth and Planetary Sciences* (Vol. 37, pp. 47–66). https://doi.org/10.1146/annurev.earth.36.031207.124300

Turetsky, M., Kotowska, A., Bubier, J., Dise, N. B., Crill, P., Hornibrook, E. R., Minkkinen, J., Moore, T. R., Myers-Smith, I. H., Nykanen, H., & Olefeldt, D. (2014). A synthesis of methane emissions from 71 northern, temperate, and subtropical wetlands. *Global Change Biology*, *20*(7), 2183–2197. https://doi.org/10.1111/gcb.12580

Tveit, A. T., Dumont, M. G., & Schmider, T. (2025). Physiology of atmospheric methane-oxidizing bacteria. *Current Opinion in Microbiology*, *88*, 102656. https://doi.org/10.1016/j.mib.2025.102656

UNEP, U. N. E. P. (2021). *Global Methane Assessment: Benefits and Costs of Mitigating Methane Emissions | UNEP - UN Environment Programme*. https://www.unep.org/resources/report/global-methane-assessment-benefits-and-costs-mitigating-methane-emissions

Vainio, E., Haikarainen, I. P., Machacova, K., Putkinen, A., Santalahti, M., Koskinen, M., Fritze, H., Tuomivirta, T., & Pihlatie, M. (2022). Soil-tree-atmosphere CH4 flux dynamics of boreal birch and spruce trees during spring leaf-out. *Plant and Soil*, *478*(1–2), 391–407. https://doi.org/10.1007/S11104-022-05447-9/FIGURES/4

van Haren, J., Brewer, P. E., Kurtzberg, L., Wehr, R. N., Springer, V. L., Espinoza, R. T., Ruiz, J. S., & Cadillo-Quiroz, H. (2021). A versatile gas flux chamber reveals high tree stem CH4 emissions in Amazonian peatland. *Agricultural and Forest Meteorology*, *307*. https://doi.org/10.1016/j.agrformet.2021.108504

Vigano, I., Röckmann, T., Holzinger, R., Dijk, A. van, Keppler, F., Greule, M., Brand, W. A., Geilmann, H., & Weelden, H. van. (2009). The stable isotope signature of methane emitted from plant material under UV irradiation. *Atmospheric Environment*, *43*(35), 5637–5646. https://doi.org/10.1016/J.ATMOSENV.2009.07.046

Vihermaa, L. E., Waldron, S., Garnett, M. H., & Newton, J. (2014). Old carbon contributes to aquatic emissions of carbon dioxide in the Amazon. *Biogeosciences*, *11*, 3635–3645. https://doi.org/10.5194/bg-11-3635-2014

Viitanen, H. A. (1997). Modelling the Time Factor in the Development of Brown Rot Decay in Pine and Spruce Sapwood—The Effect of Critical Humidity and Temperature Conditions. *Hfsg*, *51*(2), 99–106. https://doi.org/10.1515/hfsg.1997.51.2.99

Vroom, R. J. E., Van Den Berg, M., Pangala, S. R., Van Der Scheer, O. E., & Sorrell, B. K. (2022). Physiological processes affecting methane transport by wetland vegetation – A review. *Aquatic Botany*, *182*, 103547. https://doi.org/10.1016/j.aquabot.2022.103547

Wagener, W., & Davidson, R. (1954). Heart rots in living trees. *The Botanical Review*, *20*, 61–134.

Wagner, D. (2017). Effect of varying soil water potentials on methanogenesis in aerated marshland soils. *Scientific Reports*, *7*(1), 1–9. https://doi.org/10.1038/S41598-017-14980-Y;SUBJMETA

Wang, Z. P., Gu, Q., Deng, F. D., Huang, J. H., Megonigal, J. P., Yu, Q., Lü, X. T., Li, L. H., Chang, S., Zhang, Y. H., Feng, J. C., & Han, X. G. (2016). Methane

emissions from the trunks of living trees on upland soils. *The New Phytologist*, *211*(2), 429–439. https://doi.org/10.1111/nph.13909

Wang, Z. P., Han, S. J., Li, H. L., Deng, F. D., Zheng, Y. H., Liu, H. F., & Han, X. G. (2017). Methane Production Explained Largely by Water Content in the Heartwood of Living Trees in Upland Forests. *Journal of Geophysical Research: Biogeosciences*, *122*(10), 2479–2489. https://doi.org/10.1002/2017JG003991

Wang, Z. P., Li, H. L., Wu, H. H., Han, S. J., Huang, J. H., Zhang, X. M., & Han, X. G. (2021). Methane Concentration in the Heartwood of Living Trees and Estimated Methane Emission on Stems in Upland Forests. *Ecosystems*, *24*(6), 1485–1499. https://doi.org/10.1007/S10021-020-00596-3/METRICS

Wang, Z. P., Zeng, D., & Patrick, W. H. (1996). METHANE EMISSIONS FROM NATURAL WETLANDS. *Environmental Monitoring and Assessment*, (42), 143–143.

Warner, D. L., Villarreal, S., McWilliams, K., Inamdar, S., & Vargas, R. (2017). *Carbon dioxide and methane fluxes from tree stems, coarse woody debris, and soils in an upland temperate forest*. *20*(6), 1205–1216.

Welch, B., Gauci, V., & Sayer, E. J. (2019). Tree stem bases are sources of CH4 and N2O in a tropical forest on upland soil during the dry to wet season transition. *Global Change Biology*, *25*(1), 361–372.

Whalen, S. C. (2005). Biogeochemistry of Methane Exchange between Natural Wetlands and the Atmosphere. *Https://Home.Liebertpub.Com/Ees*, *22*(1), 73–94. https://doi.org/10.1089/EES.2005.22.73

Whiticar, M. J. (1999). *Carbon and hydrogen isotope systematics of bacterial formation and oxidation of methane* (Chemical Geology, Vol. 161, pp. 291–314). www.elsevier.comrlocaterchemgeo

Whiticar, M. J., Faber, E., & Schoell, M. (1986). Biogenic methane formation in marine and freshwater environments: CO2 reduction vs. Acetate fermentation—Isotope evidence. *Geochimica et Cosmochimica Acta*, *50*, 693–709.

Wittmann, C., & Pfanz, H. (2014). Bark and woody tissue photosynthesis: A means to avoid hypoxia or anoxia in developing stem tissues. *Functional Plant Biology*, *41*(9), 940. https://doi.org/10.1071/FP14046

Wittmann, F., Anhuf, D., & Funk, W. J. (2002). Tree species distribution and community structure of central Amazonian várzea forests by remote-sensing techniques. *Journal of Tropical Ecology*, *18*(6), 805–820. https://doi.org/10.1017/S0266467402002523

Wittmann, F., Householder, J. E., Piedade, M. T. F., Schöngart, J., Demarchi, L. O., Quaresma, A. C., & Junk, W. J. (2022). A Review of the Ecological and Biogeographic Differences of Amazonian Floodplain Forests. *Water (Switzerland)*, *14*(21). https://doi.org/10.3390/w14213360

Wittmann, F., Schöngart, J., & Junk, W. J. (2010). Phytogeography, Species Diversity, Community Structure and Dynamics of Central Amazonian Floodplain Forests. In W. J. Junk, M. T. F. Piedade, F. Wittmann, J. Schöngart, & P. Parolin (Eds), *Amazonian Floodplain Forests* (Vol. 210, pp. 61–102). Springer Netherlands. https://doi.org/10.1007/978-90-481-8725-6_4

Wittmann, F., Schöngart, J., Montero, J. C., Motzer, T., Junk, W. J., Piedade, M. T. F., Queiroz, H. L., & Worbes, M. (2006). Tree species composition and diversity

gradients in white-water forests across the Amazon Basin. *Journal of Biogeography*, *33*, 1334–1347. https://doi.org/10.1111/j.1365-2699.2006.01495.x

Wittmann, F., Schöngart, J., Parolin, P., Worbes, M., Piedade, M. T. F., & Junk, W. J. (2006). Wood specific gravity of trees in Amazonian white-water forests in relation to flooding. *IAWA Journal*, *27*(3), 255–268. https://doi.org/10.1163/22941932-90000153

Worbes, M. (1997). *The forest ecosystem of the floodplains. In The Central Amazon floodplain: Ecology of a pulsing system* (W. J. Junk, Ed.; Vol. 126, p. 265). Springer Berlin Heidelberg. https://doi.org/10.1007/978-3-662-03416-3

Wycherley, P. R. (1992). The Genus Hevea—Botanical Aspects. In *Developments in Crop Science* (Vol. 23, pp. 50–66). Elsevier. https://doi.org/10.1016/B978-0-444-88329-2.50009-X

Yang, H., Wang, S., Son, R., Lee, H., Benson, V., Zhang, W., Zhang, Y., Zhang, Y., Kattge, J., Boenisch, G., Schepaschenko, D., Karaszewski, Z., Stereńczak, K., Moreno-Martínez, Á., Nabais, C., Birnbaum, P., Vieilledent, G., Weber, U., & Carvalhais, N. (2024). Global patterns of tree wood density. *Global Change Biology*, *30*(3), e17224. https://doi.org/10.1111/gcb.17224

Yip, D. Z., Veach, A. M., Yang, Z. K., Melissa A Cregger, & Schadt, C. W. (2019). Rapid report Methanogenic Archaea dominate mature heartwood habitats of Eastern Cottonwood (Populus deltoides). *New Phytologist*, *222*, 115–121. https://doi.org/10.1111/nph.15346

Zeikus, J. G., & Ward, J. C. (1974). Methane Formation in Living Trees: A Microbial Origin. *Science*, *4142*(184), 1181–1183.

Zhang, J., & Khoshelham, K. (2020). 3D reconstruction of internal wood decay using photogrammetry and sonic tomography. *The Photogrammetric Record*, *35*(171), 357–374. https://doi.org/10.1111/PHOR.12328

Zhang, Z., Zimmermann, N. E., Stenke, A., Li, X., Hodson, E. L., Zhu, G., Huang, C., & Poulter, B. (2017). Emerging role of wetland methane emission in driving 21st century climate change. *PNAS*, *114*(36), 9647–9652. https://doi.org/10.1073/pnas.1618765114

Zhou, X., Zhang, M., Krause, S. M. B., Bu, X., Gu, X., Guo, Z., Jia, Z., Zhou, X., Wang, X., Chen, X., & Wang, Y. (2021). Soil aeration rather than methanotrophic community drives methane uptake under drought in a subtropical forest. *Science of the Total Environment*, *792*. https://doi.org/10.1016/j.scitotenv.2021.148292